BIOMECHANICS OF FLEXIBLE JOINTS

IN THE CALCIFIED SEAWEED *CALLIARTHRON CHEILOSPORIOIDES*

A DISSERTATION

SUBMITTED TO THE DEPARTMENT OF BIOLOGICAL SCIENCES

AND THE COMMITTEE ON GRADUATE STUDIES

OF STANFORD UNIVERSITY

IN PARTIAL FULFILLMENT OF THE REQUIREMENTS

FOR THE DEGREE OF

DOCTOR OF PHILOSOPHY

Patrick Ted Martone

June 2007

I certify that I have read this dissertation and that, in my opinion, it is fully adequate in scope and quality as a dissertation for the degree of Doctor of Philosophy.

_____

Mark W. Denny (Principal Adviser)

I certify that I have read this dissertation and that, in my opinion, it is fully adequate in scope and quality as a dissertation for the degree of Doctor of Philosophy.

_____

George N. Somero

I certify that I have read this dissertation and that, in my opinion, it is fully adequate in scope and quality as a dissertation for the degree of Doctor of Philosophy.

_____

Fiorenza Micheli

I certify that I have read this dissertation and that, in my opinion, it is fully adequate in scope and quality as a dissertation for the degree of Doctor of Philosophy.

_____

Judith L. Connor

Approved for the University Committee on Graduate Studies

_____

ABSTRACT

Macroalgae that inhabit the intertidal zone of rocky shores must resist drag forces imposed by breaking waves. One common survival strategy is flexibility, which allows intertidal seaweeds to reconfigure into streamlined shapes and reduce the thallus area exposed to flow. The paradigm of flexibility extends even to calcified coralline algae that produce uncalcified joints (genicula) to enable the growth of flexible upright fronds. Articulated corallines evolved from crustose coralline ancestors three times in evolutionary history, and the thrice repeated emergence of genicula is an apparent example of convergent evolution. In this dissertation, I explore the biomechanics and tissue construction of genicula in the Corallinoid *Calliarthron cheilosporioides*. I quantify the variation in geniculum size and strength along individual fronds and demonstrate that genicular tissue is stronger than fleshy algal tissues and strengthens as fronds age. This tissue strengthening is a consequence of thickening cell walls, and mature genicula may be more than 50% cell wall. The strength of genicular cell wall is similar to the strength of cell wall from a freshwater green alga, suggesting that it is the quantity, not the quality, of cell wall that makes genicular tissue strong. By combining genicular geometry and mechanical properties, I construct a numerical model to predict deflections of articulated fronds and evaluate the effects of various morphological dimensions on flexibility and amplification of stress in genicula. I predict the size to which fronds can safely grow in the intertidal zone by comparing breaking force of genicula to drag measured on fronds in a high speed water flume. Field measurements support these predictions, suggesting that intertidal frond size is limited by wave forces. I describe important differences in cell wall polysaccharides between genicula and intergenicula, which may influence genicular properties and the decalcification process, and I document the presence of secondary cell walls and lignin monomers in genicula, two features found in terrestrial plant xylem but unknown in marine algae. By exploring the biomechanics of genicula at a variety of scales, this study explores how nature has orchestrated their functional design.

ACKNOWLEDGEMENTS

Wible was an incredible reference sleuth who would sometimes hand-deliver papers to my office mere hours after they were requested from across the globe. Freya Sommer helped identify all the pesky animals living in my seaweeds and helped make me feel comfortable when diving in the frigid waters (with mixed success). Jim Watanabe was always available to lend statistical advice and to help argue my points to reviewers. Judy Thompson made the marine station run as smoothly as possible, and it frightens me to think what will happen when she retires.

My love of marine phycology (and phycologists!) started at Friday Harbor Laboratories when Paul Gabrielson and Charley O'Kelly taught the marine botany summer course in 2001. Paul and Charley were palpably passionate and knowledgeable about seaweeds and I credit them with initially fostering my interest in phycological research. Since then, I have been inspired by several phycologists who share Paul and Charley's zeal for life. Kathy Ann Miller helped me identify "weeds" in the field, sent me samples and photos from southern California, and was a great sounding board for my ideas. Mike Lakeman and Laura Carney were close phycological friends with whom I balanced annual meetings with camping trips and fun excursions into nature.

Over the last six years, I have had the opportunity to work with many brilliant and creative people in the Denny lab who taught me how to be both productive and not-so-productive. Luke Miller, Moose O'Donnell, and Mike Boller all possess an amazing ability to design and build gadgets with staggering efficiency – in the time it would take me to find a drill bit, they would have equipment up and running: from water flumes to blowguns. Luke John Hoot Hunt was perpetually stoked on life, equally comfortable helping solve difficult equations or leaping from rock to rock in the intertidal zone. Chris Harley showed me the right balance of hard work and hilarity. Joanna Nelson and Elizabeth Nelson both lent important moral support throughout my PhD, even after they had moved away from the lab.

Thanks to my parents, Sherry and David, for their boundless support and love. Snorkeling in the Bahamas, fishing off the Florida coast, shaking critters out of floating *Sargassum* seaweed, rescuing newborn sea turtles, and spending day after day at the beach all contributed to my passion for marine biology. Is it any wonder that I chose graduate school over medical school? Thank you for believing in me.

Finally, thanks to my beautiful wife and best friend Rebecca for her love and support over the years. Becca inspired me when I lost my confidence, comforted me even when she was equally stressed, loved me when my blood sugar levels plummeted, and more than lived up to her vow to share my passion for seaweeds. Living and laughing with Becca gave me a valuable perspective on the Ph.D. and was a constant reminder of life outside graduate school. I couldn't have finished without her.

TABLE OF CONTENTS

To Be a Coralline:
Size, strength, and allometry of joints in the articulated coralline *Calliarthron*

To Break a Coralline:
Impact of wave-induced forces on articulated frond survival

To Transform a Coralline:
Changes in cell wall polysaccharides during genicula development

To Fortify a Coralline:
Secondary cell walls and lignin precursors in *Calliarthron* genicula

LIST OF FIGURES

xiii

xiv

LIST OF TABLES

INTRODUCTION

"How many of us would suspect that evolution could have led to such unlikely plants as coralline algae… plants that few people know about and some do not dream exist."

H. W. Johansen (1981)

The importance of flexibility

The intertidal zone of wave-swept rocky shores is one of the most physically stressful habitats on Earth. At low tide, marine organisms are subjected to the rigors of the terrestrial environment and must contend with severe desiccation and temperature stresses. At high tide, breaking waves generate water velocities that may exceed 20 m s^{-1}, imposing potentially lethal drag forces on intertidal inhabitants (e.g., Denny et al. 2003, Helmuth and Denny 2003, O'Donnell 2005). Despite, and perhaps because of, this physical adversity, wave-swept shores support a diverse assemblage of macroalgae (Hurd 2000).

Researchers have investigated the morphological and mechanical characteristics that allow algae to survive the hydrodynamic stress of their environment (e.g., Gerard and Mann 1979, Koehl 1986, Armstrong 1987, Denny et al. 1989, Carrington 1990, Gaylord et al. 1994, Carrington et al. 2001, Hale 2001, Milligan and DeWreede 2004), and three themes have emerged. Drag increases with the area of an alga's body (the thallus), and as a consequence, many intertidal seaweeds remain small (Denny et al. 1985, Gaylord et al. 1994, Denny 1999). But there are notable exceptions. For example, *Egregia*, the feather-boa kelp, reaches lengths in excess of 5 m in wave-swept intertidal habitats. Thus, small size alone cannot explain the survival of wave-swept algae. Macroalgae could potentially reduce their risk of mechanical failure by being strong, but seaweed tissues are generally weak (Koehl 1986, 2000, Hale 2001). Some macroalgae, such as kelps, grow large in cross-section to compensate for their weak materials, but the benefits are limited because, as explained above, increased size also increases drag. Thus, strength of materials cannot explain the survival of intertidal algae.

Instead, the design criterion that best accounts for the ability of algae to withstand hydrodynamic forces is *flexibility*. Flexibility (a function of both thallus shape and material properties) allows macroalgae to reconfigure, which in turn allows them to reduce the area exposed to flow, to assume a more streamlined shape, and to bend over into slower moving water in the benthic boundary layer (e.g., Koehl 1984, 1986, Vogel 1994, Denny and Gaylord 2002). Furthermore, flexibility and the high extensibility of weak seaweed materials (Koehl 1986, 2000, Hale 2001) allow algae to "go with the flow," which under some circumstances reduces the shock of impinging waves. Flexibility has its limitations (Koehl 1998) (e.g., large kelps may develop destructive momentum (Gaylord and Denny 1997, Denny et al. 1998) or experience harmful whiplash effects (Friedland and Denny 1995) as they reorient), but in general, flexible reconfiguration has been described as a "prerequisite for survival" of wave-swept macroalgae (Harder et al. 2004).

Coralline algae

The role of flexibility in the evolution of algal design has been difficult to demonstrate, in large part, because fleshy algae have a very limited fossil record. If (as seems likely) ancestral fleshy algae were made from weak, extensible materials, present-day flexibility might be a matter of default rather than of design. In contrast, coralline algae (Corallinales, Rhodophyta) reinforce their cell walls with calcite (Borowitzka 1977, 1982), and have an extensive fossil record extending back hundreds of millions of years (Johnson 1961, Wray 1977, Steneck 1983). Ancestors of modern-day corallines (Corallinaceae) are thought to have emerged in the early Jurassic, approximately 200 million years ago (Johnson 1961, Wray 1977, Steneck 1983). According to the fossil record, an important event occurred approximately 100 million years ago: crustose corallines evolved articulations that gave flexibility to their otherwise rigid fronds. Thus, at least for coralline algae, the shift from rigidity to flexibility is clear, and this evolved mechanical innovation has been highly successful. Articulated coralline algae are abundant in oceans worldwide and frequently dominate very low-intertidal habitats where wave forces are most severe.

Extant coralline algae include both crustose and articulated species. Crustose corallines are rigid and generally grow prostrate on hard substrata (see Johansen 1981, Steneck 1986, Woelkerling 1988), thereby avoiding drag and using the rock for mechanical support. In contrast, articulated corallines consist of an alternating sequence of calcified segments (intergenicula) and uncalcified joints (genicula), which allow them to produce upright fronds that may extend 20-30 cm above the substratum (Ganeson 1971, Abbott and Hollenberg 1976, Johansen 1981) (Figure I-1).
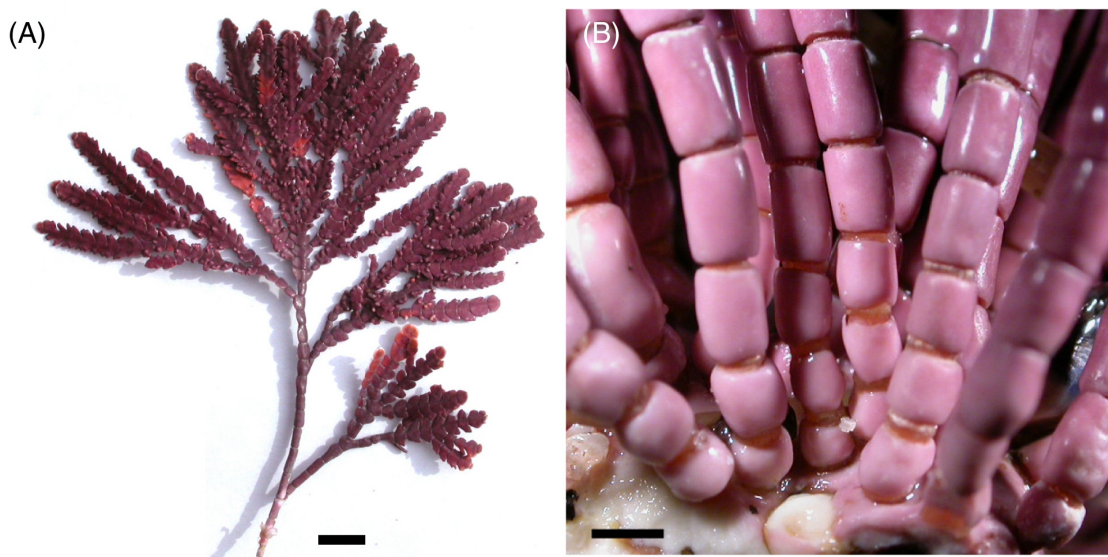
Figure I-1. The articulated Corallinoid *Calliarthron cheilosporioides*, illustrating (A) an entire frond, scale = 1cm, and (B) detail of basal genicula and intergenicula, scale = 2mm.

Moreover, this structural innovation evolved more than once. Sequences from nuclear small-subunit rRNA genes suggest that articulated corallines evolved from crustose coralline ancestors three separate times (Bailey and Chapman 1998, Bailey et al. 2004), a result that is strongly supported by structural and developmental differences in their genicula (Johansen 1969a, b, Johansen 1974, Johansen 1981). In other words, genicula, the "joints" that provide flexibility, are non-homologous structures, which evolved independently in each lineage of articulated corallines. These three lineages are currently represented by three distinct subfamilies, Corallinoideae, Amphiroideae, and Metagoniolithoideae (Johansen 1969a, 1981), and according to the current

coralline phylogeny, representatives of the three articulated subfamilies are more closely related to crustose corallines than they are to each other (Bailey et al. 2004).

Genicula from each subfamily are thought to be functionally similar, but they develop quite differently (Figure I-2). Corallinoid and Amphiroid genicula form when specific regions of the thallus decalcify (Johansen 1974, Johansen 1981), whereas Metagoniolithoid genicula are produced at the meristem as cells alternate between producing calcified and uncalcified tissue (Ganeson 1971, Johansen 1974, Ducker 1979, Johansen 1981). Corallinoid genicula consist of a single tier of uncalcified medullary cells (Johansen 1974, Johansen 1981), whereas Amphiroid and Metagoniolithoid genicula may be composed of several tiers of uncalcified medullary and cortical cells which do not differ structurally from calcified regions of their thalli (Ganeson 1971, Johansen 1974, Ducker 1979, Johansen 1981, Dolan 2001).
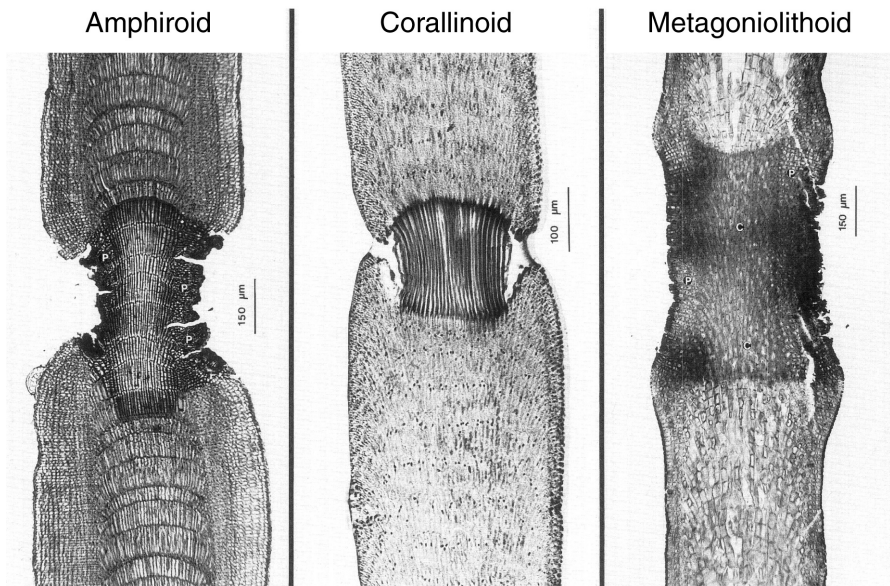
Figure I-2. Genicula from the three subfamilies of articulated coralline algae. Photo from Woelkerling (1988).

All three lineages of articulated corallines occur in hydrodynamically stressful environments. For example, in California, many Corallinoids and Amphiroids inhabit the low intertidal zone (Abbott and Hollenberg 1976), where impacts of wave forces are well-studied and stressful (e.g., Denny and Gaylord 2002, Denny et al. 2003,

Helmuth and Denny 2003, O'Donnell 2005). Other Corallinoids and Amphiroids live along the reef fringes of barrier reef systems in Australia (Huisman 2000, Littler and Littler 2003) and islands in the South Pacific (Littler and Littler 2003, South and Skelton 2003). Metagoniolithoids grow in low intertidal and shallow subtidal environments in southern and western Australia (Ganeson 1971, Ducker 1979) where they, too, likely experience intense hydrodynamic stress. Because articulated fronds are flexible, several researchers have hypothesized that genicula play a critical role in the mechanical and ecological success of articulated coralline fronds (Borowitzka and Vesk 1978, Johansen 1981, Hale 2001).

The thrice repeated emergence of articulated fronds is an apparent—but currently untested—example of convergent evolution of functional morphology. The ultimate goal of this research is to explore the biomechanical performance of genicula in the three lineages, at multiple levels of organization (molecules, cells, tissues, whole organisms), to evaluate the extent and precision of their convergent evolution. However, that is a career's worth of work. Surprisingly little is currently known about coralline genicula – novel soft tissues produced by calcifying algae – and the last six years have been dedicated to collecting baseline data for genicula in one Corallinoid species, *Calliarthron*.

Biomechanics of joints in Calliarthron

Given the broader context of genicula biomechanics and convergent evolution, this dissertation focuses exclusively on the articulated coralline *Calliarthron*, exploring the morphology and performance of segmented fronds in flow, the structure and mechanics of genicula, and the cellular and chemical basis for genicular mechanical properties. By describing *Calliarthron* genicula at multiple levels of organization, this study raises many questions about other Corallinoid and non-Corallinoid species and erects a solid framework of methods and results upon which to expand.

In Chapter 1: *To Be a Coralline*, I explore the variation in geniculum size and strength along individual *Calliarthron* fronds. I show that genicular tissue is far stronger than

fleshy algal tissues, but similar in strength to coral skeleton, with the added benefit of flexibility. By comparing genicula from young and old fronds, I demonstrate that genicula strengthen over time but that frond growth outpaces the ability of genicula to strengthen. Assuming larger fronds experience greater drag force, I predict that fronds become increasingly prone to mechanical failure as they grow and that genicula near (but not necessarily at) the bases of fronds are most likely to break.

In Chapter 2: *To Build a Coralline*, I compare alternative growth strategies to resisting breakage in the intertidal zone: growing in girth versus growing strong tissues. I demonstrate that, due to developmental constraints, *Calliarthron* genicula are unable to increase their cross-sectional area, but compensate by producing tissues that are much stronger than other algae. Using histological techniques, I show that genicular tissue strengthens over time as a consequence of cell wall thickening. I estimate the tensile strength of genicular cell wall and show that *Calliarthron* cell wall is similar in strength to cell walls in a freshwater green alga, suggesting that it is the quantity and not the quality of cell wall that gives *Calliarthron* its great strength. This raises many questions about the other intertidal algae that may ultimately rely on cell walls for mechanical support.

In Chapter 3: *To Bend a Coralline*, I describe the geometry of *Calliarthron* genicula and construct a numerical model that combines genicula morphology and material properties to predict deflection of articulated fronds in flow. I evaluate the effect of various genicular features on flexibility and stress amplification, and demonstrate that genicula near the base of *Calliarthron* fronds, which experience the most bending stress, are morphologically well-adapted to maximizing flexibility while limiting stress amplification.

In Chapter 4: *To Break a Coralline*, I measure the force to break *Calliarthron* genicula in bending, and I propose that, in the field, *Calliarthron* fronds are actually more likely to break in tension. Data suggest that the morphology of basal genicula and the thickened cell walls at the periphery of genicula effectively fortifies fronds against

mechanical failure in bending. I measure drag force on fronds at environmentally-relevant water velocities and predict the maximum size to which *Calliarthron* fronds can grow in the intertidal zone before breaking. Field measurements support model predictions, suggesting that the size of intertidal *Calliarthron* fronds may be limited by wave-induced drag forces.

Experiments described in Chapters 5 and 6 were conducted in fruitful collaboration with Dr. Jose Estevez, an expert in red algal cell walls, at the Carnegie Institute of Washington at Stanford University. In Chapter 5: *To Transform a Coralline*, I describe important differences in cell wall polysaccharides among flexible genicula and calcified intergenicula in *Calliarthron*, suggesting that previous studies of coralline chemistry, which pooled both tissue types, may be misleading. Differences in genicular and intergenicular chemistry may partially explain mechanical properties of genicula and contribute to our limited understanding of calcification and decalcification in coralline taxa.

Experiments described in the final chapter were conducted in further collaboration with Drs. John Ralph and Fachuang Lu, experts in terrestrial lignin chemistry, at the University of Wisconsin, Madison. In Chapter 6: *To Fortify a Coralline*, I document the presence of secondary cell walls in *Calliarthron* genicular cells – common features of terrestrial xylem tissue but a first for marine algae. Furthermore, I demonstrate that genicular cell walls contain three types of monolignols, precursors to terrestrial lignins, including two types found in gymnosperms and one type known only from angiosperms. Chemical data are supported by histological stains used to detect lignin in terrestrial plants. Monolignols may help explain the unique material properties of genicular tissue. I propose that secondary cell walls and monolignols may have evolved convergently in terrestrial xylem and *Calliarthron* genicula in response to mechanical stress.

In addition to revealing many interesting facets of articulated coralline biology, this study raises a wealth of questions for future consideration. For example, do genicula

in other coralline subfamilies contain monolignols and secondary cell walls? Can differences in the material properties of other genicula be explained by differences in cellular structure and cell wall chemistry? Do different combinations of genicular morphology and material properties in other coralline taxa have similar effects on articulated frond flexibility and survival? Is growth of other coralline fronds limited by wave-induced drag? By exploring the biomechanics of genicula, from molecules to macroalgae, this study probes the interaction of chemistry and mechanics in the development of these novel biological structures and lends insight into how nature has orchestrated their functional design.

TO BE A CORALLINE:
SIZE, STRENGTH, AND ALLOMETRY OF JOINTS
IN THE ARTICULATED CORALLINE *CALLIARTHRON*

1.1. Abstract

Articulated coralline algae (Corallinales, Rhodophyta) dominate low intertidal, wave-exposed habitats around the world, yet the mechanics of this diverse group of organisms has been almost completely unexplored. In contrast to fleshy seaweeds, articulated corallines consist of calcified segments (intergenicula) separated by uncalcified joints (genicula). This jointed construction makes calcified fronds as flexible as fleshy seaweeds, allowing them to "go with the flow" when struck by breaking waves. In addition to functioning as joints, genicula act as breakage points along articulated fronds. Here, I describe the allometric scaling of geniculum size, breaking force, and tissue strength along articulated fronds in two species of *Calliarthron*. Genicular material is much stronger than tissue from fleshy macroalgae. Moreover, genicular tissue strengthens as fronds grow, helping them resist breakage. Within individual fronds, larger branches, which presumably experience greater drag force, are supported by bigger, stronger genicula. However, frond growth greatly outpaces genicular strengthening. As a result, *Calliarthron* fronds most likely break at or near their bases when critically stressed by incoming waves. Shedding fronds probably reduces the drag force that threatens to dislodge coralline crusts and may constitute a reproductive strategy.

1.2. Introduction

Organisms that live in wave-exposed, intertidal habitats must contend with remarkable mechanical stresses on a daily basis. Breaking waves can generate water velocities greater than 20 m s^{-1} (e.g., Denny et al. 2003, O'Donnell 2005) and impose considerable forces on intertidal inhabitants (Helmuth and Denny 2003). Moreover, sessile organisms, such as marine macroalgae, cannot seek shelter when

environmental conditions worsen; they must endure wave impacts wherever they settle and grow. Thus, for intertidal seaweeds, the threats of breakage and dislodgement are ever-present.

1.2.1. *Lessons from fleshy macroalgae*

For decades, researchers have studied the mechanical properties and morphological adaptations that allow macroalgae to survive intertidal wave forces (e.g., Delf 1932, Gerard and Mann 1979, Koehl 1986, Armstrong 1987, Denny et al. 1989, Carrington 1990, Gaylord et al. 1994, Carrington et al. 2001, Hale 2001, Milligan and DeWreede 2004). Collectively, these studies have revealed general patterns in the interactions between algal thalli and their fluid environment, material composition, and physical morphology that help macroalgae resist mechanical failure. For instance, the predominant hydrodynamic force applied to intertidal macroalgae by breaking waves is drag (Denny and Gaylord 2002), not hydrodynamic acceleration (Gaylord 2000), although wave impingement forces have yet to be properly quantified (Gaylord 2000). Thus, the risk (R) of mechanical failure of an algal thallus can be described by:

$$R = \frac{F_d}{F_b}$$

1-1

where F_d is the drag force applied to the algal thallus and F_b is the force with which the alga resists breakage. Note that risk is the inverse of the engineer's safety factor (Alexander 1981). Seaweeds that experience excessive drag force relative to their strength are at greatest risk of failure. By comparing drag force to breaking force, past studies have successfully predicted the wave-induced failure of macroalgae in the field (e.g., Carrington 1990, Dudgeon and Johnson 1992, Shaughnessy et al. 1996, Bell 1999). An evaluation of risk suggests that, to reduce their risk of failure and increase their chance of survival, algae can decrease the effective drag force on their thalli or increase their physical strength.

Drag force (F_d) can be described in terms of thallus and fluid characteristics:

$$F_d = \frac{1}{2}\rho U^2 S C_d \qquad\qquad 1\text{-}2$$

where ρ is the density of seawater, U is the water velocity, S is the planform area of the alga (approximately half the wetted surface area), and C_d is the drag coefficient, an index of thallus shape. To reduce drag force, an alga must reduce at least one of these components. For instance, many intertidal seaweeds stay relatively small (Denny et al. 1985, Gaylord et al. 1994, Denny 1999), thereby limiting S. In addition, most macroalgal thalli are flexible. Flexible seaweeds that "go with the flow" reconfigure into more streamline shapes (reducing C_d) and may find refuge from intense water velocities (U) by hugging the substratum (see Koehl 1984, Koehl 1986, Vogel 1994, Denny and Gaylord 2002). Furthermore, the time that flexible fronds spend reorienting and reconfiguring may exceed the duration of brief hydrodynamic loads, such as the wave impingement force, potentially allowing them to evade these maximal forces (Gaylord 2000, Gaylord et al. 2001). Flexibility has its limitations, as particularly massive macroalgae sometimes develop substantial momentum as they reorient (Gaylord and Denny 1997, Denny et al. 1998) and, under some circumstances, experience a harmful whiplash effect (Friedland and Denny 1995). However, in general, flexibility is thought to be beneficial to marine macroalgae and flexible reconfiguration has been described as a "prerequisite for survival" in unstable flow conditions (Harder et al. 2004).

An increase in the force required to break algal thalli also decreases risk. Breaking force is affected by both material composition and cross-sectional area. For example, a single steel thread resists more force than one made of cotton, but cotton threads woven into a sturdy rope are considerably stronger than a slim steel thread. Unlike materials from other wave-exposed organisms, such as barnacle tests and limpet shells, seaweed tissues are rather weak (see summaries in Koehl 1986, Hale 2001). Some macroalgae, such as kelps, grow large in cross-section to compensate for their weak material construction, but large size may deleteriously increase drag force as

well (see Eqn 1-2). Instead, weak seaweed materials are compliant, allowing them to stretch and absorb considerable energy from impinging waves before they break (Koehl 1986, Hale 2001). The utility of being stretchy, however, is not entirely clear cut and depends upon the duration of an applied force and whether an alga is deformed in bending or in tension (Gaylord et al. 2001). In some circumstances, compliance may actually exacerbate the consequences of an applied load (Gaylord et al. 2001). Nevertheless, the mechanical success of macroalgae in the wave-swept intertidal zone can be attributed, at least in part, to their flexibility and their weak but extensible material composition.

Unfortunately, previous studies of algal biomechanics (except Gaylord et al. 2001, Hale 2001) have focused exclusively on fleshy macroalgae and neglected an entire taxonomic order of organisms: the coralline algae (Corallinales, Rhodophyta). Unlike fleshy seaweeds, corallines reinforce their cell walls with calcite, a crystalline form of calcium carbonate ($CaCO_3$) (Borowitzka 1977, Johansen 1981). In other words, coralline algae are composed of cells which are essentially encased in limestone. At the cellular level, such rigidity appears to stand in stark contrast to the flexible body plan that helps fleshy algae survive – yet coralline algae are abundant in oceans worldwide, frequently dominating low-intertidal habitats, where wave forces are expected to be most severe. Thus, coralline algae represent a significant gap in our understanding of algal biomechanics and provide an opportunity to test generalizations about how macroalgae survive breaking waves. In this chapter, I take the first steps in incorporating coralline algae into the paradigm of algal biomechanics.

1.2.2. *Articulated coralline algae*

Most coralline species grow prostrate on the substratum, forming calcified crusts of varied morphology (see Woelkerling 1988), but many extend upright into the water column, forming complex fronds. One might imagine that, without an ability to "go with the flow," upright, calcified fronds would be highly susceptible to breakage or dislodgement in the wave-swept intertidal zone. However, in contrast to their crustose

relatives, most species of upright coralline algae have evolved an "articulated" morphology that reduces the overall stiffness of their fronds. That is, specific regions of the calcified fronds remain uncalcified or actively decalcify to form discrete flexible joints (Figure 1-1). This jointed architecture, which consists of an alternating sequence of calcified segments (intergenicula) and uncalcified joints (genicula), lends flexibility to otherwise rigid coralline fronds. Thus, despite their largely calcified thalli, articulated corallines fit the flexible generality proposed for fleshy macroalgae. But are they, too, structural weaklings?

Several researchers (Borowitzka and Vesk 1978, Johansen 1981, Hale 2001) have hypothesized that genicula play a critical role in the mechanical success of articulated coralline algae; however, little has been published about genicula physical characteristics, mechanical ability, or material composition. Johansen (1969a, 1974, 1981) published the most comprehensive studies of articulated coralline algae, yet many questions about genicula remain.
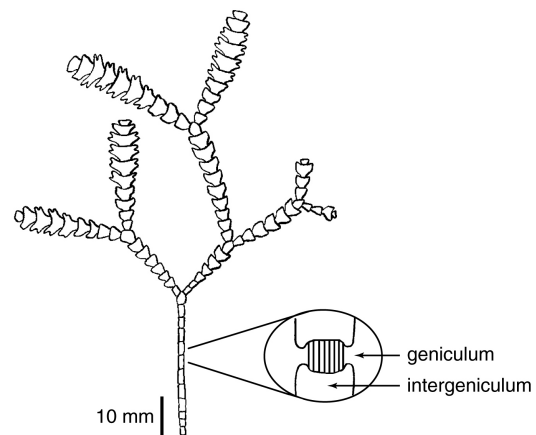
Figure 1-1. Diagram of a representative frond from *Calliarthron cheilosporioides.*

Articulated corallines in the genus *Calliarthron* have genicula composed of a single tier of decalcified cells, which span the entire gap between adjacent intergenicula (Figure 1-1). According to Johansen (1969a), all cells in *Calliarthron* are calcified as they are initiated at the apical meristem, but certain medullary cells pre-destined to form a geniculum soon begin to decalcify and elongate. Shortly thereafter, the cortex surrounding the decalcified cells ruptures to reveal the mature geniculum. In *Calliarthron*, this decalcification process must strike a balance between providing flexibility and catastrophically weakening the fronds. Besides functioning as joints, genicula may, of necessity, act as weak breakage points along articulated fronds. The effect of decalcification on material strength is entirely unknown. Moreover, the

material strength of this novel flexible tissue derived from calcified cells deserves further investigation.

Johansen (1969a) reported that, as *Calliarthron* genicula develop, genicular cells lose most of their cytoplasm, and their nuclei disappear. This study suggests that mature genicula may consist of empty cell walls whose primary function is structural support, as wood provides support for terrestrial trees. However, without nuclei, genicular cells may be incapable of cell division, growth, or repair, thereby imposing severe mechanical and growth limitations upon actively growing fronds. Are genicula static components within dynamically growing fronds?

Finally, the modular nature of articulated coralline algae provides a unique opportunity to quantify the scaling of material strength and mechanical ability along the length of algal thalli. Fleshy macroalgae have tapered homogenous fronds, which make it difficult to force breakage at pre-specified positions. By taking multiple measurements along articulated fronds, I can predict the position within coralline thalli most prone to mechanical failure in the field. The segmented body plan also facilitates comparisons among younger and older thalli, making it possible to estimate physical and material changes in specific genicula over time.

In this paper, I explore the mechanics, growth, and allometric scaling of genicula in the wave-swept articulated corallines *Calliarthron cheilosporioides* Manza and *Calliarthron tuberculosum* (Postels *et* Ruprecht) Dawson. For the first time, I report the breaking strengths of individual genicula and compare them to the strengths of fleshy macroalgal materials. I describe the effects of decalcification on the strength of genicular tissue and provide results suggesting that genicula are not static entities, but strengthen as fronds grow. I measure the variation in genicula characteristics along articulated thalli and, by estimating drag force, predict at what positions thalli are likely to break when hydrodynamically stressed.

1.3. Materials & Methods

1.3.1. *Mechanical test overview*

Because articulated coralline algae are composed of both calcified and uncalcified tissue, two separate mechanical tests were employed to measure their material strength (Figure 1-2). When articulated fronds were pulled in tension, genicula behaved like other fleshy seaweeds (e.g., Hale 2001), stretching until they broke. In contrast, intergenicula behaved more like other calcified materials, such as mollusc shell and coral skeleton, and rarely broke in tension. Furthermore, individual intergenicula were too small to grip in order to force tensile breakage. Thus, three-point bending tests were conducted on intergenicula (Figure 1-2A) to measure their moduli of rupture (M_r), as has been done with other calcified biological materials (Currey 1980, Vosburgh 1982, Boller et al. 2002), while pull-to-break tests were conducted on genicula (Figure 1-2B) to measure their tensile breaking stresses (σ).

Moduli of rupture and tensile breaking stresses are not directly comparable. Moduli of rupture are generally greater than tensile strength measurements because the localized breaks have a decreased likelihood of including pre-existing flaws (Currey and Taylor 1974). Fortunately, data on both tensile breaking stress and modulus of rupture have been reported for mollusc shells (n = 25: Currey 1980) and coral skeleton (n = 1: Vosburgh 1982). A linear regression was fitted to these 26 data points extracted from the literature, and the breaking stress of intergenicula was estimated from their modulus of rupture.

1.3.2. *Three-point bending test*

Fourteen *Calliarthron cheilosporioides* fronds were collected from tidepools above a moderately wave-exposed surge channel at Hopkins Marine Station in Pacific Grove, California (36° 36' N, 121° 53' W). Presumably, the fronds had been broken off the substratum in the surge channel and recently cast ashore. Fronds exhibited healthy pigmentation, no decomposition, and no extensive grazer damage or epiphytism; aside from their dislodgement, all fronds appeared perfectly healthy. Specimens were kept

in a flow-through, seawater table for a maximum of 48 hours before testing. Prior to each experiment, fronds were removed from the seawater, briefly patted dry, and tested immediately while still damp.

To measure the force required to break the calcified intergenicula, three-point bending tests were performed using a custom-made tensometer. The tensometer used a linearly variable differential transformer (LVDT; model 100HR, Schaevitz Engineering, Pennsauken, New Jersey) to measure the bending of a beam, and thereby the force applied to algal tissue between two clamps. The tensometer did not measure tissue strain. In this experiment, one clamp was outfitted with two dulled razor blades (2.25 mm apart) and the other clamp was outfitted with a single dulled razor blade aligned halfway between the other two.
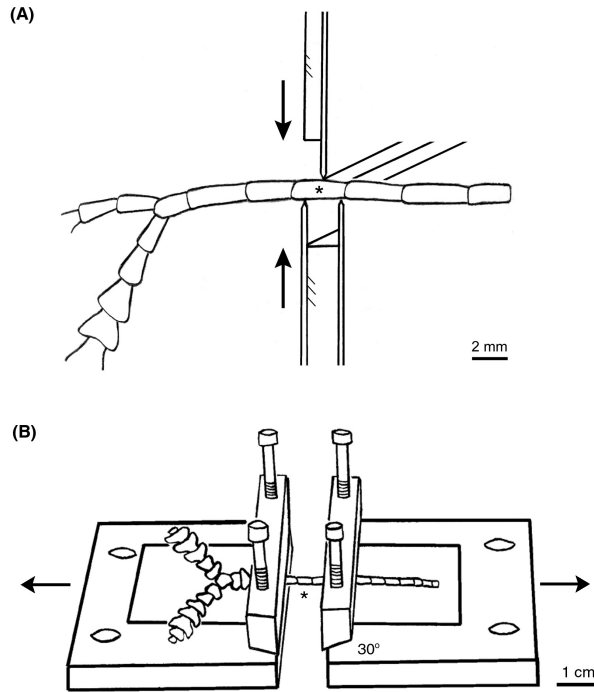
Figure 1-2. Mechanical tests used to measure the strength of genicula and intergenicula. (A) Three-point bending test. Fronds were compressed between three razor blades until intergenicula snapped. (B) Pull-to-break test. Fronds were stretched until genicula broke. The asterisks (*) indicate approximate break locations.

Each frond was positioned so that a single, cylindrical intergeniculum was held between the three razor blades (Figure 1-2A). The razor blades were driven together along the tensometer track at 1 mm/s until the intergeniculum broke, and the applied force was recorded on a chart recorder. The dulled razor blades did not introduce cuts or flaws into the calcified tissue, and most intergenicula broke cleanly in half. The lengths of the major and minor axes of the broken intergenicula were measured, and the following equation was used to calculate the modulus of rupture (M_r):

$$M_r = \frac{F_b\,L\,r}{4\,I}$$

<div align="right">1-3</div>

where F_b is the breaking force, L is the length of the stressed tissue (i.e., the distance between the outer two razor blades), r is the intergeniculum radius parallel to the applied force, and I is the second moment of area, defined for an elliptical cross-section (Roark and Young 1975).

Two intergenicula were broken per frond, and the modulus of rupture of each frond was calculated by averaging these two measurements. Mean intergeniculum modulus of rupture was calculated by averaging the moduli of the fourteen fronds. As explained in section 1.3.1, the tensile breaking stress of intergenicula was estimated from the mean modulus of rupture using the linear regression calculated from Currey (1980) and Vosburgh (1982).

1.3.3. *Pull-to-break tests*

Twenty-nine *Calliarthron* fronds were collected from a single study site (approx. 1 m^2) within the surge channel mentioned above. The site was at mean lower low water (MLLW) near the landward end of the channel. Articulated coralline fronds comprising two size classes were collected: small fronds (n=16; mean length = 38.8 mm ± 8.1 S.D.) and large fronds (n=13; mean length = 101.4 mm ± 24.8 S.D.). Large fronds had at least one dichotomy and proliferous lateral branching, while most small fronds were short, unbranched sprouts. The large fronds were composed of both *Calliarthron tuberculosum* (n=6) and *Calliarthron cheilosporioides* (n=7). The small fronds were generally unidentifiable to the species level, but were assumed to include both *Calliarthron* species. All fronds were completely intact with healthy meristems (i.e., small fronds did not appear to be remains of broken large fronds), and therefore, small fronds were assumed to represent a younger phase in the life of *Calliarthron*. A knife was used to separate each frond from its crustose holdfast at the first geniculum. Extra care was taken to ensure that each frond was removed from a different holdfast,

so that the fronds were presumably representative of 29 distinct individuals. Fronds were kept in a flow-through seawater table, and all thalli were tested within 48 hours to avoid tissue degradation. Prior to each experiment, fronds were removed from the seawater, briefly patted dry, and promptly tested while still damp. Fronds were re-submerged in seawater between trials.

The forces required to break individual genicula were determined by conducting pull-to-break tests using the same tensometer from the three-point bending tests. In this experiment, algal tissue was stretched between two aluminum wedge clamps, designed specifically for this purpose (Figure 1-2B). In each clamp, fronds were held between a flat plat and a 30° wedge, both lined with 2 mm thick rubber pads. The clamps effectively gripped the coralline fronds without crushing the calcified intergenicula.

The clamps were secured along articulated fronds so that 2-4 intergenicula were left "floating" between them. The wedge clamps were driven apart along the tensometer track at 1 mm/s, and the floating series of intergenicula and genicula was stretched until one geniculum broke. The force applied to the geniculum was recorded on a chart recorder. Breaks that occurred at an intergeniculum or at a clamp interface were noted, but not included in this

Figure 1-3. Diagram of a *Calliarthron* frond after it has been broken. (A) Broken genicula were numbered according to their original position in the frond. Data from each broken geniculum was paired with the planform area of the frond that it would have supported in flow (e.g., encircled segments would be paired with geniculum #24). (B) Transverse view of a broken frond segment.

analysis. After each break, the broken segment was set aside, the clamps were shifted down the frond, and the pull-to-break test was repeated. Broken genicula were numbered according to their relative position within a frond (Figure 1-3A). Between

two and four genicula were broken in each small frond and between five and eleven genicula were broken in each large frond, for a total of 157 genicula measurements. Broken segments were organized and taped to a sheet of paper for planform area analysis and archived collection (as depicted in Figure 1-3A).

1.3.4. *Cross-section measurements*

For every genicular break, broken segments were turned up on end and the boundary between the calcified, intergenicular tissue and the decalcified, genicular tissue was identified (Figure 1-3B). The dimensions of the genicular boundary and adjacent intergeniculum were measured using an ocular dial-micrometer. These values were used to calculate the cross-sectional area (A) of the broken geniculum and to estimate the cross-sectional area of the adjacent intergeniculum, assuming both were elliptical. Measurement error was estimated by repeatedly measuring the dimensions of five representative genicula. On average, repeated area measurements deviated from the mean by 5%. Cross-sectional areas of genicula and intergenicula from the large size class were plotted against geniculum position to summarize the relative variation in these values within an average frond and among *Calliarthron* species. The effect of geniculum position (covariate) and species (fixed factor) on geniculum cross-sectional area (response #1) and intergeniculum cross-sectional area (response #2) were analyzed using two separate ANCOVA.

The cross-sectional areas of the basal genicula (#0) were recorded for the small fronds (n=10) and large fronds (n=11) that were not chipped by the knife during collection. The cross-sectional areas of genicula #2, 4, 6, 8, and 10 were measured similarly. To avoid any effect of branching on geniculum size, only genicula below the first branching dichotomy were analyzed. Additional geniculum data collected from large fronds were incorporated into the interspecific ANCOVA described above. The effects of size class (fixed factor) and geniculum position (fixed factor) on cross-sectional area (response) were analyzed using a two-way ANOVA, and the cross-

sectional areas of genicula from the two size classes were compared at specific positions using post-hoc planned comparisons.

Geniculum breaking forces (F_b) were plotted against cross-sectional areas (A) for all broken genicula within each size class. The effects of size class (fixed factor) and cross-sectional area (covariate) on breaking force (response) were initially analyzed with ANCOVA. However, size class regressions had significantly different slopes and were treated separately.

1.3.5. *Breaking stress calculations*

The breaking stress (σ) of each broken geniculum was calculated by dividing breaking force (F_b) by cross-sectional area (A) (Denny 1988). Measurement error in cross-sectional area was propagated into calculation error in breaking stress; reported breaking stresses are assumed to be within 5% of the actual value.

The mean breaking stress of each frond was calculated by averaging together the breaking stresses of its broken genicula. Interspecific variation in the large size class was evaluated using a Student's *t*-test. *Calliarthron* species were not significantly different and breaking stress data from the large size class were pooled. The mean breaking stresses of fronds from each size class were compared using a Student's *t*-test. Mean breaking stresses of fronds from the large size class were nominally compared with the breaking stresses of flexible macroalgae.

1.3.6. *Planform area measurements*

Digital photographs were taken of the broken fronds once they were arranged and taped down. This organization of frond segments allowed each broken geniculum to be paired with all segments distal to it, as these segments comprise the portion of the frond the geniculum must support in flow (Figure 1-3A). The planform areas (S) of the distal segments were measured using an image analysis routine written in LabView (version 6.0.2, National Instruments Corporation, Austin, TX).

Measurement error was estimated by repeatedly calculating the planform areas of seven frond segments. On average, repeated planform area measurements deviated from the mean by 4%. For each large frond, the breaking force (F_b), cross-sectional area (A), and breaking stress (σ) of each broken geniculum were correlated to the planform area of the frond (S) distal to and supported by that geniculum in flow. Data from each frond were tested separately using regression analyses. The effect of planform area (covariate) on geniculum breaking force (response) for all fronds from the large size class (fixed factor) was analyzed using ANCOVA.

1.3.7. *Risk index*

Ideally, to predict where articulated fronds will fail, the risk (R) at each geniculum would be calculated according to Eqn 1-1. However, it is difficult to measure the force of drag pulling on each geniculum in flow. Instead, assuming a constant drag coefficient (C_d) and water velocity (U), frond planform area (S) can be used as a proxy for drag force (F_d) (see Eqn 1-2). This assumption is supported by previous studies which demonstrated that thallus area explains most of the variation in drag (e.g., Carrington 1990, Milligan and DeWreede 2004). See further support for this assumption in Chapter 4. All else being equal, genicula that support larger branches experience proportionately more drag force. Thus, instead of calculating risk (R), the planform area of the frond (S) distal to each geniculum was divided by its breaking force (F_b) to calculate risk index (I_r):

$$I_r = \frac{S}{F_b} \qquad\qquad 1\text{-}4$$

where risk index was assumed to be proportional to risk (R). Risk indices were calculated for all broken genicula from the large frond size class. Data were log-transformed, and regression analysis was used to test the correlation between genicula risk indices and the planform areas of the branches they support. The trend was used to predict at what geniculum position an average frond would be most likely to break.

1.3.8. *Statistics*

JMPIN (version 3.2.1, SAS Institute Inc., Cary, NC) was used to perform all statistical analyses.

1.4. Results

1.4.1. *Intergeniculum tissue strength*

The mean modulus of rupture of intergenicular tissue from *C. cheilosporioides* was 54.6 MN/m^2 ± 2.6 S.E. (Table 1-1). The linear regression fitted to data extracted from Currey (1980) and Vosburgh (1982) showed a significant correlation ($R^2 = 0.57$, $p < 0.001$) between the moduli of rupture (M_r) of calcified materials and their tensile breaking stresses (σ):

$$\sigma = 0.29 M_r + 12.65 \qquad\qquad 1\text{-}5$$

Based on this regression, the mean intergeniculum breaking stress was estimated to be 28.5 MN/m^2.

Table 1-1. Tissue strengths of calcified and uncalcified biological materials.

Division	Species	Tissue	σ (MN m^{-2})	M_r (MN m^{-2})	Reference
	Calcified				
	Gastropod (average)	Sh	50.1	130.0	(Currey, 1980)[†]
	Bivalve (average)	Sh	49.1	124.8	(Currey, 1980)[†]
	Plexaura kuna	Gor	–	75.0	(Boller et al., 2002)
Red	*Calliarthron cheilosporioides*	I	28.5*	54.6	This study
	Acropora reticulata	C	25.6	36.1	(Vosburgh, 1982)
	Uncalcified macroalgae				
Red	*Calliarthron cheilosporioides*	G	25.9		This study
Red		G	25.1		(Hale, 2001)
Red	*Calliarthron tuberculosum*	G	25.2		This study
Red	*Mastocarpus stellatus*	S	18.9		(Dudgeon and Johnson, 1992)
Red		S	11.1		(Pratt and Johnson, 2002)
Red	*Chondrus crispus*	S	10.5		(Dudgeon and Johnson, 1992)
Red		S	7.0		(Pratt and Johnson, 2002)
Red	*Endocladia muricata*	Br	8.1		(Hale, 2001)
Red	*Mazzaella splendens*	S	7.8		(Shaughnessy et al., 1996)
Red	*Prionitis lanceolata*	Br	7.3		(Hale, 2001)
Brown	*Pterygophora californica*	S	7.5		(Biedka et al., 1987)
Brown		S	6.6		(DeWreede et al., 1992)
Red	*Mastocarpus papillatus*	S	6.7		(Carrington, 1990)
Red		S	6.3		(Kitzes and Denny, 2005)
Brown	*Eisenia arborea*	S	6.0		(DeWreede et al., 1992)
Brown	*Egregia menziesii*	S	5.1		(Hale, 2001)
Brown	*Fucus gardneri*	S	4.3		(Hale, 2001)
Brown	*Nereocystis luetkeana*	S	3.6		(Koehl and Wainwright, 1977)
Brown	*Laminaria setchellii*	B	2.3		(Hale, 2001)
Brown	*Postelsia palmaeformis*	S	2.1		(Hale, 2001)
Brown	*Hedophyllum sessile*	B	1.5		(Armstrong, 1987)
Brown	*Lessonia nigrescens*	S	1.2		(Koehl, 1986)
Brown	*Durvillaea antarctica*	S	0.7		(Koehl, 1986)
Green	*Enteromorpha intestinalis*	B	0.7		(Hale, 2001)
Green	*Codium fragile*	Br	0.2		(Hale, 2001)

Species are listed in decreasing order of tissue strength.
σ, breaking stress; M_r, modulus of rupture.
Macroalgae divisions: Red, Rhodophyta; Brown, Ochrophyta, Phaeophyceae; Green, Chlorophyta.
B, blade; Br, branch; C, coral; Gor, gorgonian; G, geniculum; I, intergeniculum; S, stipe; Sh, shell.
*Tensile breaking stress of *Calliarthron* intergeniculum was estimated from its modulus of rupture using Eqn 5.
[†]Only average values (Currey, 1980) are reported here.

1.4.2. *Geniculum cross-sectional areas*

Genicula sizes varied greatly (CV = 48%), spanning an order of magnitude difference (min A = 0.13 mm^2; max A = 1.30 mm^2; mean A = 0.52 mm^2). Overall, genicula near the bases of large fronds had significantly larger cross-sections than genicula near the frond tips (Figure 1-4; ANCOVA $F_{1,151}$ = 176.98, $p < 0.001$). Linear regressions fitted to genicula data from the two *Calliarthron* species had similar slopes (ANCOVA $F_{1,151}$ = 0.88, $p = 0.35$) and revealed no significant interspecific differences (Figure 1-4; ANCOVA $F_{1,151}$ = 0.22, $p = 0.63$). At any given geniculum position, intergenicula from *C. cheilosporioides* (mean A = 1.44 mm^2 ± 0.51 S.D.) and from *C. tuberculosum*

(mean A = 2.40 mm^2 ± 0.70 S.D.) were larger than adjacent genicula; this difference was barely measurable near frond bases, but substantial near frond tips (Figure 1-4). Cross-sectional areas of intergenicula from the two species followed similar patterns (ANCOVA $F_{1,78}$ = 0.30, p = 0.58), but did not vary predictably with geniculum position (Figure 1-4; ANCOVA $F_{1,78}$ = 0.05, p = 0.82). Intergenicula from *C. tuberculosum* were significantly thicker in cross-section than intergenicula from *C. cheilosporioides* (Figure 1-4; ANCOVA $F_{1,78}$ = 8.09, p < 0.01).
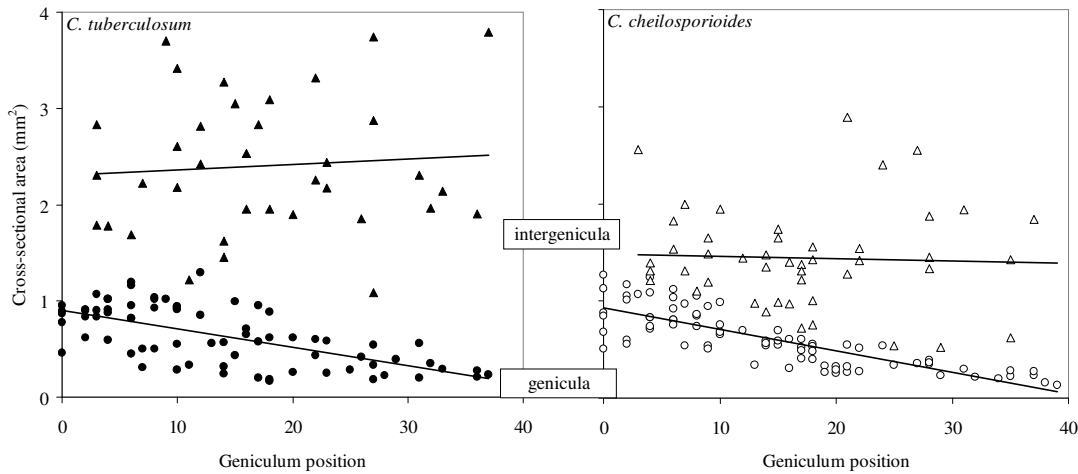
Figure 1-4. Cross-sectional areas of genicula (circles) and intergenicula (triangles) from *C. tuberculosum* (black symbols) and *C. cheilosporioides* (white symbols) from the large size class as functions of geniculum position. Lines represent linear regressions fitted to each data set.

Cross-sectional areas of genicula from the two size classes followed similar patterns over comparable geniculum positions (Figure 1-5; ANOVA $F_{5,133}$ = 0.39, p = 0.85). The effect of geniculum position on cross-sectional area was insignificant in the first ten positions (ANOVA $F_{5,133}$ = 0.34, p = 0.89). Overall, genicula from large fronds had significantly larger cross-sections than genicula from small fronds (Figure 1-5; ANOVA $F_{1,133}$ = 41.83, p < 0.001). Post-hoc planned comparisons revealed that the cross-sectional areas of genicula from large and small fronds were more different at geniculum positions #4-10 (all p < 0.01) than at geniculum position #2 (p < 0.05) or at geniculum position #0 (p = 0.13), where differences between genicula from large and small fronds were not detectable (Figure 1-5). Variances were not significantly

different among large and small fronds at any geniculum position (Levene test: minimum $p = 0.10$).
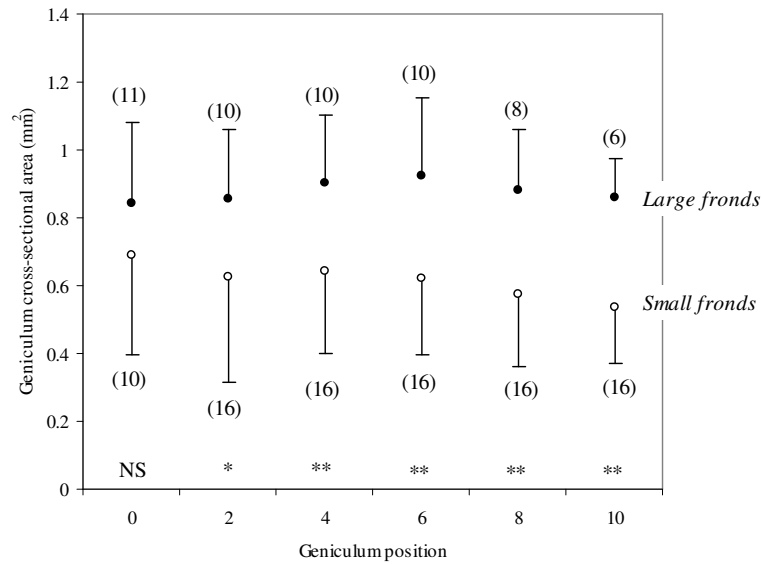
Figure 1-5. Comparison of mean cross-sectional areas ($A \pm$ S.D.) of genicula from small fronds (white circles) and large fronds (black circles). Central error bars were omitted to clarify the graph. Numbers of genicular measurements are reported in parentheses. [NS = not significantly different, * = p < 0.05, ** = p < 0.01]

1.4.3. *Geniculum breaking forces*

Geniculum breaking forces spanned nearly an order of magnitude: the weakest geniculum resisted 2.9 N before breaking, and the strongest geniculum resisted 24.5 N before breaking (Figure 1-6). In general, bigger genicula required more force to break than smaller genicula (Figure 1-6). Linear regressions fitted to genicula data from the two size classes had significantly different slopes (ANCOVA $F_{1,153} = 5.01$, $p < 0.05$) and were analyzed separately. Regressions fitted to both large frond ($R^2 = 0.76$, $p < 0.001$) and small frond ($R^2 = 0.72$, $p < 0.001$) datasets were significant.

Genicula from large fronds: $F_b = 18.49\,A + 2.81$ 1-6

Genicula from small fronds: $F_b = 14.42\,A + 3.49$ 1-7

The slope of the large frond regression was 28% steeper than the slope of the small frond regression.
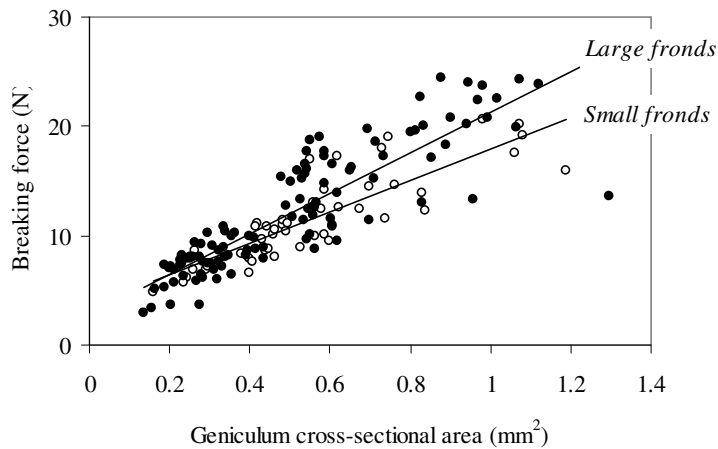
Figure 1-6. Breaking forces of genicula from large fronds (black circles; n=107) and small fronds (white circles; n=50) as functions of their cross-sectional areas.

1.4.4. *Geniculum tissue strength*

The mean breaking stresses of genicular tissue from *C. cheilosporioides* and *C. tuberculosum* were 25.9 MN/m^2 ± 0.9 S.E. and 25.2 MN/m^2 ± 1.7 S.E., respectively (Table 1-1). These genicular measurements were not significantly different (Figure 1-7; Student's $t = 0.42$, $df = 11$, $p = 0.68$), and data from large fronds of both species were pooled. The mean breaking stress of genicula from small fronds, 21.5 MN/m^2 ± 1.0 S.E., was significantly weaker than the mean breaking stress of genicula from large fronds, 25.6 MN/m^2 ± 0.9 S.E. (Figure 1-7; Student's $t = 2.98$, $df = 27$, $p < 0.01$). Variances among the two size classes were not significantly different (Levene test: $p = 0.56$).
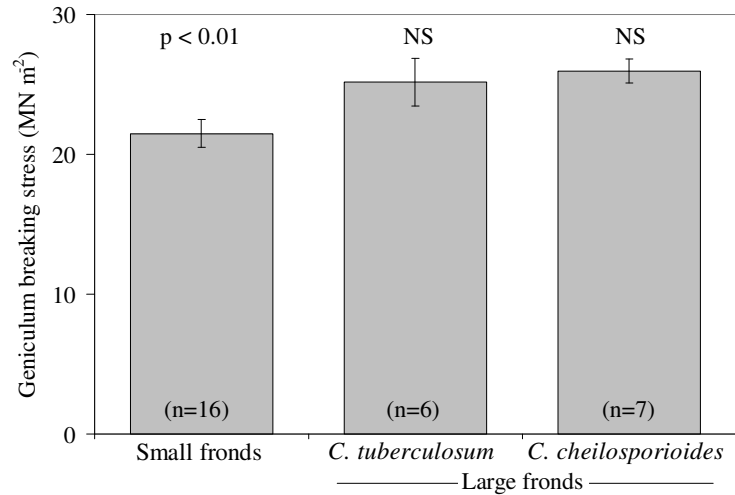
Figure 1-7. Comparison of the mean breaking stress ($\sigma \pm$ S.E.) of large and small *Calliarthron* fronds.

1.4.5. *Variation within fronds*

Genicula at the bases of large fronds required more force to break than genicula near the tips (Figure 1-8A). In general, genicula supporting large branches resisted more force than genicula supporting small branches, and thallus planform area distal to genicula explained most of the variation in breaking force (mean: $R^2 = 0.75$, $p < 0.05$). Similarly, genicula at the bases of large fronds were bigger in cross-section than genicula near the tips (Figure 1-8B). Large branches were supported by large genicula, small branches were supported by small genicula, and thallus planform area distal to genicula explained most of the within-frond variation in cross-sectional area (mean: $R^2 = 0.72$, $p < 0.05$). In contrast, breaking stresses of genicula within a given frond were similar regardless of location (Figure 1-8C). Thallus planform area distal to genicula explained little of the within-frond variation in breaking stress (mean: $R^2 = 0.17$, $p = 0.45$).
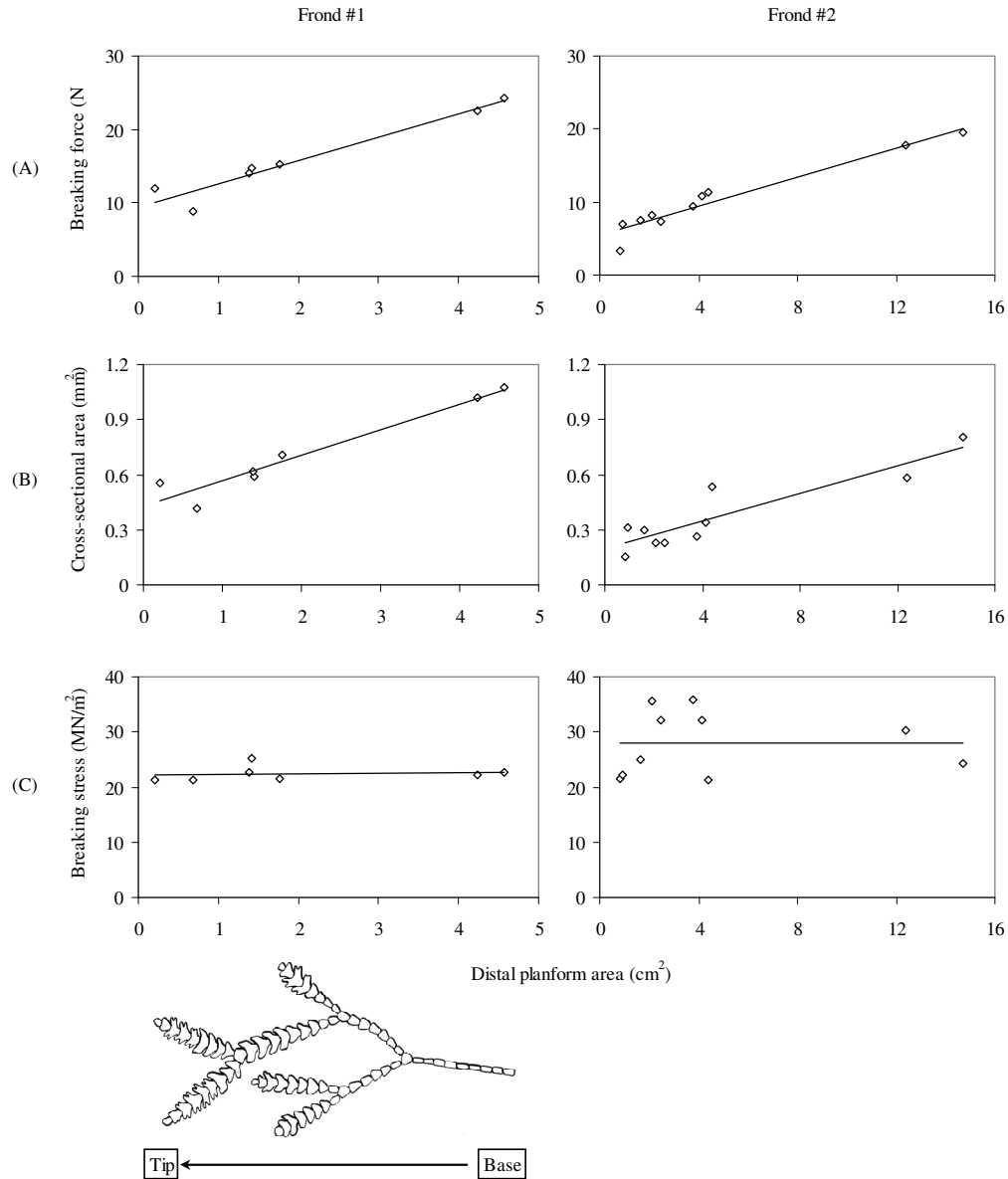
Figure 1-8. Data collected from broken genicula in two representative fronds: (A) Breaking forces, (B) cross-sectional areas, and (C) breaking stresses of genicula as functions of the planform areas of distal frond segments supported in flow.

When fronds from the large size class were all graphed on the same linear scale, the slopes of breaking force - planform area regressions were significantly different (Figure 1-9A; ANCOVA $F_{12,81} = 9.81$, $p < 0.001$). Regressions of larger fronds had lower slopes than regressions of smaller fronds (Figure 1-9A). On average, basal genicula from the large size class supported 30-times more thallus planform area than basal genicula from the small size class.
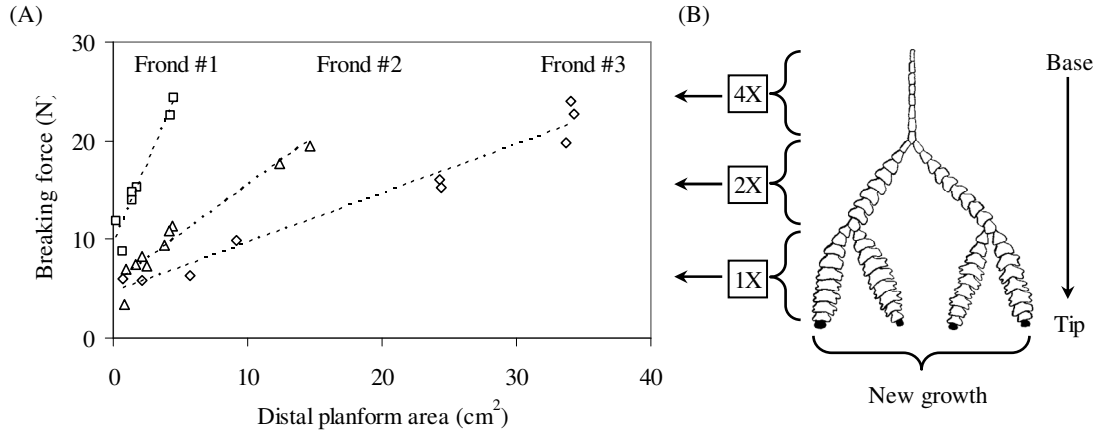
Figure 1-9. (A) Breaking forces of genicula from three representative fronds as functions of the planform areas of distal frond segments supported in flow. (B) Diagram of hypothetical *Calliarthron* frond, explaining the pattern of decreasing slope with increasing frond size. 1X, 2X, and 4X refer to the number of new growth units distal to genicula in the specified regions. See text for details.

1.4.6. *Risk index*

Risk index increased significantly with distal planform area (Figure 1-10; $R^2 = 0.88$, $p < 0.001$). Genicula which support the largest branches have the greatest risk of breaking (Figure 1-10).
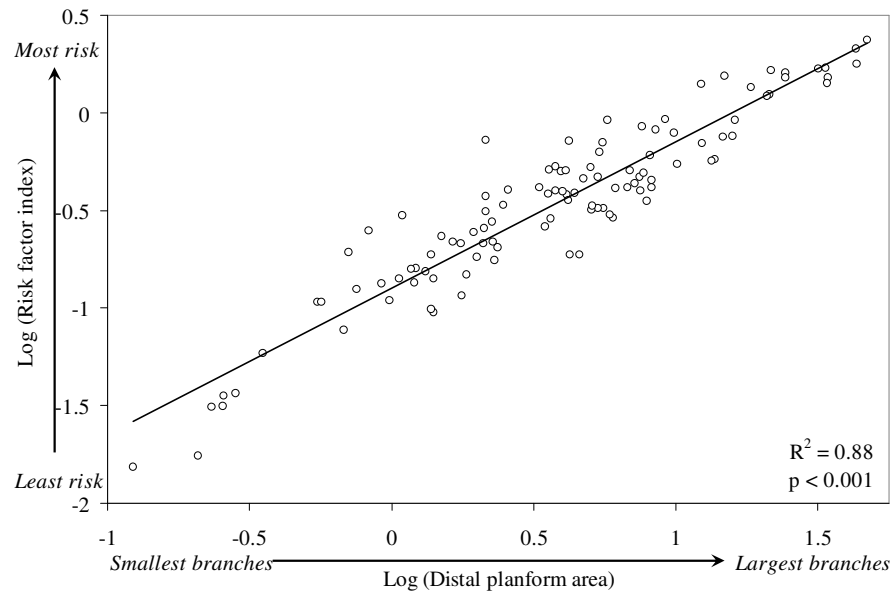
Figure 1-10. Risk indices (I_r) of genicula from the large size class as a function of the planform areas of distal frond segments supported in flow.

1.5. Discussion

1.5.1. *Effect of decalcification*

The modulus of rupture of calcified intergenicular tissue is greater than that of coral skeleton, less than that of gorgonian skeleton, and about half that of mollusc shell (Table 1-1). However, based on Eqn 1-5, the tensile strength of *Calliarthron* intergenicula is estimated to be quite similar to that of coral skeleton, suggesting a material commonality among coral and coralline tissues, at least when stressed in tension. Furthermore, *Calliarthron* intergenicula and genicula are estimated to have similar tensile strengths (Table 1-1). This suggests that as calcified coralline tissue decalcifies to form genicula, tensile strength may not be affected.

However, decalcification produces genicula that are smaller in cross-section than the nearest intergenicula (Figure 1-4) and, because of that simple morphological difference, fronds almost always fail at genicula when loaded in tension. For example, an average-sized *C. cheilosporioides* intergeniculum is predicted to resist approximately 41 N in tension before breaking, but an average-sized *C. cheilosporioides* geniculum snaps at 13 N. Over the course of conducting pull-to-break tests on 157 genicula, intergenicula broke before genicula only 10 times. Many of these incidental breaks occurred at geniculum/intergeniculum interfaces or near the frond tips where reproductive conceptacles form, suggesting that tissue decalcification in these areas may have compromised the intergenicular material in unpredictable ways. Thus, genicula function as pre-defined breakage points along articulated fronds, not because of their weaker material strength, but because of their smaller cross-sectional area. In addition, stress may be amplified in bending genicula (Chapter 3) and the reader is advised to read the discussion of genicular breakage in Chapter 4.

1.5.2. *Geniculum strength*

Tissue from *Calliarthron* genicula is more than an order of magnitude stronger than many brown and green algal materials, several times stronger than other red algal materials, and even 35% stronger than *Mastocarpus stellatus*, the previous record-

holder (Table 1-1). Moreover, genicular tissue is as strong as coral skeleton with the added benefit of flexibility. Although seaweed materials are weaker than several other biological materials (see Gordon 1978, Koehl 1986), the dissimilarity of *Calliarthron* tissues compared to most other macroalgal tissues casts some doubt on the broad generalization that seaweeds are all "weaklings." Rather, macroalgal materials encompass a wide range of tissue strengths (e.g., Table 1-1).

From this widening strength distribution, two patterns are starting to emerge. First, in general, red algal materials are stronger than most brown algal materials which, in turn, are stronger than most green algal materials (Table 1-1). Second, algae with large cross-sectional areas, such as *Durvillaea*, are composed of some of the weakest materials, while skinnier algae, such as *Calliarthron*, possess the strongest materials (Table 1-1). To what degree these two patterns interact is unclear, but the continuum of fat-but-weak and skinny-but-strong is intriguing and merits further study. Strong materials and large cross-sectional area both contribute equally to algal breaking force and, as such, comprise two distinct strategies of mechanical design. By being ten-times stronger, *Calliarthron* can resist the same breaking force as a typical brown alga with ten-times the cross-sectional area. See further discussion of this pattern in Chapter 2.

Data presented here suggest that, as *Calliarthron* grows, genicula increase in both cross-sectional area (but see Chapter 2) and material strength, employing both strengthening strategies. On average, genicula from large fronds were composed of a material that was 20% stronger than tissue from small fronds (Figure 1-7) – a conclusion which is generally supported by the 28% difference in large and small frond regression slopes in Eqns 1-6 & 1-7 (depicted in Figure 1-6). Thus, for a given cross-sectional area, genicula from large fronds resist 20-28% more force than genicula from small fronds. Furthermore, genicula from large fronds were as much as 60% bigger, on average, than genicula from small fronds (Figure 1-5, see geniculum position #10) (but see contrasting results in Chapter 2). These two processes would work together to help genicula avoid breaking when stressed by intertidal waves.

According to these patterns, an average geniculum that grows larger and strengthens its material composition could almost double its ability to resist breakage (i.e., $1.20 \, \sigma$ x $1.60 \, A = 1.92 \, F_b$).

1.5.3. *Geniculum growth*

Although correlative, data from the two size classes support hypotheses of genicular activity, calling into question Johansen's (1969a) note that mature genicula do not have nuclei. Data presented here are not likely the result of a selective process, where only the small fronds with big genicula composed of strong materials survive to become large fronds. If that had been the case, data from large fronds would have comprised a small subset of measurements from small fronds, resulting in differing variances between the two datasets. However, material strength and cross-sectional area data from large fronds do not represent a subset of small frond measurements, as seen in variances that were not significantly different. Correlative data, such as these, may have to suffice for now, as breaking stress and cross-sectional area measurements require destructive sampling, precluding repeated testing of individual genicula through time. Data in Chapter 2 differ from genicular growth data presented here, underscoring the difficulty in quantifying growth using correlative data.

Previous studies have hinted that genicular cells may change their material properties through time. Johansen (1974) noted that genicular cell walls change in staining properties as they age, and Borowitzka and Vesk (1978) found, in their study of a closely-related articulated coralline, that the amount of fibrillar material in the genicular cell walls increases with age. Both of these observations support a shift in material properties and, potentially, strengthening of genicular tissue through time. The present study takes the first steps toward quantifying and proposing the functional effects of such a change. Recent studies have confirmed this tissue strengthening, and the histological basis for the process is presented in Chapters 2 and 6.

That genicula breaking stress increases as fronds grow is in sharp contrast to recent studies of size-dependent breaking stress in fleshy macroalgae. For instance, the stipe / holdfast junctions of long and short blades of the red alga *Mazzaella splendens* have similar tissue strengths (Shaughnessy et al. 1996). Furthermore, no correlation has been found between breaking stress and blade area (*Nereocystis luetkeana*: Johnson and Koehl 1994), thallus size (*Mastocarpus stellatus* and *Chondrus crispus*: Dudgeon and Johnson 1992), or thallus length (*Chondracanthus exasperatus*: Koehl 2000). However, the specimens in these last three studies were approximately the same size, and only Shaughnessy *et al.* (1996) explicitly compared young plants to mature, adult plants. Conversely, Delf (1932) briefly noted that young *Laminaria digitata* had weaker breaking stresses than adult plants and, on this basis, discarded young plants from her analysis. Future work on size-dependent breaking stress in fleshy macroalgae would help resolve these patterns.

1.5.4. *Geniculum allometry*

Geniculum size and breaking force vary predictably along articulated fronds: the largest/strongest genicula are positioned at the bases of fronds, where they support the majority of the frond in flow, and the smallest/weakest genicula are positioned near the tips, where they support smaller branches (Figure 1-8A & B). If larger branches experience greater drag force (see Eqn 1-2), then genicula of a given strength appear ideally situated to support branches of a given size. Ostensibly, such a correlation is consistent with the engineering theory of optimal design (also known as Maxwell's Lemma), which states that each unit should be exactly as strong as it needs to be, without wasting energy or materials in its construction (see Wainwright et al. 1982, Niklas 1992). Although natural selection is not necessarily an optimizing process, comparisons to such theoretical optima can be useful in exploring the adaptive significance of specific traits (Endler 1986). If *Calliarthron* fronds were optimally designed to resist drag force, then all genicula within a given frond would be stressed equally in flow and risk indices (I_r) would necessarily be constant. In other words, all genicula would be predicted to fail simultaneously. In addition, all force-planform

area regressions would need to be parallel, implying that, as fronds grow bigger and drag force increases, the force to break supporting genicula increases proportionately. That genicula increase their breaking force by growing bigger and increasing their material strength as fronds develop lends support to such a hypothesis. However, the force-planform area regressions are not parallel (Figure 1-9A), and risk indices varied significantly within large fronds (Figure 1-10).

Instead, the force to break individual genicula changes relatively little compared to the planform area of a growing frond. For example, genicula toward the bases of fronds #1 and #3 resisted a similar breaking force, but basal genicula from frond #3 supported seven times the distal planform area (Figure 1-9A). Such a pattern of regressions may be explained by the largely dichotomous branching structure of *Calliarthron* fronds (Figure 1-9B). If one new unit of growth is added to each of four apical meristems, basal genicula suddenly support four new drag elements, while genicula near the tips only support one. Thus, data from basal genicula move to the right in Figure 1-9 four-times faster than data from apical genicula. As fronds transition from the small to the large size class, the average planform area of the fronds increases 30-fold, but the basal genicula which support those growing fronds may only double their ability to resist breakage. Therefore, genicula which support the largest branches have the greatest risk of breaking (Figure 1-10) and, consequently, fronds are predicted to break near the base. Observations of entire fronds cast ashore in tidepools and on beaches lend credibility to this prediction. *Calliarthron* are clearly not optimally designed to resist drag force. However, *Calliarthron* fronds can resist tremendous wave velocities before breaking, and the reader is encouraged to read Chapter 4 for detailed discussion of frond survival.

1.5.5. *Benefits of breakage*

Data presented here suggest that *Calliarthron* fronds are not optimally designed to withstand drag force and, instead, break near the base when critically stressed. Although significantly different from optimal, could this mechanical design be

adaptive? Like many red algae, *Calliarthron* have a perennial crustose base that maintains numerous upright fronds concurrently and replenishes those fronds over a lifetime (Johansen 1969a, Abbott and Hollenberg 1976). As wave force increases, upright fronds may be designed to fail in order to reduce the drag force imposed on the crustose base and decrease the risk of dislodgement of the crust itself. Several other wave-swept red algae, including *Mastocarpus* spp. (Carrington 1990, Dudgeon and Johnson 1992, Pratt and Johnson 2002), *Mazzaella* spp. (Shaughnessy et al. 1996), *Chondracanthus exasperatus* (Koehl 2000) and *Chondrus crispus* (Dudgeon and Johnson 1992, Carrington et al. 2001, Pratt and Johnson 2002), employ a similar breakage strategy. Jettisoned fronds may also be favorably linked to the reproductive cycle of *Calliarthron*, just as fragmentation plays a critical role in coral reproduction (Highsmith 1982). Johansen (1969a) found that *Calliarthron* intergenicula are capable of re-attaching to hard substratum, forming new crustose bases, and eventually growing new upright fronds. Moreover, *Calliarthron* fronds remain healthy and continue to grow for months after separation from their crustose base (*pers. obs.*). Thus, broken fronds may continue to release sexual material after breakage, assuming they do not get buried or cast ashore.

Chapter 2

TO BUILD A CORALLINE:
CELLULAR BASIS FOR MECHANICAL STRENGTH IN THE WAVE-SWEPT ALGA *CALLIARTHRON*

2.1. Abstract

Previous biomechanical studies of wave-swept macroalgae have revealed a trade-off in growth strategies to resist breakage in the intertidal zone: increasing girth versus growing strong tissues. Brown macroalgae, such as kelps, grow thick stipes but have weak tissues, while red macroalgae grow slender thalli but have much stronger tissues. For example, genicular tissue in the articulated coralline *Calliarthron cheilosporioides* Manza is more than an order of magnitude stronger than some kelp tissues, but genicula rarely exceed 1 mm in diameter. The great tissue strength of *Calliarthron* genicula results, at least in part, from a lifelong strengthening process. Here I present a histological analysis to explore the cellular basis for mechanical strengthening in *Calliarthron* genicula. Genicula are composed of thousands of fiber-like cells, whose cell walls thicken over time. Thickening of constitutive cell walls likely explains why older genicula have stronger tissues: a mature geniculum may be more than 50% cell wall. However, the material strength of the genicular cell wall is similar to the strength of cell wall from a freshwater green alga, suggesting that it may be the quantity – not the quality – of cell wall material that gives genicular tissue its strength. Apparent differences in tissue strength across algal taxa may be a consequence of tissue construction rather than material composition.

2.2. Introduction

In order to survive along wave-swept shores, intertidal macroalgae must have thalli whose breaking forces exceed the drag forces imposed on their fronds by breaking waves. Many studies of intertidal algal biomechanics have focused primarily on flow-induced forces (e.g., Koehl 1984, 1986, Denny 1994, Denny et al. 1997, Gaylord and Denny 1997, Denny et al. 1998, Bell 1999, Denny 1999, Gaylord et al. 2001, Denny and Gaylord 2002) and how wave-swept thalli remain generally small (e.g., Denny et

al. 1985, Gaylord et al. 1994, Blanchette 1997, Denny 1999) or reorient and reconfigure in flow (e.g., Koehl 1986, Bell 1999, Boller and Carrington 2006) to limit these forces. And while many researchers have explored thallus breakage (e.g., Koehl and Wainwright 1977, Carrington 1990, Gaylord et al. 1994, Shaughnessy et al. 1996, Duggins et al. 2003, Kitzes and Denny 2005), few studies have examined the dynamics of the supportive tissues and composite materials that allow macroalgae to resist drag forces as they grow.

Given an imposed force, algae can follow two basic growth strategies to avoid breaking: increase either the (1) cross-sectional area or (2) tissue strength of thalli. Both strategies increase the ability of algal thalli to resist applied loads. Data from past biomechanical studies reveal that these two growth strategies are indeed traded against one another (Figure 2-1). That is, algae with thick thalli tend to be composed of weaker tissues, while algae with slender thalli have the strongest tissues. In general, brown macroalgae (Ochrophyta, Phaeophyceae), including the kelps, follow the first strategy. While their tissues are quite weak (Koehl 1986, also see summary in Chapter 1, Hale 2001), many brown macroalgae have secondary meristems, called "meristoderms" in kelps, which allow their stipes to increase greatly in girth (Graham and Wilcox 2000). Thus, brown algal stipes gain much of their strength from their large cross-sectional areas, rather than from inherently strong tissues, as a braided rope exceeds the strength of a single fiber. The giant intertidal alga *Durvillaea antarctica* has taken this strategy to an extreme. Its tissues are among the weakest (0.7 MN m^{-2}, Koehl 1986), but it can grow to more than 50 mm in diameter (Stevens et al. 2002) and therefore resist more than 1000 N before breaking.
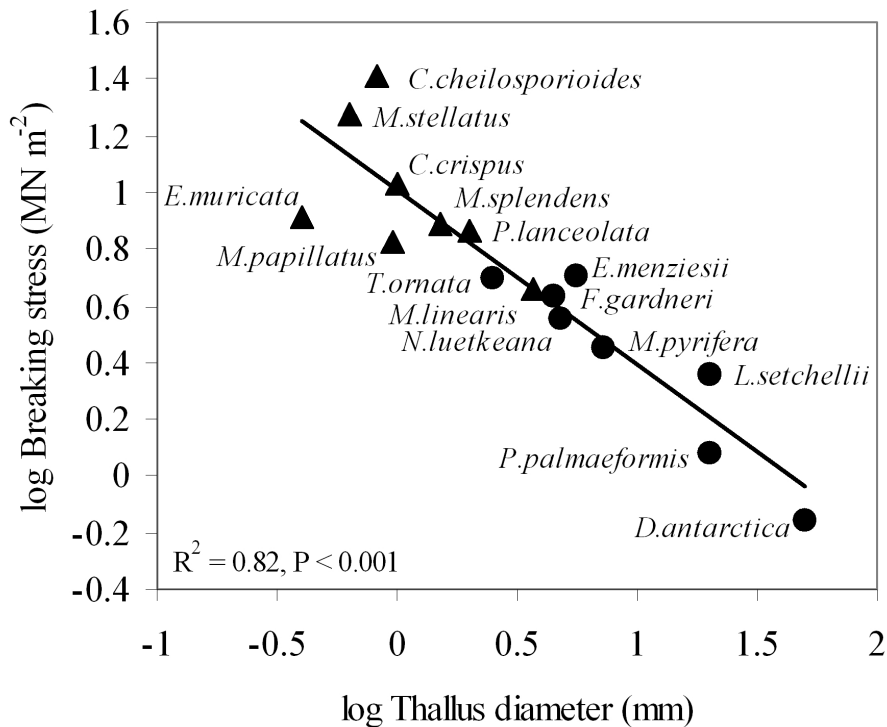
Figure 2-1. Mean breaking stresses of various red macroalgae (triangles) and brown macroalgae (circles) as a function of their mean stipe diameters. Data were extracted from the following references: *Calliarthron cheilosporioides* (Chapter 1), *Mastocarpus stellatus* (Dudgeon and Johnson 1992), *Chondrus crispus* (Carrington et al. 2001), *Endocladia muricata* (Hale 2001), *Mazzaella splendens* (Shaughnessy et al. 1996), *Prionitis lanceolata* (Hale 2001), *Mastocarpus papillatus* (Carrington 1990), *Egregia menziesii* (Friedland and Denny 1995), *Turbinaria ornata* (Stewart 2006a, b), *Nereocystis luetkeana* (Koehl and Wainwright 1977), *Macrocystis pyrifera* (Utter and Denny 1996), *Fucus gardneri* (Hale 2001), *Laminaria setchellii* (Klinger and DeWreede 1988, Hale 2001), *Postelsia palmaeformis* (Holbrook et al. 1991), *Durvillaea antarctica* (Koehl 1986, Stevens et al. 2002). If diameters were not explicitly reported, mean stipe diameter was estimated by dividing mean breaking force (N) by mean breaking stress (N m^{-2}) and assuming a circular cross-section. Diameter measurements of *F. gardneri* were taken by the author at Hopkins Marine Station. Error bars were excluded to increase the readability of the graph.

Red algae (Rhodophyta) generally follow the second strategy, constructing their thalli from stronger tissues but rarely growing large in cross-section (Figure 2-1). Of particular interest are the flexible joints, or "genicula," in the wave-swept articulated coralline *Calliarthron cheilosporioides* Manza (Figure 2-2). Genicular tissue is extremely strong – more than ten times stronger than some kelp tissues – but genicula rarely exceed 1 mm in diameter (Chapter 1). In addition, *Calliarthron* genicula are formed secondarily via thallus decalcification and may be developmentally incapable of increasing in cross-section (Johansen 1981, but see Chapter 1). Despite this

physical size limitation, genicular tissue strengthens as fronds age (Chapter 1). In a sense, *Calliarthron* genicula may grow stronger to compensate for their inability to grow larger.
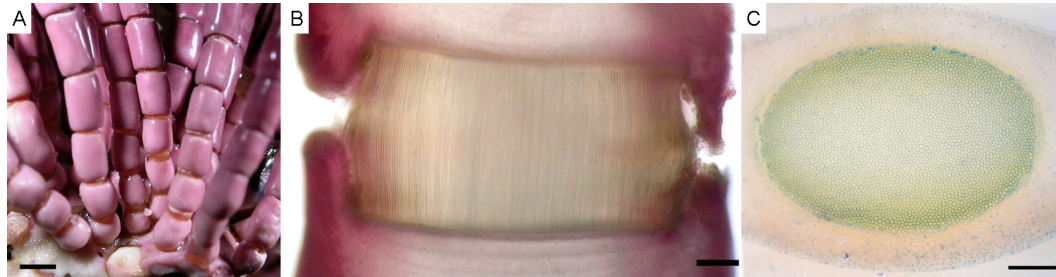
Figure 2-2. (A) Basal segments of *Calliarthron* fronds, illustrating calcified intergenicula separated by uncalcified genicula (Scale=2 mm). (B) Long-section of *Calliarthron* geniculum (Scale=0.2 mm). (C) Cross-section of *Calliarthron* geniculum (Scale=0.1 mm), visualized by staining the surface of the resin block with methylene blue.

Strengthening by growing in girth is easily understood, as meristematic growth in algae has been well-studied (e.g., Klinger and DeWreede 1988, Kogame and Kawai 1996). But strengthening by altering material properties or tissue construction has been largely unexplored. We know relatively little about the material properties of algal tissues or about the effects of material properties or composition on tissue performance. Several studies have observed increases in algal tissue strength along gradients of wave exposure (e.g., Armstrong 1987, Johnson and Koehl 1994, Kitzes and Denny 2005), but whether these patterns resulted from selection or responses to environmental conditions is unknown. A few studies have observed changes in tissue properties associated with thallus ontogeny (Kraemer and Chapman 1991, Stewart 2006b, also see Chapter 1), but none has demonstrated a mechanism underlying such a shift in tissue performance. For example, hypothesized differences in cell wall polysaccharides (alginic acid) did not explain differences in tissue strength (Kraemer and Chapman 1991). Similarly, Carrington et al. (2001) were unable to link tissue properties to carrageenan content in tissue where thalli typically broke.

Genicula in the articulated coralline alga *Calliarthron* present an ideal system for studying mechanical strengthening at the cellular level. Genicula are composed of single tiers of elongated cells, which span the entire distance between calcified

intergenicula (Fig. 2B, Johansen 1969a, 1981). Thus any change in genicular tissue is a direct result of changes to genicular cells. Unfortunately, the characteristics of these constitutive cells (e.g., dimensions, quantities) are poorly described, severely limiting our understanding of genicular tissue and material dynamics. Yet, genicula comprise a wide range of sizes and breakage strengths and differ significantly in their mechanical abilities depending on their age (Chapter 1), all suggesting differences at the cellular level. Most notably, genicula enrich their cell walls with an unknown fibrillar substance as they develop, which makes them thicker than the calcified intergenicular cell walls from which they are derived (Johansen 1974, Borowitzka and Vesk 1978). Genicular cell walls may continue to thicken as genicula age (Yendo 1904), but data supporting this claim are scant. Such cell wall thickening would help explain differences in tissue strengths among young and old *Calliarthron* genicula (Chapter 1).

Here I present results from a histological study to characterize the cellular basis for the great tissue strength of *Calliarthron* genicula and to explore mechanisms underlying the tissue strengthening process. I investigate limitations to genicular growth by comparing equivalent genicula from young and old fronds. I quantify the characteristics of individual genicular cells and estimate the contribution of a single cell to overall geniculum strength. By measuring the proportion of genicular cross-section filled with cell wall, I estimate the material strength of the cell wall proper, and I explore how changes in cell wall dimensions may explain differences in observed tissue strengths.

2.3. Materials & Methods

2.3.1. *Remarks on estimating growth*

Ideally, to assess growth in algal thalli, one should monitor and repeatedly measure individual thalli over time. Unfortunately, this method is impractical to apply to genicula or to their constitutive cells. First, each geniculum is partially obscured from view by calcified flanges that grow down from adjacent intergenicula. Thus accurate

measurements of geniculum cross-sectional areas require destructive sampling (i.e., breaking the fronds). Furthermore, whole genicula are impervious to vital stains, such as Calcofluor White (pers. obs.), which previous studies used to pre-stain algal cells and to measure new growth after stain application (e.g., Waaland and Waaland 1975). This imperviousness is likely a consequence of the densely packed, thick-walled genicular cells. Thus, comparing genicula across different age classes may be the only practical option for estimating growth.

2.3.2. *Sample collection and preparation*

Twenty fronds of *Calliarthron cheilosporioides* were collected haphazardly from a single study site at Hopkins Marine Station in Pacific Grove, California (36°36'N, 121°53'W). The site was located in the low-intertidal zone at the landward end of a moderately wave-exposed surge channel. The collection site was also used and described in Chapter 1. Fronds consisted of two age classes, old (n=10; 14.0 ± 2.5 cm, mean length ± s.d.) and young (n=10; 4.0 ± 0.5 cm), corresponding to the large and small size classes used in Chapter 1.

Fronds were removed from their crustose bases by cutting the basal geniculum with a knife. Fronds were immersed in dilute fixative (1% glutaraldehyde, 1% formaldehyde, 98% filtered seawater) for 24 hours and then decalcified in 1 N HCl for 24 hours. The first and tenth genicula (counting up from the basal geniculum) were dissected out of young and old fronds by cutting through neighboring decalcified intergenicula. For additional comparison, "apical" genicula were also dissected near the tips of old fronds, approximately 1 cm from apices. The distances from tenth genicula to the tips of young fronds were roughly equivalent to the distances from "apical" genicula to the tips of old fronds. Given that *Calliarthron* fronds exhibit apical growth (Johansen and Austin 1970), tenth genicula from young fronds and "apical" genicula from old fronds were assumed to be similar in age.

Samples (n=50) were dehydrated with ethanol (25%, 50%, 75%: 2 hours each), infiltrated with Spurr's resin (Standard "Firm" recipe, 33%, 50%, 66%, 100%: 24 hours each), and cured overnight in a 70° C oven. Thin cross-sections (4 µm) were cut through genicula using a microtome (DuPont Instruments, Sorvall®, model MT2-B),stained with 2% methylene blue, mounted with Permount, and allowed to set for 24 hours before imaging.
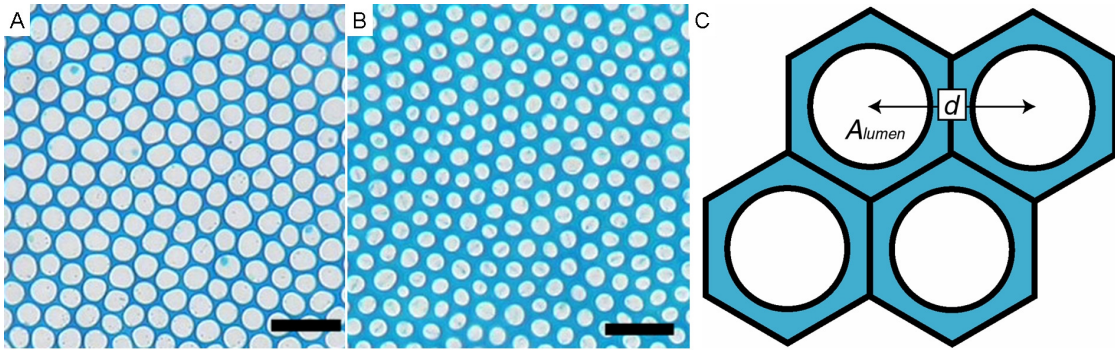
Figure 2-3. Histological cross-sections of a young geniculum (A) and an old geniculum (B), both stained with methylene blue. (C) Cells were assumed to be hexagonal in shape and were characterized by measuring areas of cell lumens (A_{lumen}) and distances to nearest neighbors (d).

2.3.3. *Histological calculations*

Cross-sections of whole genicula were digitally photographed under low magnification. The major and minor diameters of genicula were measured using an image-analysis program written in LabView, and the cross-sectional areas (A_{gen}) were calculated assuming elliptical cross-sections.

Genicular cross-sections were digitally photographed under high magnification (Figure 2-3A & B). Methylene blue stained genicular cell walls but not cell lumens, allowing these components of individual cells to be distinguished and measured. Resin embedding had no measureable effect on cell dimensions, based on measurements of fresh genicula. In cross-section, cells resembled hexagons packed tightly together (Figure 2-3C), an arrangement also noted by Yendo (1904). Preliminary measurements revealed that cells situated at the genicular periphery (within the outer 1/6th of any radius) were distinct from central cells (within the inner

5/6th of any radius) and were analyzed separately. An image-analysis program was written in LabView to measure genicular cells as follows. Representative regions, containing approximately 100 cells, were selected from the center and periphery of each geniculum. Partial cells at the edge of the regions of interest were not measured, and data in excess of 100 cells per region were later discarded at random. Within each region, the program identified all cell lumens and measured their areas (A_{lumen}), based on the number of pixels (Figure 2-3C). The program then measured the distance (d) between the center of each cell lumen and the center of its nearest neighbor (Figure 2-3C). Thus the radius of each cell (r_{cell}) was estimated to be d/2, and the cross-sectional area of each cell (A_{cell}) was calculated according to the area of a hexagon:

$$A_{cell} = \frac{d^2 \sqrt{3}}{2}$$
2-1

Assuming circular cell lumens, the radius of each lumen (r_{lumen}) was calculated from its area:

$$r_{lumen} = \sqrt{\frac{A_{lumen}}{\pi}}$$
2-2

The thickness of each cell wall (w) was calculated as the difference between radii,

$$w = r_{cell} - r_{lumen}$$
$$= \frac{d}{2} - \sqrt{\frac{A_{lumen}}{\pi}}$$
2-3

and the area of each cell wall (A_{wall}) was estimated to be the difference between lumen and cell areas,

$$A_{wall} = A_{cell} - A_{lumen}$$
$$= \frac{d^2 \sqrt{3}}{2} - A_{lumen}$$
2-4

The LabView program measured these cell characteristics in each geniculum (n=50), thereby providing a complete characterization of 10,000 genicular cells.

The average cross-sectional area of central cells was used to estimate the number of cells (N_{cells}) in each geniculum:

$$N_{cells} = \frac{A_{gen}}{(mean\ A_{cell})_{center}}$$ 2-5

Since central and peripheral cells had similar cross-sectional areas, only central cell measurements were used in this calculation.

The percent of genicular cross-sections occupied by cell wall was deduced from the percent of central and peripheral cell cross-sections occupied by cell wall:

$$\%cellwall_{gen} = \frac{5}{6}(\%cellwall_{center}) + \frac{1}{6}(\%cellwall_{periphery})$$
$$= \frac{5}{6}(\frac{mean\ A_{wall}}{mean\ A_{cell}})_{center} + \frac{1}{6}(\frac{mean\ A_{wall}}{mean\ A_{cell}})_{periphery}$$ 2-6

Since cell wall areas (A_{wall}) differed substantially among central and peripheral cells, measurements from both regions were used in this calculation.

2.3.4. *Data analysis*

The average girths of equivalent genicula (i.e., first genicula, tenth genicula) from young and old fronds were compared using Student's t-tests.

The effects of cell position, age class, and frond identity on cell cross-sectional area (A_{cell}) were evaluated using three-way ANOVAs. In order to ensure independence, data were sub-sampled such that, for each age class, central cells were analyzed from half the fronds (selected randomly) and peripheral cells from the other half. In order to retain statistical power, first and tenth genicula were analyzed separately. Variances were significantly different (Cochran's test, $p < 0.05$) and transformations had negligible effects. Because ANOVA interpretation is generally robust given very large sample sizes (Underwood 1999), untransformed data were analyzed.

The effects of age class (fixed factor) and geniculum area (A_{gen}; covariate) on average cross-sectional area of central cells (mean (A_{cell})$_{center}$; n=50) were determined using

ANCOVA. The effects of age class (fixed factor) and geniculum area (A_{gen}; covariate) on the numbers of genicular cells (N_{cells}; n=50) were also determined by ANCOVA. In both analyses, variances were not significantly different (Cochran's test, $p > 0.05$), and slopes were not significantly different ($p = 0.40$ and $p = 0.29$, respectively). A single linear regression was used to predict the number of genicular cells comprising genicula of a given size.

According to data presented in Chapter 1, *Calliarthron* genicula resisted a breaking force (F_b) in newtons according to their cross-sectional area and age class, such that for old genicula, $F_b = 18.49 A_{gen} + 2.81$ ($R^2=0.76$, $p < 0.001$), and for young genicula, $F_b = 14.42 A_{gen} + 3.49$ ($R^2=0.72$, $p < 0.001$). These regressions were used to predict the breaking forces of all genicula measured in this study. Estimated breaking forces were plotted against the number of cells in each geniculum, and linear regressions were fitted to data from each age class. An ANCOVA (age class, fixed factor; N_{cells}, covariate) was used to compare regression slopes, which represented the breaking force per cell from a given age class.

The effects of age class, geniculum, and frond identity on cell wall thickness (w) were evaluated using three-way ANOVAs. In this case, central and peripheral cells were analyzed separately in order to retain statistical power. In addition, cell wall thicknesses of cells from apical genicula in old fronds and tenth genicula in young fronds were compared using a three-way ANOVA with age class, cell position, and frond as factors. All data were sub-sampled, as described above, to ensure independence. As with the first ANOVA, variances were significantly different (Cochran's test, $p < 0.05$), but given the very large sample sizes, untransformed data were analyzed.

Data presented in Chapter 1 also demonstrated that old genicula were significantly stronger per cross-sectional area (mean $\sigma_{old} = 25.9$ MN m^{-2}) than young genicula (mean $\sigma_{young} = 21.5$ MN m^{-2}). Here, the average percent of genicular cross-sectional areas occupied by cell wall (mean %cellwall$_{gen}$) was compared across young (n=20)

and old (n=20) genicula, averaging over first and tenth genicula. To estimate the breaking stresses of genicular cell walls, mean breaking stresses of young and old genicula were divided by respective mean %cellwall$_{gen}$.

The effects of age class, cell position, and frond identity on cell wall thickness (w) were evaluated using three-way ANOVAs. Data were sub-sampled, as described above, and first and tenth genicula were analyzed separately. Again, variances were significantly different (Cochran's test, $p < 0.05$), but the high degree of replication ensured that untransformed data could be interpreted reliably.

ANOVAs were performed using GMAV (Version 5, University of Sydney, Australia). All other statistical tests were performed using JMPIN (Version 3.2.1, SAS Institute, Inc.).

2.4. Results

2.4.1. *Geniculum size*

First genicula from young and old fronds were not significantly different in cross-sectional area (Table 2-1; Student's t-test, df = 18, p = 0.26). The same was true for tenth genicula from young and old fronds (Table 2-1; Student's t-test, df = 18, p = 0.13). Apical genicula in old fronds were smaller than all first and tenth genicula (Table 2-1).

Table 2-1. Genicular cross-sectional areas and constitutive cell dimensions, means ± 95% C.I., measured in three genicula (first, tenth, and apical), two age classes (young and old), and two cell positions (center and periphery).

		A_{gen} (mm^2)			A_{cell} (μm^2)			w (μm)		
		First	Tenth	Apical	First	Tenth	Apical	First	Tenth	Apical
Old	Center	0.61 ±0.10	0.64 ±0.08	0.21 ±0.03	38.8 ±0.5	39.3 ±0.4	38.9 ±0.6	0.82 ±0.02	1.01 ±0.02	0.62 ±0.02
Old	Periphery				39.5 ±0.5	35.5 ±0.5	36.6 ±0.5	1.28 ±0.02	1.35 ±0.02	1.28 ±0.02
Young	Center	0.69 ±0.10	0.56 ±0.06		40.1 ±0.4	35.4 ±0.5		0.46 ±0.01	0.35 ±0.01	
Young	Periphery				37.4 ±0.5	33.2 ±0.5		1.04 ±0.02	0.72 ±0.02	

2.4.2. *Cell area*

On average, *Calliarthron* genicular cells measured $37.5 \pm 0.2 \ \mu m^2$ (mean $\pm$ 95% C.I.; n=10,000). Significant differences in genicular cell area (A_{cell}) were found among fronds, representing normal variability within the population, but this variability was not partitioned in any predictable way (Table 2-2). Cell area did not vary significantly among the centers and peripheries of genicula or among young and old age classes in either first or tenth genicula (Tables 2-1 & 2-2). Moreover, large and small genicula were all composed of similarly-sized cells (Figure 2-4A; ANCOVA, $F_{1,46} = 0.64$, p = 0.42). In sum, all genicula were made of cells of comparable cross-sectional area (Figure 2-4A, Table 2-1).

Table 2-2. ANOVA results for the cross-sectional area of cells, A_{cell}, in (A) first genicula and (B) tenth genicula. ANOVA factors were Age class (2 levels: young and old; fixed, orthogonal), Position (2 levels: center and periphery; fixed, orthogonal), and Frond (5 levels; random, nested) given 100 replicates.

Source of Variation	df	*F*	*P*
A) First genicula			
Age	1	0.01	0.97
Position	1	0.02	0.88
Age x Position	1	2.29	0.15
Frond (Age x Position)	16	123.84	**<0.001**
B) Tenth genicula			
Age	1	0.37	0.55
Position	1	0.63	0.43
Age x Position	1	0.51	0.49
Frond (Age x Position)	16	159.76	**<0.001**
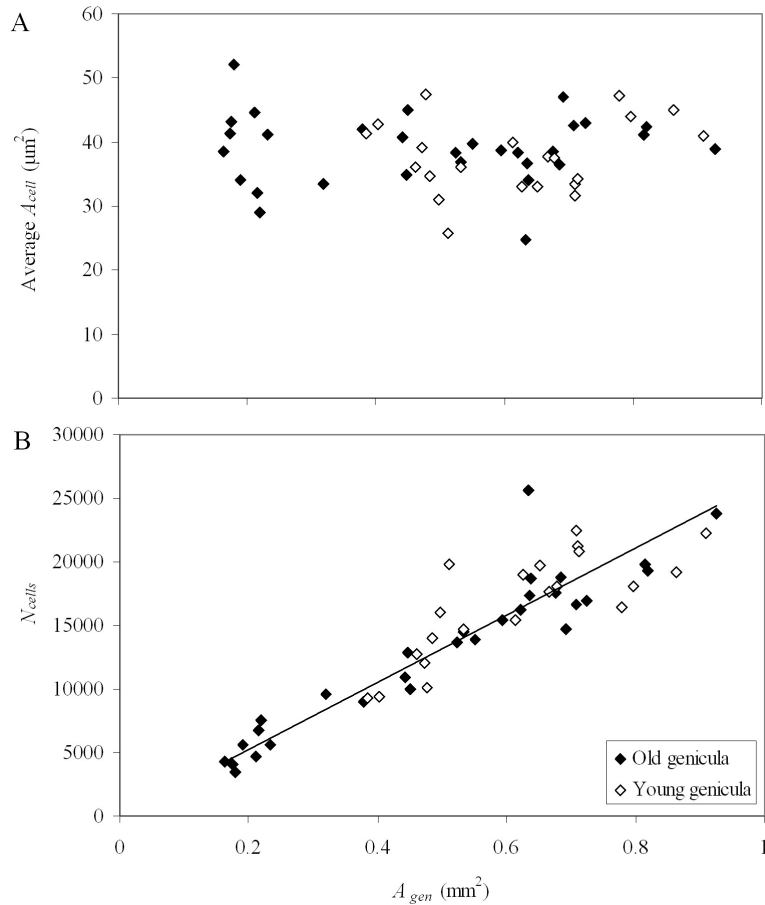
Figure 2-4. (A) Average cross-sectional area of central cells and (B) number of constitutive cells as functions of geniculum cross-sectional area, comparing young genicula (white diamonds) and old genicula (black diamonds).

2.4.3. *Cell number*

Differences in geniculum cross-sectional area can be explained by differences in numbers of genicular cells. That is, larger genicula were composed of significantly more cells (Figure 2-4B; ANCOVA, $F_{1,46} = 133.86$, $p < 0.001$). The smallest geniculum ($A_{gen} = 0.16$ mm^2), an apical geniculum from an older frond, had approximately 4,242 cells, while the largest geniculum ($A_{gen} = 0.93$ mm^2), the first geniculum of an older frond, had approximately 23,806 cells. This correlation was independent of geniculum age; for a given geniculum size, young and old genicula had similar numbers of cells (Figure 2-4B; ANCOVA, $F_{1,46} = 1.69$, $p = 0.20$). In general,

$N_{cells} = 26{,}323$ (A_{gen}); that is, a 1 mm^2 geniculum has approximately 26,323 cells (Figure 2-4B).

Genicula with more constitutive cells resisted greater breaking forces (Figure 2-5). This correlation was significant in both young genicula ($F_b = 0.0004\,N_{cells} + 5.42$, $R^2 = 0.63$, $p < 0.001$) and old genicula ($F_b = 0.0006\,N_{cells} + 3.59$, $R^2 = 0.89$, $p < 0.001$). Regression slopes were significantly different (ANCOVA, $F_{1,46} = 6.26$, $p < 0.05$).
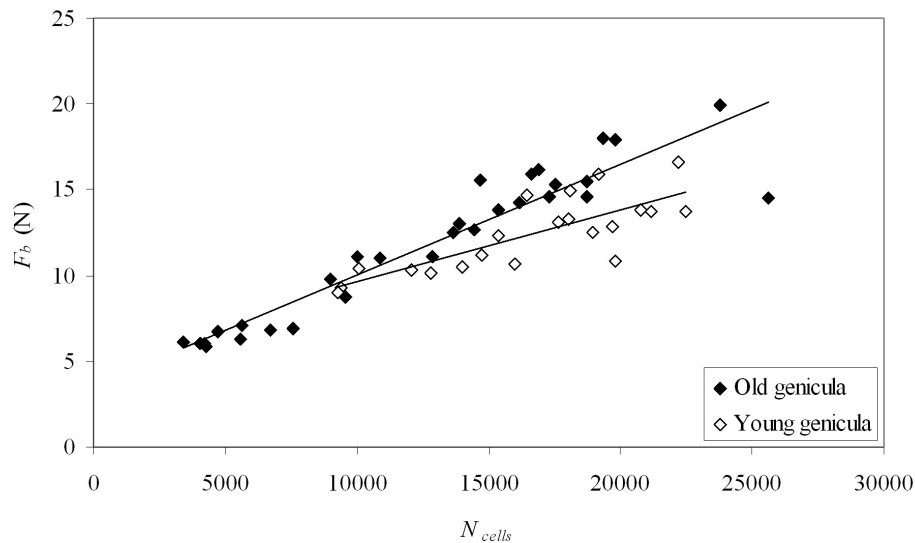
Figure 2-5. Estimated breaking force as a function of number of constitutive cells, comparing young genicula (white diamonds) and old genicula (black diamonds). The slopes of these regressions are used to estimate the forces to break individual cells.

2.4.4. *Cell wall thickness*

Cell wall thickness varied significantly among cells in the various fronds (Table 2-3). Cells in old genicula had significantly thicker cell walls than cells in young genicula (Tables 2-1 & 2-3, Figure 2-6). This pattern was evident in both first and tenth genicula (Figure 2-6), and parallel ANOVA results were obtained from both centers and peripheries of genicula (Table 2-3). Cells from the apical genicula in old fronds had significantly thicker cell walls than cells from the tenth genicula in young fronds (Tables 2-1 & 2-4, Figure 2-6). This pattern was evident at both centers and peripheries of genicula (Table 2-4).

Table 2-3. ANOVA results for cell wall thickness, w, at the (A) center and (B) periphery of genicula. ANOVA factors were Age class (2 levels: young and old; fixed, orthogonal), Geniculum (2 levels: first and tenth; fixed, orthogonal), and Frond (5 levels; random, nested) given 100 replicates.

Source of Variation	df	F	P
A) Center			
Age	1	51.42	**<0.001**
Geniculum	1	0.29	0.6
Age x Geniculum	1	3.15	0.1
Frond (Age x Geniculum)	16	78.75	**<0.001**
B) Periphery			
Age	1	15.65	**<0.001**
Geniculum	1	2.75	0.12
Age x Geniculum	1	2.73	0.12
Frond (Age x Geniculum)	16	129.59	**<0.001**

Table 2-4. ANOVA results for cell wall thickness, *w*, in genicula of approximately the same age: apical genicula from old fronds and tenth genicula in young fronds. ANOVA factors were Geniculum (2 levels: tenth and apical; fixed, orthogonal), Position (2 levels: center and periphery; fixed, orthogonal), and Frond (5 levels: random, nested in Geniculum x Position) given 100 replicates.

Source of Variation	df	F	P
Geniculum	1	32.92	**<0.001**
Position	1	65.67	**<0.001**
Geniculum x Position	1	7.18	**<0.05**
Frond (Geniculum x Position)	16	49.98	**<0.001**
SNK post-hoc tests*:*			
Apical > Tenth (both cell positions)			**<0.05**
Periphery > Center (both genicula)			**<0.01**
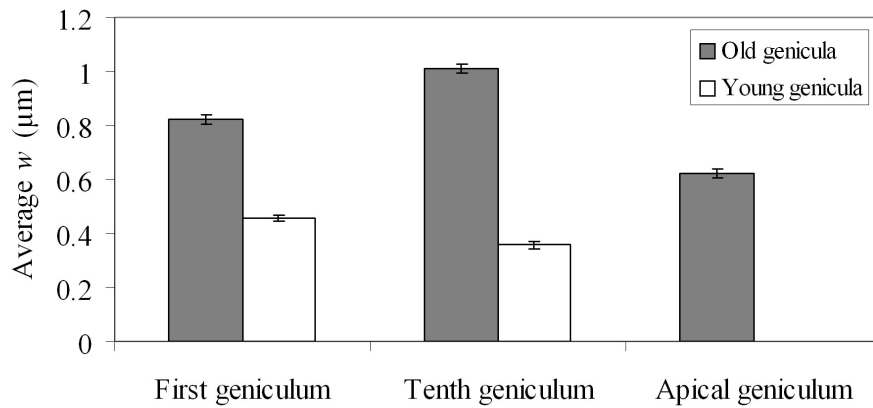
Figure 2-6. Average thickness of cell walls in central cells from first, tenth, and apical genicula in old genicula (gray bars) and young genicula (white bars). Error bars represent 95% C.I. (n=1000).

On average, young genicula were $33.6 \pm 0.3\%$ cell wall (mean $\pm$ 95% C.I.) and old mature genicula were $54.2 \pm 0.3\%$ cell wall (Figure 2-7). Given the tissue strengths of young and old genicula in *Calliarthron* (Chapter 1), young cell wall material was calculated to have a breaking strength of 64.0 MN m^{-2}, and old cell wall material was calculated to have a breaking strength of 47.8 MN m^{-2} (Figure 2-7).
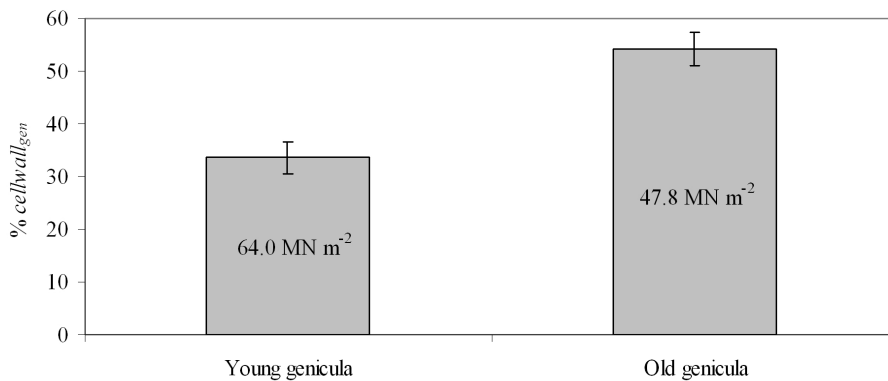
Figure 2-7. Percent of old and young geniculum cross-sectional areas filled with cell wall, averaged over first and tenth genicula. Error bars represent 95% C.I. (n=20). Calculated cell wall breaking strengths are also reported. Note that old cell wall material is weaker than young cell wall material.

Cells near the periphery of genicula had thicker cell walls than central cells (Tables 2-1 & 2-5, Figure 2-8). This pattern was consistent among both young and old genicula, although older genicula had significantly thicker cell walls (Tables 2-1 & 2-5, Figure 2-8). Data from first and tenth genicula gave parallel ANOVA results (Table 2-5).

Table 2-5. ANOVA results for cell wall thickness, w, in (A) first genicula and (B) tenth genicula. ANOVA factors were Age class (2 levels: young and old; fixed, orthogonal), Position (2 levels: center and periphery; fixed, orthogonal), and Frond (5 levels: random, nested in Age x Position) given 100 replicates.

Source of Variation	df	F	P
A) First genicula			
Age	1	6.34	**< 0.05**
Position	1	14.72	**< 0.01**
Age x Position	1	0.27	0.61
Frond (Age x Position)	16	189.32	**<0.001**
B) Tenth genicula			
Age	1	48.66	**<0.001**
Position	1	10.05	**< 0.01**
Age x Position	1	0.12	0.73
Frond (Age x Position)	16	96.44	**<0.001**
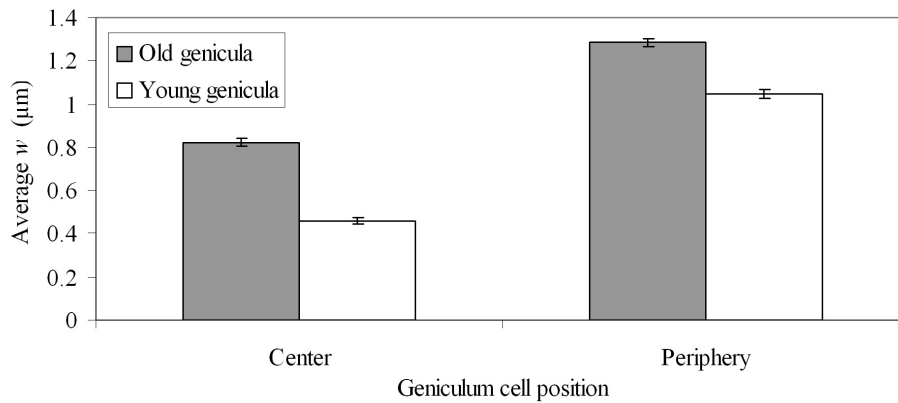
Figure 2-8. Average thickness of cell walls in central and peripheral cells from old first genicula (gray bars) and young first genicula (white bars). Error bars represent 95% C.I. (n=1000).

2.5. Discussion

2.5.1. *Constraints on geniculum growth*

Old genicula were not significantly larger than young genicula at either the first or the tenth geniculum position, suggesting that genicula do not grow in cross-sectional area once they have decalcified. This result highlights a major difference in growth – and thus strengthening – strategies between genicula and other algal tissues and is consistent with our understanding of genicular development: the cortical cells responsible for increasing thallus girth dissolve as the geniculum is revealed (Johansen 1969a). Conversely, data presented in Chapter 1 suggest significant, albeit slight, changes in cross-sectional area using similar methods to those reported here. Such conflicting results emphasize the difficulty in assessing growth via comparisons, where population variability may confound any effect of age. Thus, without direct measurements of individual genicula through time, whether genicula grow after maturation remains somewhat of an open question. However, such growth seems contrary to normal coralline development and, even if it occurs, genicula remain quite small.

2.5.2. *Building blocks of genicula*

Calliarthron genicula are composed of thousands of long fiber-like cells. The large number of cells is routinely misrepresented, for the sake of simplicity, in drawings from previous publications (e.g., Johansen 1981, see also Chapter 1). In this study, an average geniculum (0.54 mm^2) was composed of approximately 14,300 cells. The average size of these constitutive cells is quite consistent across genicula, regardless of the size or age of the geniculum; genicular cells are approximately 37.5 μm^2 in cross-section or about 6.5 μm in diameter.

Geniculum cross-sectional area varies greatly (up to an order of magnitude), even within a single *Calliarthron* frond (Chapter 1). Given the uniformity of constitutive cell size, differences in cross-sectional area can be explained by differences in cell numbers. For instance, larger genicula, generally situated near the bases of fronds,

may have five times as many cells as smaller genicula, situated near the frond apices. This suggests that each new geniculum has fewer cells than the one before it, possibly defining an inherent size limit to which *Calliarthron* fronds can grow. Whether any single geniculum can grow by increasing the number of constitutive cells is unknown, but unlikely; cell division is probably difficult, given that the ends of genicular cells are firmly calcified and embedded in adjacent intergenicula, and evidence of such a process would likely be seen in cells of varying size.

Larger genicula are capable of resisting more force than smaller genicula (Chapter 1), mainly because they are composed of more cells. It therefore seems pertinent to describe the breaking strength of a geniculum building block: a single cell. This can be estimated from the regression slopes in Figure 2-5, measured in force (N) per cell. In an old mature geniculum, an average cell can resist 0.0006 N, a seemingly modest strength capable of supporting, for example, a couple grains of rice. Yet when combined with 25,000 other cells to form a geniculum, these cells can support a 2 kg hanging mass.

2.5.3. *Cell wall thickening*

Data clearly suggest that genicular cell walls thicken over time, a surprising result given that cell wall thickening has not been observed in other algal taxa and is generally considered a developmental process associated with terrestrial plant tissues, such as xylem (Niklas 1992, Raven et al. 2003). Nevertheless, older genicula had cell walls up to three times thicker than younger genicula. Because old and young genicular cells are not significantly different in size, new material must be added to the inside of each cell wall, as indicated by the smaller lumens of old genicular cells (Figure 2-3). Cell walls provide structural support to algal cells, and differences in cell wall thickness help explain observed differences in genicular tissue strengths among young and old fronds (Chapter 1). For instance, judging from the differing regression slopes in Figure 2-5, older thick-walled cells may be able to resist 50% more force than young thin-walled cells. Thus, by fortifying their cells with additional

cell wall material, genicula increase their ability to resist breakage. Interestingly, cells from apical genicula in old fronds had significantly thicker cell walls than cells from tenth genicula in young fronds, even though these genicula are assumed to be roughly similar in age. This suggests that cell wall thickening may be more than a simple ontogenetic process and may also depend upon environmental parameters which may differ between basal and apical genicula, such as light interception, nutrient delivery, or drag force experienced by genicula in a given wave climate.

Within any geniculum, peripheral cells have thicker cell walls than central cells, a possible adaptation to resisting bending stresses. Intertidal *Calliarthron* fronds are constantly pulled back and forth by breaking and receding waves, and when genicula bend, the cells furthest from the center and nearest the periphery experience the most stress (see Denny 1988). Thus, by reinforcing these peripheral cells, fronds may resist bending. With few exceptions (e.g., Koehl and Wainwright 1977), most studies of algal biomechanics assume thalli are homogeneous in cross-section and mechanical differences within algal tissues have largely been unexplored. Investigations into the distribution of materials within other macroalgal tissues may improve biomechanical models of algal breakage, especially those that consider complex loading regimes, such as bending.

2.5.4. *Cell wall material strength*

Because genicular tissue is rather homogenous with uniform cells packed tightly together, we can assume that applied forces are resisted directly by the cell walls of constitutive cells. This provides a unique opportunity to estimate the strength of geniculum cell wall – the true "material" strength of genicula – by adjusting the published tissue strengths of genicula by the percent cell wall, essentially factoring out the cell lumens which presumably contribute little to tissue strength.

This novel approach to estimating mechanical strength at the sub-cellular level has provided insight into tissue biomechanics. First, young cell wall material is stronger

than old cell wall material (Figure 2-7). This difference implies that the thickening process is more complicated than simply accreting more of the same material in the same way into each cell wall. One explanation is that cell walls weaken over time as new material is added to wall interiors. Another hypothesis is that wall thickening is a two-fold process resulting in two distinct cell wall layers. Cell wall layers may be chemically similar but laid down differently, as microfibril orientation can differ among primary and secondary cell walls in terrestrial plants (Niklas 1992). Primary cell wall material is likely accreted as genicular cells elongate, suggesting that cell wall microfibrils might be oriented longitudinally and therefore ideal for resisting tensile stresses, whereas secondary cell wall material is added after genicular cells cease elongating, suggesting that secondary microfibrils might be oriented more radially, making them less effective in resisting tension. Alternatively, secondary cell wall material could be accreted in the same orientation, but might be composed of a mechanically weaker substance – at least when stressed in tension. Distinct layers have been documented within primary walls of genicula (Borowitzka and Vesk 1979), but the development of true secondary cell walls has never been described in marine algae, yet would be consistent with the findings of Yendo (1904). Descriptions of the ultra-structure and chemical composition of genicular cell walls can be found in Chapters 5 and 6.

Data summarized in Chapter 1 demonstrate that *Calliarthron* genicular tissue is stronger than other algal tissues. But is genicular tissue really made of uniquely strong materials? Cell walls in a mature *Calliarthron* geniculum have a breaking strength of 47.8 MN m^{-2} (Figure 2-7). This study is the first to report the strength of cell wall, independent of overall tissue strength, from a wave-swept macroalga. Interestingly, cell walls in the filamentous freshwater green alga *Chara corallina* have a breaking strength of 47.0 MN m^{-2} (Toole et al. 2001), remarkably similar to *Calliarthron* cell wall strength, considering *Calliarthron* likely experiences significantly more hydrodynamic stress in the wave-swept intertidal zone. This comparison suggests that genicula probably gain their great strength from packing their cross-section full of cell wall (up to 50%), and not from using especially strong materials in their construction.

This comparison also suggests that much of the variation in macroalgal tissue strength (e.g., Figure 2-1) may be explained by tissue construction, rather than by material composition. Further exploration into other macroalgal tissues is needed to resolve these patterns.

2.5.5. *Kelp versus coralline*

That red macroalgae have more slender thalli than brown macroalgae (Figure 2-1) may not be surprising, as brown macroalgae are often larger than red macroalgae in every dimension. However, size differences cannot explain the apparent pattern in tissue breaking stress across this wide range of algal taxa. Such a pattern clearly suggests a trade-off between growing thicker thalli and developing stronger tissues (e.g., we have not identified macroalgae with both thick thalli and strong tissues). Kelps, although generally composed of weak tissues, can grow large in cross-section to increase their mechanical ability, while *Calliarthron* genicula are probably incapable of growing in girth but have relatively strong tissues.

These two strengthening strategies are not entirely mutually exclusive. For example, the feather boa kelp, *Egregia menziesii*, develops stronger tissues when experimentally grown in high flow conditions (Kraemer and Chapman 1991), although the ultimate breaking strength they report (2.5 MN m^{-2}) was still not very strong: only half that reported for *Egregia* in Figure 2-1. Likewise, although red algae lack true secondary meristems, they are still generally capable of increasing their girth, albeit less so than kelps. Future tests of the trade-off between girth and tissue strength will undoubtedly prove informative. Do small wave-swept brown algae, such as *Petalonia* or *Scytosiphon*, have strong tissues like small red algae? Can differences in tissue strengths be universally explained by differing tissue construction rather than by differing material composition? That is, are the strengths of all macroalgal cell walls comparable?

The growth strategies of kelps and corallines both increase mechanical strength, but differ widely in their scope. For instance, kelps grow outward in girth by adding new cells at the stipe surface, a process limited only by an ability to support underlying medullary tissue. Conversely, *Calliarthron* genicula grow inward by thickening their cell walls, a process limited by space, as the cells slowly compress their organelles and cytoplasm. Thus, in general, the brown algal strategy of growing in girth conveys a much greater potential for resisting drag forces. Perhaps as a consequence, kelps and other brown macroalgae can successfully produce the largest fronds in the wave-swept intertidal zone, while *Calliarthron* and most red algal fronds must remain relatively small.

TO BEND A CORALLINE:
EFFECT OF GENICULAR MORPHOLOGY ON FROND FLEXIBILITY
AND STRESS AMPLIFICATION

3.1. Abstract

Previous studies have demonstrated that fleshy seaweeds resist wave-induced forces in part by being flexible. Flexibility allows fronds to "go with the flow," reconfiguring into streamlined shapes and reducing frond area projected into flow. Unlike fleshy algae, articulated coralline algae have discrete joints (genicula) that lend flexibility to otherwise rigid calcified fronds. In this chapter, I describe the geometry of *Calliarthron* genicula and demonstrate how segmentation affects the bending performance of articulated fronds and amplifies bending stresses within genicula. A numerical model successfully predicted the deflection of articulated fronds, assuming genicula to be assemblages of cables connecting adjacent calcified segments (intergenicula). By varying the dimensions of genicula numerically, I explore the effects of genicular morphology on frond flexibility and stress amplification and predict the optimal genicular morphology to maximize flexibility while minimizing stress amplification. Morphological dimensions of genicula most prone to bending stresses (i.e., genicula near the base of fronds) match model predictions.

3.2. Introduction

Researchers have long studied morphological adaptations that allow intertidal macroalgae to survive the hydrodynamic forces imposed by breaking waves (e.g., Delf 1932, Koehl 1986, Carrington 1990, Dudgeon and Johnson 1992, Friedland and Denny 1995, Blanchette 1997, Gaylord 1997, Bell 1999, Denny and Gaylord 2002, Boller and Carrington 2006, Harder et al. 2006). Despite a staggering range of morphological diversity, one common theme has emerged: flexibility. By being flexible, macroalgae "go with the flow," limiting drag forces by reducing the thallus area projected into rapid flow, reconfiguring into more streamlined shapes, and

bending over into slower moving water (Koehl 1986, Gaylord and Denny 1997, Denny and Gaylord 2002, Boller and Carrington 2006). For these reasons, flexibility is considered a "pre-requisite for survival" (Harder et al. 2004).

Unfortunately, because fleshy macroalgae likely evolved from soft-bodied ancestors, adaptive hypotheses are difficult to argue, since flexibility may be a matter of default, rather than of design. In contrast, coralline algae (Corallinales, Rhodophyta) are firmly calcified and have a fossil record that extends back hundreds of millions of years (Johnson 1961, Wray 1977, Steneck 1983). According to the fossil record, about 100 million years ago, coralline algae evolved articulations, called genicula, that gave flexibility to calcified fronds (Johnson 1961, Wray 1977, Steneck 1983). This evolutionary innovation allowed coralline algae to grow away from the substratum and produce elaborate articulated fronds in hydrodynamically stressful conditions. Thus, for coralline algae, the transition from inflexible to flexible thalli is clear. And articulated coralline algae have been ecologically successful: for example, the coralline *Calliarthron* often dominates wave-exposed low-intertidal habitats along the California coast.

Despite the ecological and mechanical success of articulated coralline algae, the mechanics of articulated fronds are poorly understood. In general, while fleshy algae are completely flexible along the length of their thalli, the flexibility of articulated coralline algae is limited to discrete positions along otherwise rigid thalli. The effect of this unique segmented morphology on bending performance and stress amplification in genicula is an open question.

Genicula in the articulated coralline *Calliarthron* are composed of thousands of elongated cells (see Chapter 2). The distal ends of each flexible genicular cell remain firmly calcified and embedded in adjacent intergenicula, thus effectively tethering intergenicula together like thousands of tiny cables. Moreover, unlike cells in most plant tissues, genicular cells are only loosely connected to one another. Genicular cells fray and separate as genicula break (*pers. obs.*), possibly due to weak middle

lamella between cells (see images in Chapters 5 and 6). These qualities suggest that *Calliarthron* genicula may be most appropriately modeled as a group of straight cables, capable of sliding past one another with minimal sheer resistance.

In this study, I describe the geometry of bending genicula, composed of cable-like genicular cells, and a computational model that utilizes geniculum geometry and bending moments to predict deflections of articulated fronds. By varying genicular dimensions, I test the effect of articulated frond morphology on flexibility and geniculum stress amplification. I predict the ideal genicular dimensions to maximize flexibility (thereby reducing drag force) while minimizing stress (thereby reducing risk of breakage) and I test whether genicula most prone to bending stresses (i.e., those nearest frond bases) adhere to my predictions.

3.3. Materials & Methods

3.3.1. *Geniculum geometry*

The morphology of *Calliarthron* genicula can be described by several dimensions, depicted in Figure 3-1. Genicula have initial length ω and are separated by one another by calcified intergenicula of length L. Transitions from genicula to intergenicula are obscured from view (depicted by stripes in Figure 3-1A) by intergenicular lips x. Genicula are generally elliptical with major radii r_1 and minor radii r_2 (Figure 3-1B). Because flexural stiffness of elliptical genicula is proportional to the cube of the bending radius (Denny 1988), genicula are more flexible when bent parallel to the shorter minor radius. We assume genicula always bend parallel to r_2. Genicula are circumscribed by intergenicula with minor radius y (Figure 3-1B). Genicula and intergenicula are assumed to be concentric.

(A) Long-section (B) Cross-section

Intergeniculum

Geniculum

Intergeniculum
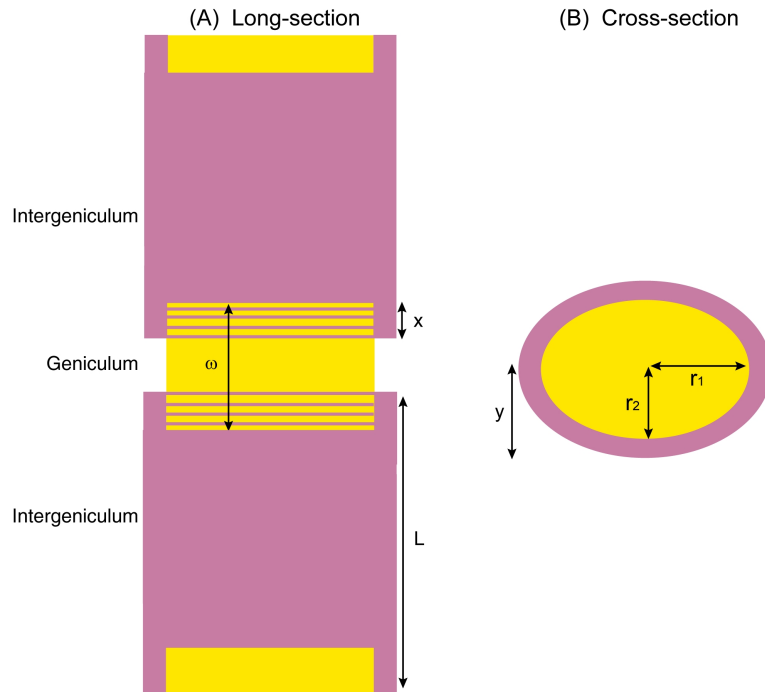
Figure 3-1. (A) Long-section and (B) cross-section diagrams of a bending geniculum.

3.3.2. *External moments*

Breaking waves apply drag force, *F*, in the direction of flow, parallel to the substratum. For an erect articulated frond, this force is perpendicular to frond orientation, and we can calculate bending moment, *M*, as

$$M = F\delta \qquad\qquad 3\text{-}1$$

where δ is the lever arm, the distance from force application to any bending geniculum (Figure 3-2A). As fronds bend, lever arms decrease (Figure 3-2B).   Ultimately, lever arms in a bent thallus are functions of total bending angle at each geniculum. For example, in Figure 3-2,

$$new\ \delta_1 = L_1\cos(\phi_1) + L_2\cos(\phi_1 + \phi_2) + L_3\cos(\phi_1 + \phi_2 + \phi_3) \qquad 3\text{-}2$$
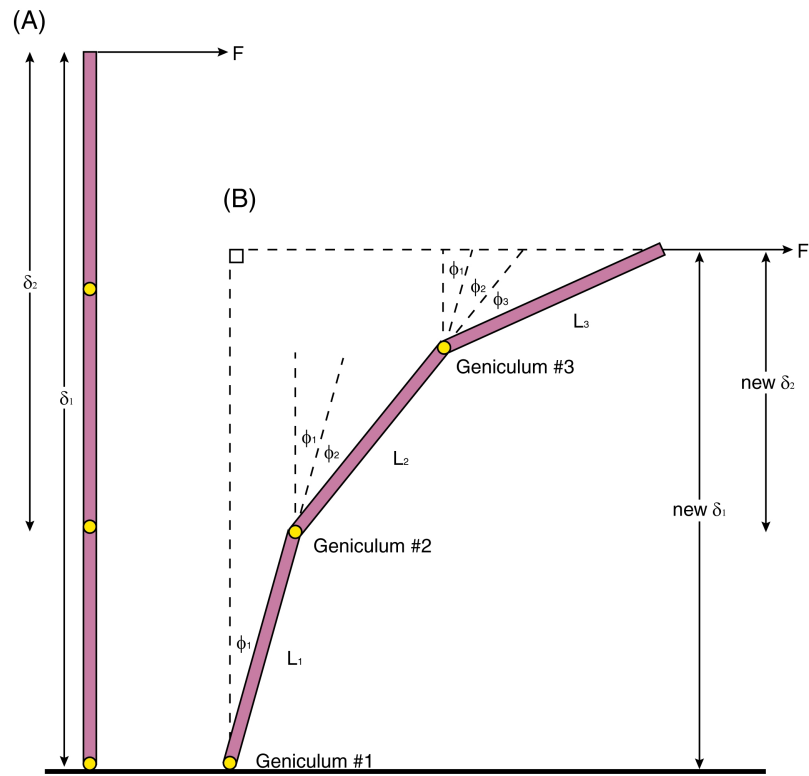
Figure 3-2. Deflection of articulated frond given an applied force, indicating (A) initial and (B) final positions. For clarity, only three segments are illustrated here.

Bending force acting around each geniculum depends upon bending angle (Figure 3-3), such that

$$F_{bending} = F \cos\left(\frac{\phi_{total}}{2}\right)$$ 3-3

so the external bending moment resisted by any geniculum is

$$M = F \cos\left(\frac{\phi_{total}}{2}\right)\delta$$ 3-4
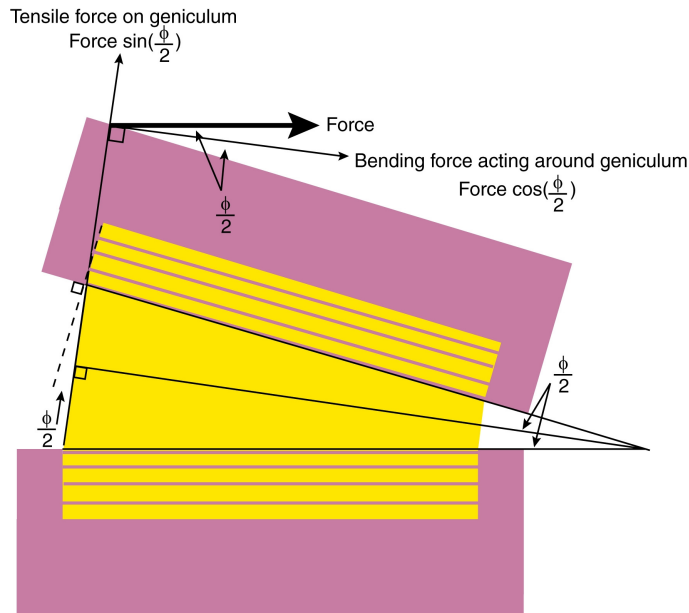
Figure 3-3. Tensile and bending components of force acting on genicula depend upon bending angle (φ).

This study focuses on the first ten genicula, where bending is expected to be greatest. Drag force experienced by *Calliarthron* fronds was simplified as a downstream force applied to the end of the tenth intergeniculum (e.g., Figure 3-2).

3.3.3. *Calculation of internal moments*

At each bending geniculum, external moments are resisted by internal moments within genicular tissue. By setting external and internal moments equal to one another, we can calculate the angle, ϕ, to which genicula must bend to attain equilibrium. As with external moments, internal moments are the products of forces and lever arms. In this case, lever arm is the distance, z, between some elemental strip of area within the geniculum and the neutral axis. The neutral axis is the position in the genicular tissue some perpendicular distance, η, away from the geniculum midline which remains unstrained during bending.

The total internal moment M resisted by any geniculum is the sum of elemental moments:

$$M = \int dM = \int z dF \qquad\qquad 3\text{-}5$$

Given the definition of tissue stress σ,

$$\sigma \equiv \frac{F}{A} \qquad F = \sigma A \qquad\qquad 3\text{-}6$$

where A is genicular cross-sectional area, M can be expressed by substituting for F:

$$M = \int z\sigma dA \qquad\qquad 3\text{-}7$$

Given that tissue stiffness E is defined as

$$E \equiv \frac{\sigma}{\varepsilon} \qquad \sigma = E\varepsilon \qquad\qquad 3\text{-}8$$

where ε is tissue strain, we can substitute for σ to yield

$$M = \int zE\varepsilon dA \qquad\qquad 3\text{-}9$$
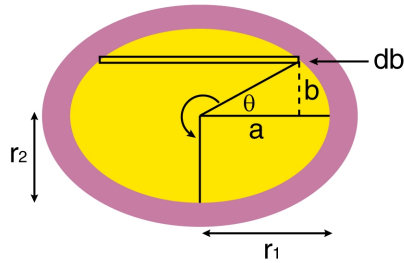
Figure 3-4. Calculating polar
coordinates of elliptical geniculum.

Using elliptical polar coordinates, we can describe positions within genicular cross-sections by

$$a = r_1 \cos\theta$$
$$b = r_2 \sin\theta \qquad\qquad 3\text{-}10$$

where θ is the angle around the geniculum center (see Figure 3-4).

Taking the derivative of the y-coordinate,

$$db = r_2 \cos\theta d\theta \qquad\qquad 3\text{-}11$$

The area of any elemental rectangular portion of ellipse is

$$dA = (2a)db$$
$$= 2r_1r_2 \cos^2 \theta d\theta$$

3-12

Substituting for Eqn 3-9, total internal moment can be expressed as

$$M = \int_{-\pi/2}^{\pi/2} zE\varepsilon \, 2r_1r_2 \cos^2 \theta d\theta$$

3-13

At this point, we use this equation in two distinct ways to separate the two sequential modes of geniculum bending that occur before and after adjacent intergenicula make contact.

3.3.3.ii Moments before intergenicula make contact

Before adjacent intergenicula touch, genicula experience pure bending (Figure 3-5), such that all tissue beyond the neutral axis, η, is stretched via tension, while all tissue inside the neutral axis is squeezed via compression. By definition, tissue along the neutral axis does not change length. The position of the neutral axis depends upon tensile and compressive moduli, such that tensile and compressive halves of genicula are balanced and no net force results. For example, when tensile and compressive moduli are equivalent, the neutral axis will pass directly through the center of the tissue. However, tensile and compressive moduli of biological materials are often not equal. Gaylord (1997) demonstrated that for several kelp tissues,

$$E_t \approx 4E_c$$

3-14

Here this conclusion is applied to genicular tissue. Tensile moduli are measured experimentally (see 3.3.6), and compressive moduli are then assumed to be 4-times lower. The result is an off-center neutral axis, shifted toward the tensile side of genicula (see Figure 3-5).

(A)

(B)
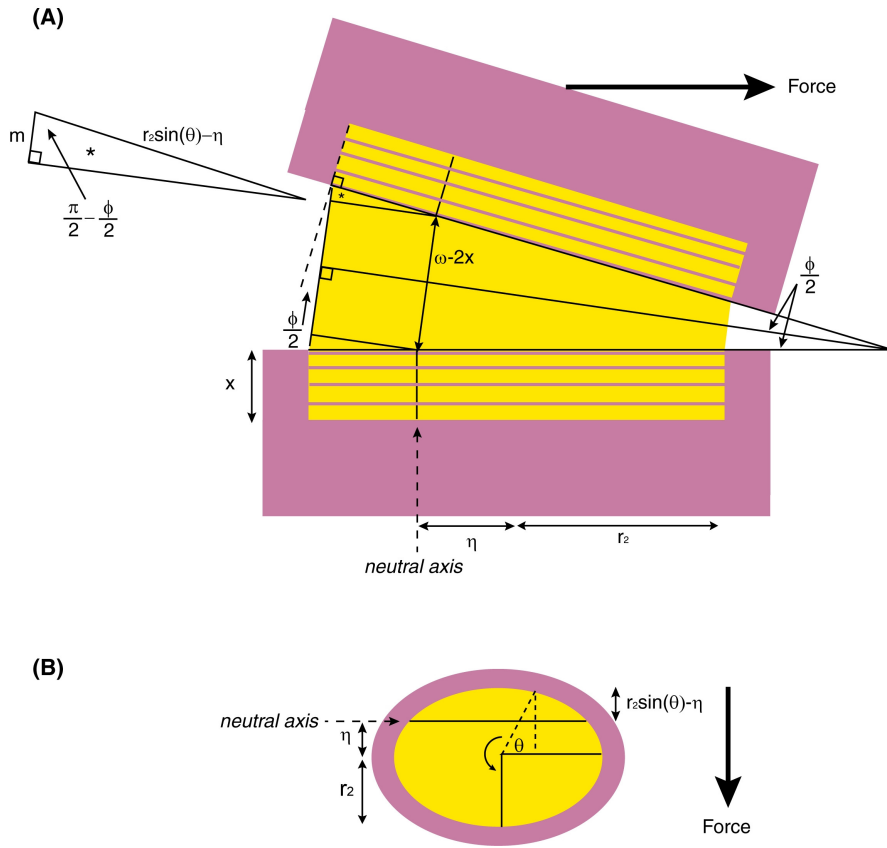
Figure 3-5. Diagram of bending geniculum before intergenicula make contact.

Using E_t and E_c, we can calculate the exact location of the neutral axis by iteratively solving for η in the following equation, derived in Appendix 7 of (Gaylord, 1997):

$$\left(E_t - E_c\right)\left(\frac{(r_2^2 - \eta^2)^{\frac{3}{2}}}{3} + \frac{\eta r_2^2}{2}\arcsin\left(\frac{\eta}{r_2}\right) + \frac{\eta^2}{2}\sqrt{r_2^2 - \eta^2}\right) - \left(E_t + E_c\right)\frac{\eta r_2^2 \pi}{4} = 0 \qquad \text{3-15}$$

The distance away from the neutral axis for any elemental area of geniculum is

$$z = r_2 \sin\theta - \eta \qquad \text{3-16}$$

(see Figure 3-5B).

Tissue strain, ε, can be calculated from the change in tissue length between intergenicula

$$\varepsilon_{pre-contact} = \frac{\omega - 2x + 2m}{\omega - 2x} - 1$$

$$= \frac{2m}{\omega - 2x}$$

3-17

where m is additional length defined by the triangle in Figure 3-5A, such that

$$\cos\left(\frac{\pi}{2} - \frac{\phi}{2}\right) = \frac{m}{r_2 \sin\theta - \eta}$$

3-18

$$m = (r_2 \sin\theta - \eta)\cos\left(\frac{\pi}{2} - \frac{\phi}{2}\right)$$

3-19

Substituting for m in Eqn 3-17 yields

$$\varepsilon_{pre-contact} = \frac{2(r_2 \sin\theta - \eta)\cos\left(\dfrac{\pi}{2} - \dfrac{\phi}{2}\right)}{\omega - 2x}$$

3-20

And finally substituting for Eqn. 3-13, we get an expression describing the internal moment resisted by genicula bent to angle ϕ before intergenicula make contact:

$$M = \int_{-\pi/2}^{\pi/2} (r_2 \sin\theta - \eta)E\left(\frac{2(r_2 \sin\theta - \eta)\cos\left(\dfrac{\pi}{2} - \dfrac{\phi}{2}\right)}{\omega - 2x}\right)2r_1 r_2 \cos^2\theta d\theta$$

3-21

3.3.3.iii Intergeniculum contact angle

When intergenicula first make contact, we can define a contact angle ($\phi=2\beta$), described by a triangle that extends from the point of intergeniculum contact to the neutral axis (Figure 3-6), such that

$$\sin\beta = \frac{\left(\dfrac{\omega - 2x}{2}\right)}{y + \eta}$$

3-22

and

$$\beta = \arcsin\left(\frac{\omega - 2x}{2(y + \eta)}\right) \qquad\qquad 3\text{-}23$$

(A)

(B)
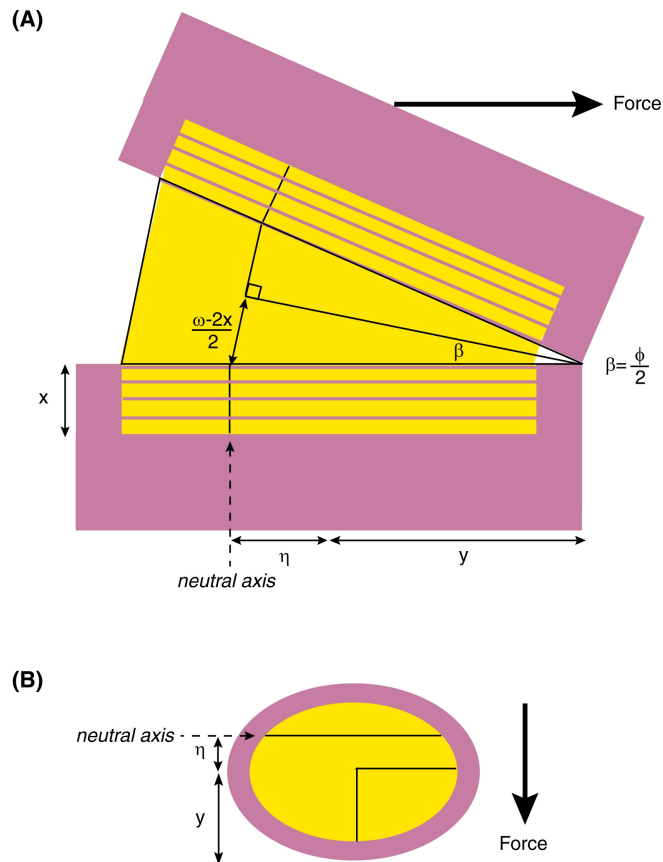
Figure 3-6. Diagram of bending geniculum precisely when intergenicula make contact. Contact angle (2β) can be calculated from genicular dimensions.

3.3.3.iv Moments after intergenicula make contact

When intergenicula touch, the neutral axis – the axis around which a geniculum rotates – abruptly shifts to the point of contact and the entire geniculum begins to stretch in tension (Figure 3-7). Compressed genicular tissue begins to expand and stretched tissue extends even more.

(A)

(B)
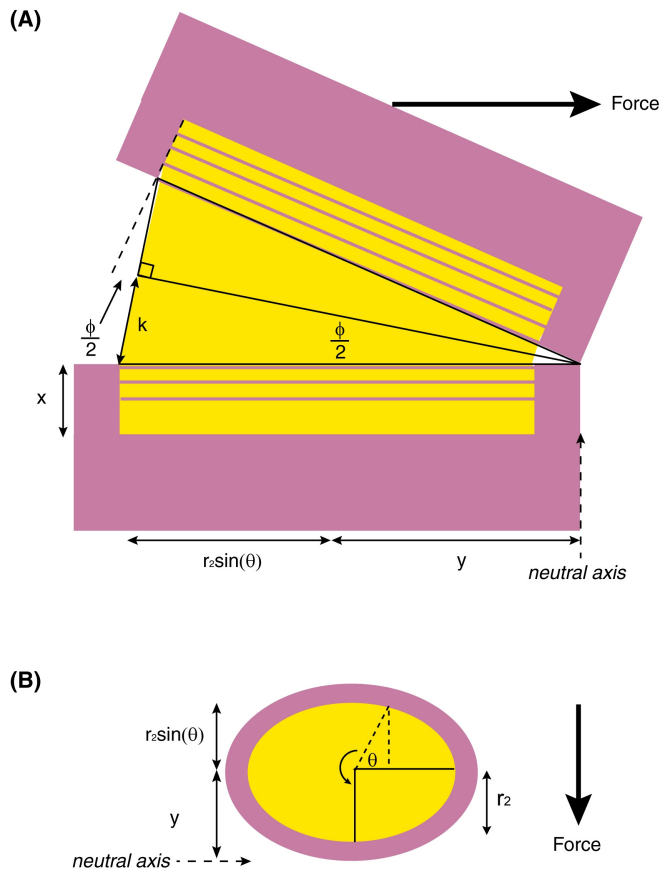
Figure 3-7. Diagram of bending geniculum after intergenicula make contact.

After contact, the distance away from the neutral axis for any elemental area of geniculum becomes the sum of the intergenicular radius y and the polar coordinate b:

$$z = y + b = y + r_2 \sin \theta \qquad \text{3-24}$$

Again, tissue strain (ε) can be calculated as the change in length of genicular tissue between intergenicula (see Figure 3-7)

$$\varepsilon_{post-contact} = \frac{2k}{\omega - 2x} - 1 \qquad \text{3-25}$$

where k is half the new length of genicular tissue defined by the triangle depicted in Figure 3-7, such that

$$\sin\left(\frac{\phi}{2}\right) = \frac{k}{y + r_2 \sin\theta} \qquad \text{3-26}$$

$$k = (y + r_2 \sin\theta)\sin\left(\frac{\phi}{2}\right) \qquad \text{3-27}$$

Substituting for k in Eqn 3-25 yields

$$\varepsilon_{post-contact} = \frac{2(y + r_2 \sin\theta)\sin\left(\dfrac{\phi}{2}\right)}{\omega - 2x} - 1 \qquad \text{3-28}$$

To account for tissue strain before intergenicula made contact ($\phi \le 2\beta$), we combine Eqns 3-20 and 3-28 as follows

$$\varepsilon_{total} = \varepsilon_{pre-contact} + \varepsilon_{post-contact}$$

$$= \frac{2(r_2 \sin\theta - \eta)\cos\left(\dfrac{\pi}{2} - \beta\right)}{\omega - 2x} + \frac{2(y + r_2 \sin\theta)\sin\left(\dfrac{\phi}{2} - \beta\right)}{\omega - 2x} - 1 \qquad \text{3-29}$$

$$= \frac{2(r_2 \sin\theta - \eta)\cos\left(\dfrac{\pi}{2} - \beta\right) + 2(y + r_2 \sin\theta)\sin\left(\dfrac{\phi}{2} - \beta\right)}{\omega - 2x} - 1$$

Finally substituting for Eqn. 3-13, we get an expression describing the internal moment resisted by genicula bent to angle ϕ after intergenicula made contact:

$$M = \int_{-\pi/2}^{\pi/2} (y + r_2 \sin\theta)E$$

$$\cdot \left(\frac{2(r_2 \sin\theta - \eta)\cos\left(\dfrac{\pi}{2} - \beta\right) + 2(y + r_2 \sin\theta)\sin\left(\dfrac{\phi}{2} - \beta\right)}{\omega - 2x} - 1 \right) 2r_1 r_2 \cos^2\theta d\theta \qquad \text{3-30}$$

3.3.4. *Implementation of geometry in MATLAB*

The above geometry was incorporated into a MATLAB routine (see Appendix 1) in order to predict the deflection of articulated fronds by applied forces. In practice, genicular dimensions for ten genicula and an applied force were read into the model.

Bending angles (2β) at which intergenicula make contact were calculated. Moments required to bend genicula before and after intergenicular contact were calculated by iteratively solving Eqns 3-21 and 3-30, respectively, for three distinct values of ϕ (0.4, 0.8, 1.0), using $E=E_c$ for negative strains and $E=E_t$ for positive strains. Linear regressions were fitted to the two sets of three (M, ϕ) datapoints and were used to quickly calculate ϕ for genicula given applied moments.

The model initially applied a small fraction (1/100th) of the total force at the frond apex and calculated external moments at all genicula (Eqn 3-4, Figure 3-2). Moments were used to calculate bending angles at all genicula, using the linear regression described above, assuming intergenicula had not yet made contact. Lever arms were re-calculated, given the bending angles (Eqns 3-2), force was incremented, and external moments were re-calculated at all genicula (Eqn 3-4). Moments were used to calculate new bending angles, using "after contact" linear regressions if previous angles exceeded 2β. Bending angles and incremented force were used to re-calculate lever arms and external moments, and new angles were calculated using moment regressions. This process was repeated until maximum force was applied. The model predicted frond deflections, based on final bending angles.

3.3.5. *Maximum stress in first geniculum*

The model computed maximum stress (that is, stress in the outermost tissue, $\theta = \pi/2$) in the first geniculum bent to ϕ_1. In general, total stress was calculated as the sum of stresses caused by bending components (Eqn 3-8) and tensile components (tensile force, Figure 3-3, per area of elliptical geniculum):

$$\sigma_{total} = \sigma_{bending} + \sigma_{tension}$$

$$= E_t \varepsilon + \frac{F \sin\left(\dfrac{\phi_1}{2}\right)}{\pi \, r_1 \, r_2} \qquad \text{3-31}$$

For $\phi_1 \le 2\beta$, Eqn 3-31 was solved using strain before intergenicula make contact (Eqn 3-20):

$$\sigma_{max} = E_t \left(\frac{2(r_2 - \eta)\cos\left(\frac{\pi}{2} - \frac{\phi_1}{2}\right)}{\omega - 2x} \right) + \frac{F \sin\left(\frac{\phi_1}{2}\right)}{\pi r_1 r_2} \qquad \text{3-32}$$

For $\phi_1 > 2\beta$, Eqn 3-31 was solved using strain after intergenicula make contact (Eqn 3-29):

$$\sigma_{max} = E_t \left(\frac{2(r_2 - \eta)\cos\left(\frac{\pi}{2} - \beta\right) + 2(y + r_2)\sin\left(\frac{\phi_1}{2} - \beta\right)}{\omega - 2x} - 1 \right) + \frac{F \sin\left(\frac{\phi_1}{2}\right)}{\pi r_1 r_2} \qquad \text{3-33}$$

3.3.6. *Measuring tensile modulus (E_t)*

Fifteen *Calliarthron* fronds were subjected to mechanical testing to determine the tensile modulus (E_t) of genicular tissue. Large fronds were collected from the low-intertidal zone in a moderately wave-exposed surge channel at Hopkins Marine Station in Pacific Grove, CA. The field site was identical to that described in Chapter 1. In each trial (N=15), a frond was secured between two grips of a custom tensometer (also described in Chapter 1), allowing several intergenicula and genicula to "float" between the grips. Two piezoelectric crystals were super-glued to intergenicula adjacent to a single geniculum. Crystals were connected to a sonomicrometer (TRX series 4, Sonometrics Corporation, Ontario, Canada). A saltwater bath was raised up to completely immerse all genicula and to ensure clear sonic contact between crystals. When the tensometer was engaged, the grips pulled the frond apart at 1 mm/s and the crystals measured geniculum strain at 175 Hz. Extension was stopped before fronds broke. Stretched genicula were cross-sectioned after they were removed from the grips, and elliptical cross-sectional areas were calculated by measuring diameters using an ocular dial-micrometer. Neighboring genicula were decalcified in 1N HCl,

long-sectioned, and their lengths measured using the ocular dial-micrometer. Stretched genicula were assumed to be identical in length to neighboring genicula. Nominal stress (F/A) versus engineering strain ($[\omega_{new}/\omega_0] - 1$) was plotted for one geniculum in each frond. Tensile moduli (E_t) were calculated as the slopes of linear stress-strain regressions forced through the origin.

3.3.7. *Testing the bending model*

Ten *Calliarthron* fronds were collected from the field site described above. Branches were removed from each frond by cutting below the first dichotomy, and the remaining straight chains of segments (generally the first 10-20 genicula) were tested as follows. For each trial, fronds were gripped by the first few genicula in clamps and held horizontal. Note the first 3-5 genicula in each test frond were hidden within the clamps and were not tested here. A thread lasso was tied around the eleventh geniculum counted from the clamp (just distal to the tenth intergeniculum), from which 5g, 20g, and 100g masses were hung. These masses applied known forces (0.05 N, 0.20 N, 0.98 N, respectively) and generated a wide range of frond deflections. Digital photos were taken of each deflection, and genicular positions were obtained using an image analysis routine (ImageJ, NIH).

After each trial, genicular dimensions were measured for all ten genicula bent in each frond. First, intergenicular lengths (L) and gaps between intergenicula (ω-$2x$) were measured using an ocular dial-micrometer. Genicula were cross-sectioned and intergenicular radii (y) and genicular radii (r_1, r_2) were measured directly. Because cross-sectioned genicula could not also be long-sectioned, the lengths (ω) of 2-3 genicula outside the chain of ten segments were measured after being decalcified and long-sectioned. Mean ω was assumed for all ten genicula. Intergenicular lip length (x) was estimated for each geniculum as half the difference between gap length and mean ω. Within-frond variance in ω and x was estimated in a separate analysis by decalcifying and long sectioning all ten genicula in six fronds. Both ω (one-way ANOVA, $p < 0.001$) and x (one-way ANOVA, $p < 0.001$) varied significantly among

fronds, but variances were not significantly different (O'Brien test p = 0.08 and p = 0.44, respectively). Mean 95% C.I. for ω (0.03 mm) and for x (0.02 mm) were assumed for estimates of mean ω and x for each test fronds.

Genicular dimensions for each frond were input into the MATLAB bending model to obtain bending predictions. Variation within genicular dimensions and moduli was incorporated by calculating stiff predictions (using ω – 95% C.I., x + 95% C.I., E_t + 95% CI) and flexible predictions (using ω + 95% C.I., x – 95% C.I., E_t – 95% C.I.) for genicula in each trial. Mean model range was calculated as half the difference between angles predicted at first genicula generated by stiff and flexible model inputs. Model accuracy was analyzed qualitatively by graphing real and model deflections together and quantitatively by comparing real and predicted angles at first genicula.

3.3.8. *Effect of genicular characteristics on stress and flexibility*

We first used the computational model to determine the effects of genicular dimensions on frond flexibility and stress. Mean values for genicular dimensions were calculated from all *Calliarthron* genicula bent in the ten trials (N=100) and assumed constant along a virtual "average" frond. Data for the "average" frond were entered in the bending model and tested at $F = 0.2$ N. Holding all other dimensions constant, each dimension was allowed to vary independently, and the resulting frond deflections were recorded. When intergeniculum length was varied, the number of intergenicula was adjusted to hold overall frond length constant (e.g., half as many intergenicula, twice as long as the mean). In one trial, genicular dimensions were all held constant but tensile modulus was allowed to vary. Flexibility and stress were quantified in each trial by calculating, respectively, the deflection angle of entire fronds (arctan of x-coordinate / y-coordinate of frond tip) and maximum stress at first genicula. Percent change (from average) of stress and flexibility were plotted against percent change (from average) in genicular dimensions. Log-transformed ratio of percent change flexibility to percent change stress was plotted against percent change of each geniculum dimension. Linear regressions were fitted to these data, and the slopes of

these lines were used to predict the changes in genicular dimensions that would increase flexibility and decrease stress.

Next, predictions derived from the computational model about genicular dimensions optimized for bending were evaluated. Genicula that experience the most bending (i.e., genicula #1 and #2) and genicula that experience little bending and mostly tension (i.e., genicula #11 and #12) were compared in ten *Calliarthron* fronds. Dimensions y, r_1, and r_2 were measured in cross-sections of genicula #1 and #11 and dimensions ω, x, and L were measured in decalcified long-sections of genicula #2 and #12 as described above. Paired t-tests were used to compare characteristics of "bending" and "tensile" genicula.

3.4. Results

3.4.1. *Tensile modulus*

Mean tensile modulus of genicular tissue was 45.4 ± 8.5 MN m^{-2} (mean ± 95% C.I.) (see Figure 3-8).

3.4.2. *Bending model*

Articulated frond deflections were generally within the range of model predictions (Figure 3-9). However, at the largest applied force (F = 0.98N), real fronds were often more flexible than the model predicted. This discrepancy was evident in the bending angle of the first geniculum, ϕ_1.
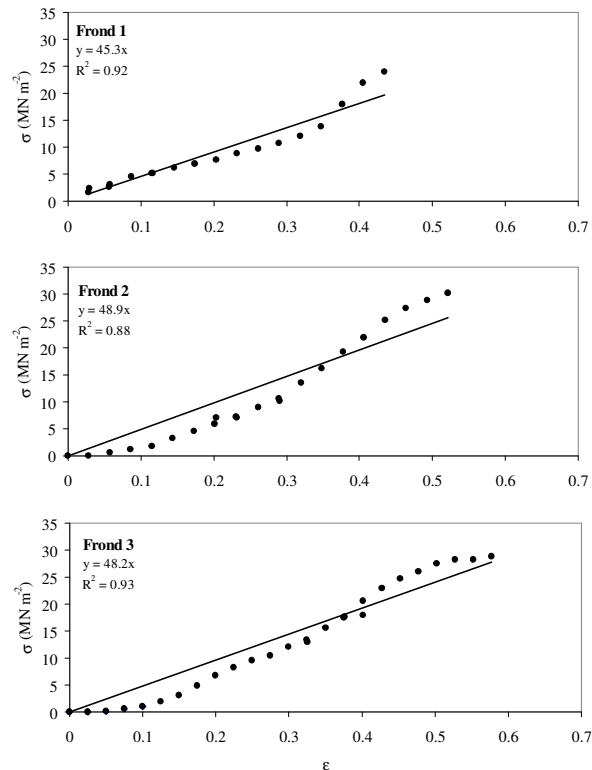
Figure 3-8. Representative stress-strain curves for three genicula. Modulus is the slope of the linear regressions.
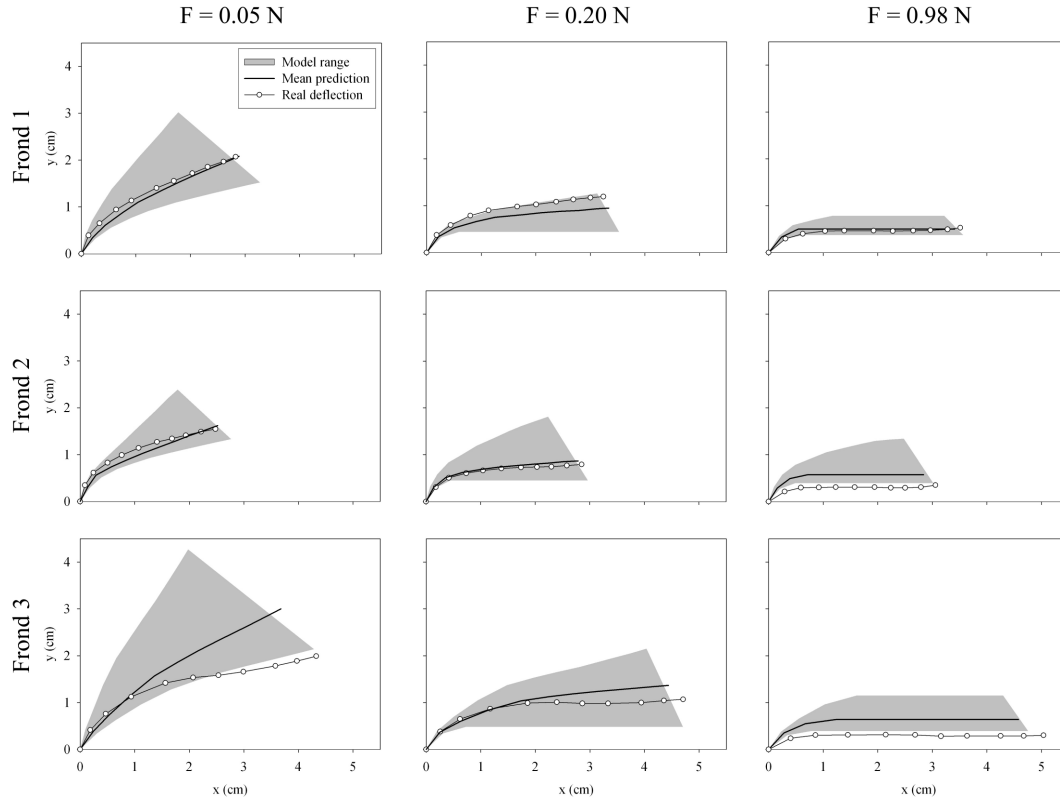
Figure 3-9. Comparison of bending model predictions and real frond deflections for three representative fronds and three applied forces. Model range (gray shaded region) is bounded by stiff and flexible model predictions.

On average, real ϕ_1 was greater than predicted ϕ_1 at all forces (Table 3-1). The difference between real and predicted ϕ_1 was greatest at the largest force, and real ϕ_1 were within the predicted range of ϕ_1 in only 20% of the bending trials (Table 3-1). Nevertheless, the simple computational model predicted ϕ_1 correctly in 60% of trials when F = 0.05N and 70% of trials when F = 0.20N. When ϕ_1 was outside the model range, differences were often slight and many unsuccessful ϕ_1 predictions were still within 5° of model range (Table 3-1).

Table 3-1. Error in predicting bending angle (ϕ_1) at first genicula (N=10).

Force (N)	Mean angle (°)	Mean predicted angle (°)	mean |real - model| (degrees ± 95% C.I.)	mean model range (degrees ± 95% C.I.)	Real angle within model range	Real angle within model range ± 5°
0.05	19.1	16.4	8.8 ± 1.6	7.3 ± 2.9	60%	70%
0.20	28.5	27.4	5.4 ± 2.5	7.3 ± 0.8	70%	90%
0.98	46.0	30.0	16.1 ± 4.9	8.2 ± 1.2	20%	50%

3.4.3. *Effect of genicular characteristics on stress and flexibility*

Average genicular dimensions are listed in Table 3-2. Adjustments to genicular dimensions had varying effects on average frond deflections (Figure 3-10). For example, quadrupling y made fronds stiffer (Figure 3-10E) than quadrupling E_t (Figure 3-10F). Increasing all geniculum dimensions increased frond stiffness, except increasing ω which decreased frond stiffness (Figure 3-10A).

Table 3-2. Mean genicular dimensions
measured in bending model analysis.

Dimension	Mean (mm) $\pm$ 95% C.I.
ω	$0.566 \pm 0.017^*$
x	$0.198 \pm 0.011^*$
y	0.693 ± 0.024
r_1	0.573 ± 0.016
r_2	0.461 ± 0.017
L	3.307 ± 0.162

*Error calculated in separate analysis (see methods)

Adjustments to genicular dimensions had varying effects on flexibility and stress (Figure 3-11). As ω increased, flexibility increased and stress decreased (Figure 3-11A). As r_1, r_2, x, L, and E_t increased, flexibility decreased and stress increased (Figure 3-11B, C, D, F). As y increased, both flexibility and stress decreased (Figure 3-11E).
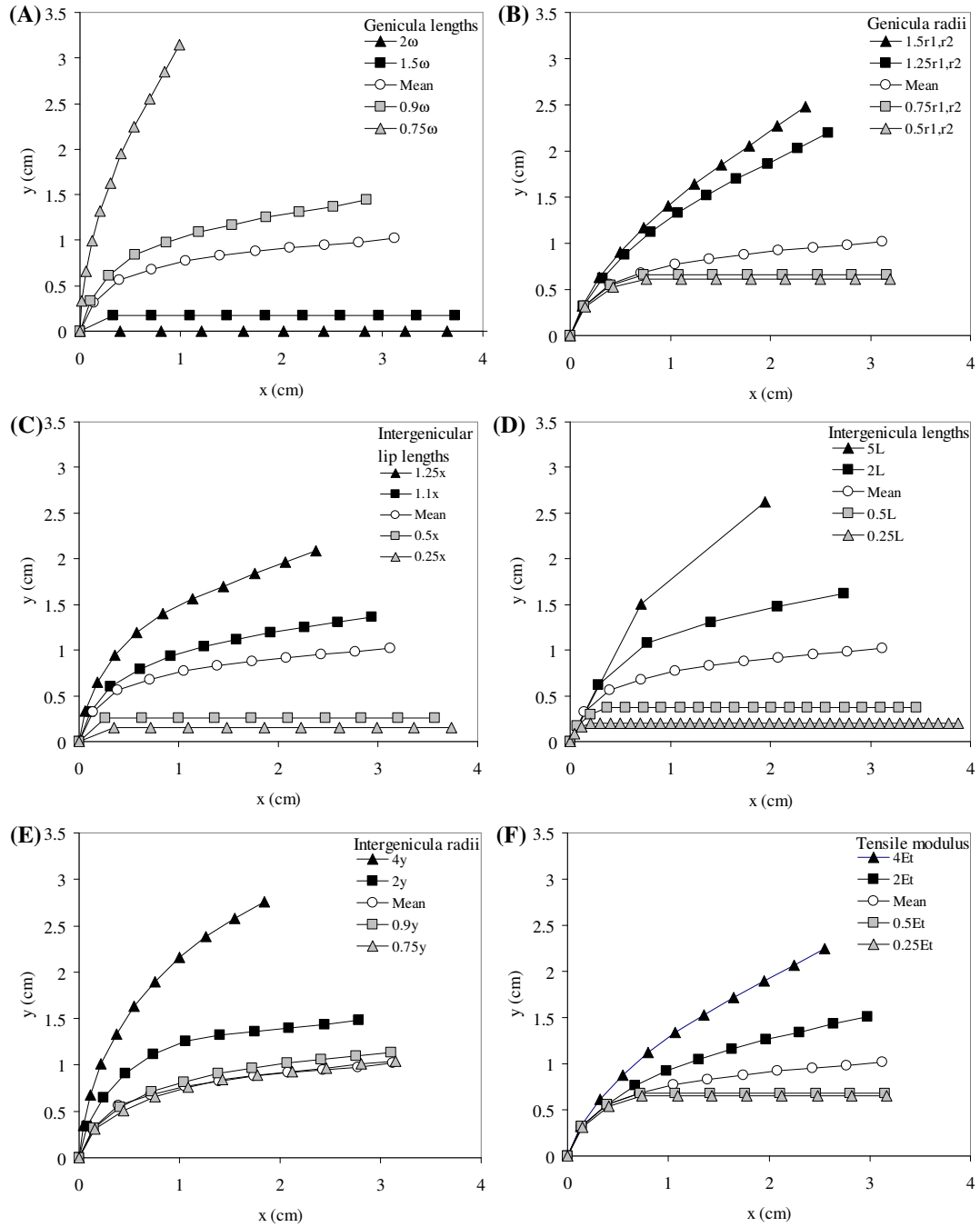
Figure 3-10. Effect of varying genicular dimensions on frond deflection. (A) Geniculum length, ω, (B) geniculum radii, r_1 and r_2, (C) intergeniculum lip length, x, (D) intergeniculum length, L, (E) intergeniculum radius, y, (F) tensile modulus, E_t.
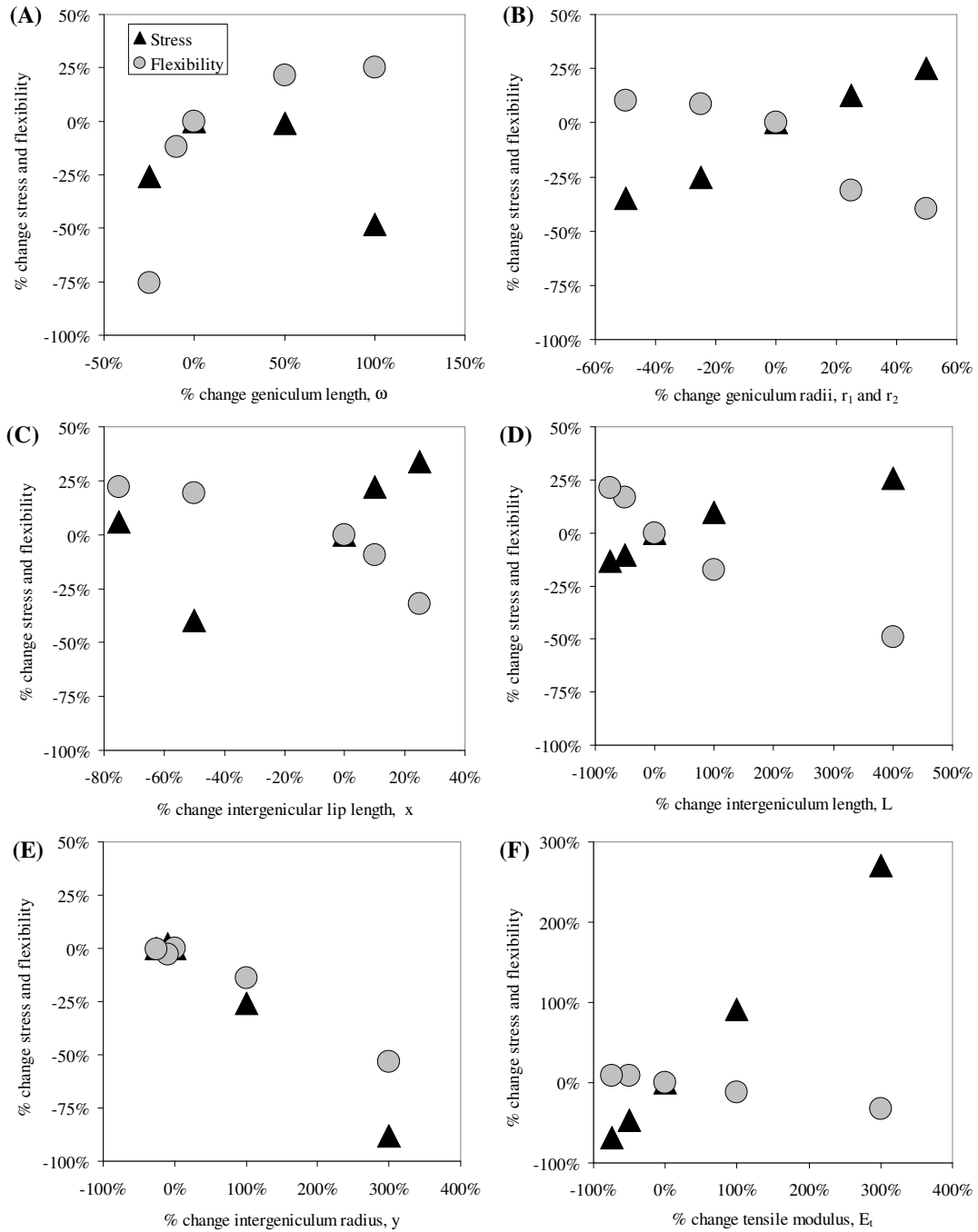
Figure 3-11. Effect of varying genicular dimensions on stress (triangles) and flexibility (circles) in first genicula. X-axes represent percent change in (A) geniculum length, ω, (B) geniculum radii, r_1 and r_2, (C) intergeniculum lip length, x, (D) intergeniculum length, L, (E) intergeniculum radius, y, (F) tensile modulus, E_t. Note that axes differ.

Contrasting effects of genicular dimensions on flexibility and stress were accounted for by analyzing the ratio of flexibility to stress (Figure 3-12). Increasing ω and y and decreasing x, r_1, r_2, E_t, and L all increased the ratio of flexibility to stress (Figure 3-12, Table 3-3).
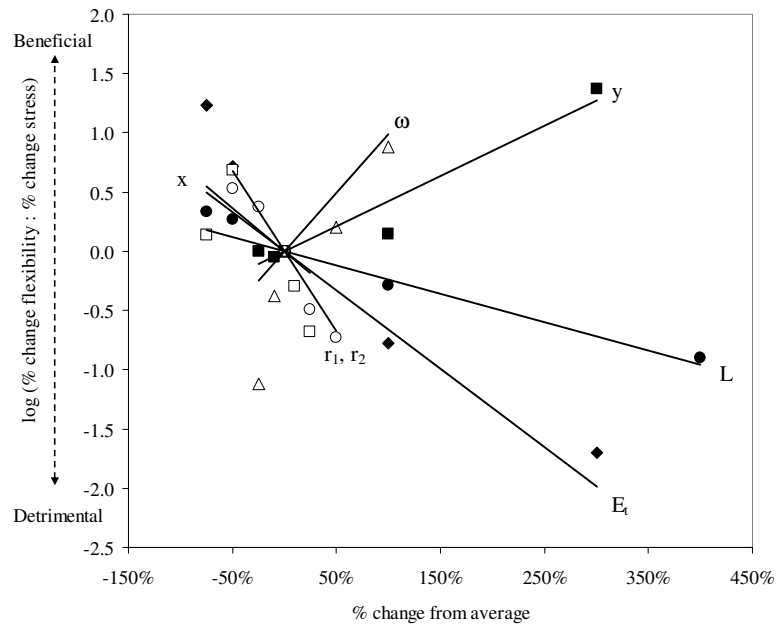
Figure 3-12. Effect of varying genicular dimensions on the ratio of flexibility to stress.

Table 3-3. List of changes to genicular dimensions that increase the ratio of flexibility to stress.

Direction	Dimension	Slope
increase	ω	0.98
decrease	x	-0.73
decrease	r_1, r_2	-1.35
decrease	E_t	-0.66
increase	y	0.42
decrease	L	-0.24

3.4.4. *Differences between "bending" and "tensile" genicula*

Several dimensions differed significantly among bending and tensile genicula (Figure 3-13). As predicted by the flexibility-stress ratio analysis, bending genicula are flanked by significantly shorter intergenicula ($p < 0.001$, Figure 3-13D) and have significantly shorter intergenicular lips ($p < 0.001$, Figure 3-13C) than tensile genicula. Bending genicula also tend to be longer than tensile genicula (Figure 3-13A), although the trend is not significant ($P = 0.08$). Genicular and intergenicular radii were not significantly different among bending and tensile genicula ($p = 0.61$ and $p = 0.15$, respectively).
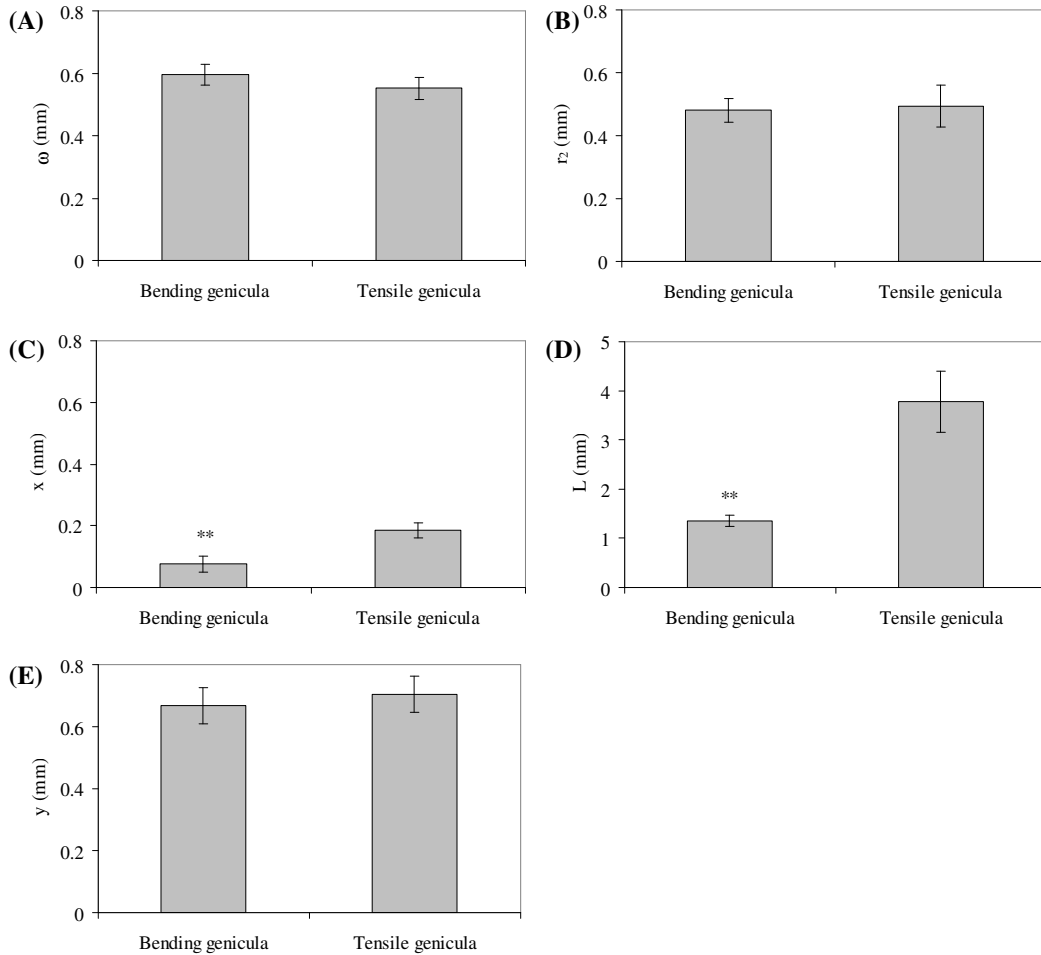
Figure 3-13. Difference in genicular dimensions between bending genicula (e.g., first and second genicula) and tensile genicula (e.g., eleventh and twelfth genicula). Note the different y-axis in part D. * $p = 0.08$, ** $p < 0.001$.

3.5. Discussion

3.5.1. *A simple bending model*

Calliarthron genicula are complex structures. They are composed of cells that are loosely connected to each other, but interact through a middle lamella of unknown composition and with unknown sheer resistance. The cells produce cell walls that vary in composition and structure through time and across individual genicula (see Chapters 2, 5, and 6). Genicula are surrounded by calcified intergenicular lips that may grind down, deform, or break upon contact. Nevertheless, the simple geometric model described here estimates frond deflections with reasonable success and allows for a detailed analysis of articulated frond performance.

Unlike previous numerical models of bending fleshy algae (Gaylord and Denny 1997), the model presented here approximates genicula as assemblages of independent cables. Early attempts to model genicular tissue like other algal tissues in pure bending predicted deflections that were far too stiff. Similarity of real deflections and cable-model predictions suggests that sheer resistance is indeed minimal in genicula, potentially a structural adaptation for increasing flexibility. Surprisingly, real deflections were even more flexible at high forces than the cable-model predicted. This may be a consequence of intergenicula sliding past one another, shifting the point of contact outward, as force increased. This phenomenon is described further in Chapter 4, when force is increased ten-fold and genicula are bent to failure.

Hypothetical adjustments to genicular dimensions affected frond flexibility and tissue stress. Increasing flexibility presumably benefits articulated fronds by decreasing thallus area projected into flow and potentially increasing reconfiguration, thereby decreasing drag. Increasing tissue stress negatively affects algae by increasing the likelihood of breakage. Thus, the ratio of flexibility to stress can be used in a cost-benefit analysis. Adjustments to genicular dimensions that increase the ratio of flexibility to stress can be considered net-benefits for articulated fronds and, potentially, adaptations to drag-induced bending.

3.5.2. *Morphological adaptations to bending articulated fronds*

3.5.2.i Long genicula

According to the computational model, longer genicula reduce tissue stress and make fronds more flexible – two qualities that benefit articulated fronds. Thus, it is reasonable to hypothesize that long genicula are adaptations to bending in articulated fronds. This hypothesis is supported by patterns of genicular development and variation in geniculum length within individual fronds. *Calliarthron* genicula consist of a single tier of cells that elongate as they develop (Johansen 1969a, 1981). Mature genicular cells are nearly 100-times longer than wide (see Chapter 2) and approximately 10-times longer than adjacent calcified cells (Johansen 1969a). Furthermore, genicula near the bases of fronds, called "bending" genicula because they likely experience the most bending, tend to be longer than genicula further up the frond. This hypothetically adaptive growth pattern may be limited, as *Calliarthron* genicular cells lose cytoplasm and organelles as they elongate and may be developmentally incapable of growing any longer.

3.5.2.ii Short intergenicular lips

Similar in effect to lengthening genicula, shortening intergenicular lips theoretically reduces tissue stress and makes fronds more flexible. In reality, the length of calcified intergenicular lips changes dynamically over time. Calcified lips initially form when genicula decalcify, separating adjacent intergenicula. The remaining intergenicular tissue becomes meristematic, recovering from the effects of localized decalcification, and calcified lips grow toward one another. Concurrently, flexible genicula convey a freedom of movement to adjacent intergenicula and calcified lips abrade and grind one another down as fronds bend in the field (Johansen 1981). Thus, the length of intergenicular lips depends upon two antagonistic processes: growth and abrasion. Growth of intergenicular lips is contrary to the adaptive hypothesis described above but may be an unavoidable phase of tissue recovery. Nevertheless, "bending" intergenicular lips are less than half the length of "tensile" intergenicular lips, likely resulting from frequent and persistent abrasion of calcified tissue.

3.5.2.iii Short intergenicula

Shortening intergenicula makes fronds more flexible by increasing the density of joints along articulated fronds. The effect of joint density on stiffness has been documented for other segmented biological beams (e.g., Etnier 2001). As a consequence of greater flexibility, shorter intergenicula reduce the lever arm of applied forces, which lowers the moment and stress in bending genicula. Thus, to minimize stress and maximize flexibility in bending genicula, intergenicula should be as short as possible. This adaptive hypothesis is borne out within individual fronds: "bending" genicula near the base of fronds are separated by intergenicula that are 1/3rd shorter than more distal "tensile" genicula. Unlike intergenicular lip length, intergenicula length is purely biologically-controlled. Shorter intergenicula likely consist of fewer tiers of calcified cells laid down during development. Whether intergeniculum length is a plastic response to wave-induced bending stresses is unknown, but subtidal *Calliarthron* likely experience lower drag forces and may be able to persist with longer intergenicula.

Articulated fronds with infinitely short intergenicula would resemble fleshy algae and would experience none of the disadvantages of segmentation. That intergenicula are not infinitely short suggests that complete decalcification might be disadvantageous. For example, calcification minimizes the impact of herbivores on coralline fronds (Steneck 1986, Padilla 1993). Alternatively, there may be a metabolic cost associated with decalcification. Future analyses will sequentially glue genicula to explore the density of joints that is sufficient to reduce stress, increase flexibility, and increase survival of articulated fronds.

3.5.3. *Inconsistent adaptive hypotheses*

3.5.3.i Slender genicula

According to the computational model, reducing genicula radii increases flexibility and decreases the maximum stress in genicula. Thinner genicula make fronds more flexible because reducing geniculum radii decreases distances to neutral axes and

increases bending angles (see Eqn 3-26). For identical reasons, thinner genicula also reduce the maximum stress in outer genicular tissue. However, slender genicula resist less force because they have less tissue. Thus, in addition to increasing flexibility, reducing genicula radii also increases risk of breakage. Interestingly, as articulated fronds bend back and forth in the field, genicular cells fray at the periphery of bending genicula. This phenomenon effectively decreases geniculum radii and increases frond flexibility but also likely makes fronds more prone to breakage. Future analyses should examine the total stress in genicula to clarify this trade-off.

3.5.3.ii Broad intergenicula

According to the model, increasing intergeniculum radius decreases flexibility and maximum stress in genicula. Broad intergenicula make fronds less flexible by increasing the distance to the neutral axis, thereby decreasing bending angles (see Eqn 3-26). In theory, decreased bending angles reduce stress and strain in genicular tissue (Eqns 3-29 and 3-32). However, the computational model does not consider the effect of flexibility on drag force. Erect fronds will experience more drag than prostrate fronds because of greater thallus area projected into the flow. With broader intergenicula, less flexible fronds likely experience greater moments, bending them to greater angles, and causing greater stresses. To properly simulate this effect, future studies could quantify the effect of frond deflection on drag force and adjust applied force in the computational model as fronds bend.

3.5.3.iii Decreased tensile modulus

According to the model, decreasing tensile modulus increases flexibility and greatly reduces genicular stress. However, contrary to model predictions, *Calliarthron* genicular tissue is stiff compared to several other algal tissues (Hale 2001). Fortunately, genicular tissue can resist greater stresses than other algal tissues (see Chapter 1), due in part to the unique composition of genicular cell walls (see Chapter 6). Thus, given a high breaking stress, genicula can remain moderately stiff without risking frond breakage. If genicula were composed of fleshy algal materials with a lower breaking stress, fronds might be more likely to break. Future analyses could

explore this hypothetical scenario by substituting fleshy algal material properties in the computational model.

3.5.4. *Other articulated algae*

The geometry and mathematical model described here will be useful in the investigation of the adaptive significance of various joint morphologies in other articulated algae. For example, genicula in all articulated Corallinoids (subfamily Corallinoideae), including *Calliarthron*, develop similarly through decalcification but differ widely in size and number. Comparisons across Corallinoid taxa would reveal if genicular dimensions scale proportionally and, if not, potentially identify functional trade-offs. Short intergenicula in *Corallina* may allow delicate fronds to survive with relatively long intergenicular lips or short genicula. The model will also be a useful tool to evaluate convergent evolution of joints across articulated lineages. For example, genicula in articulated Metagoniolithoids, which develop meristematically and not by decalcification, lack intergenicular lips ($x=0$) and are the same diameter as adjacent intergenicula ($r_2 = y$). Differences in these genicular dimensions may be offset by other material properties and genicular dimensions to yield equivalent frond deflections and stress distributions.

Chapter 4

TO BREAK A CORALLINE:
IMPACT OF WAVE-INDUCED FORCES ON ARTICULATED FROND SURVIVAL

4.1. Abstract

Previous studies have hypothesized that wave-induced drag forces may constrain the size of intertidal organisms by dislodging or breaking organisms that exceed some critical size. However, previous attempts to demonstrate that water velocities limit the size of intertidal organisms have been problematic. One common source of difficulty has been approximating intertidal water velocities in traditional re-circulating flumes. In this study, drag on *Calliarthron* fronds was measured in a gravity-accelerated water flume that generated environmentally relevant water velocities up to 11 m/s. Drag force increased in proportion to frond planform area, suggesting that fronds become increasingly prone to breakage as they grow. Breakage was characterized by applying known forces to *Calliarthron* fronds in the lab until they broke. Surprisingly, peripheral genicular tissue was well-fortified against bending stresses, and data suggested that fronds are more likely to break at "tensile" genicula than at "bending" genicula. By comparing drag force and breaking force measurements, I predicted the water velocities necessary to break fronds of given sizes. Laboratory predictions successfully correlate maximum water velocity and frond size in the field, suggesting that hydrodynamic forces may, indeed, limit the size of intertidal *Calliarthron* fronds.

4.2. Introduction

The intertidal zone of rocky shores is a hydrodynamically stressful environment, where breaking waves can generate water velocities greater than 25 m s^{-1} (e.g., Denny et al. 2003) and impose great forces on intertidal inhabitants (Helmuth and Denny 2003). The severity of wave-induced forces is hypothesized to limit the maximum size to which intertidal organisms can grow (Denny et al. 1985, Gaylord et al. 1994, Denny 1999). For example, Blanchette (1997) found that intertidal algae transplanted from sheltered to wave-exposed locations tattered back to a smaller size. Such

damage is likely the result of drag, the primary wave-induced force applied to intertidal macroalgae (Denny and Gaylord 2002):

$$F_{drag} = \frac{1}{2}\rho U^2 A C_d \qquad\qquad 4\text{-}1$$

where ρ is seawater density, U is water velocity, A is algal planform area, and C_d is drag coefficient, a dimensionless number that describes shape change and reconfiguration of flexible fronds (as in Carrington 1990, Dudgeon and Johnson 1992, Gaylord et al. 1994, Bell 1999) (but see Boller and Carrington 2006).

Several studies have measured drag on seaweeds to predict the size to which various species can grow in the intertidal zone (Carrington 1990, Dudgeon and Johnson 1992, Gaylord et al. 1994) but have had little success. This may be due in part to the characterization of drag at slow-speeds (< 3 m s^{-1}) in recirculating water flumes and the necessity to extrapolate out to environmentally-relevant water velocities (20-30 m s^{-1}). Such long range extrapolations can be misleading (Vogel 1994, Bell 1999). In particular, drag coefficient decreases as flexible macroalgae bend and reconfigure with increasing water velocity (Bell 1999, Boller and Carrington 2006), and the extent of this reconfiguration has never been characterized at high velocities.

The articulated coralline alga *Calliarthron* thrives in wave-swept intertidal habitats along the California coast. Unlike fleshy algae, *Calliarthron* thalli are calcified and have flexible joints, called genicula, that allow fronds to bend when struck by breaking waves. In providing flexibility, genicula define discrete breakage points along calcified thalli (Chapter 1). In particular, articulated fronds are hypothesized to be susceptible to bending stresses, as frond morphology may locally amplify stress in genicula (Chapter 3). However, peripheral genicular cells have thickened cell walls that may be fortified against bending stresses (Chapter 2) and the distinctive dimensions of basal genicula, which experience the most bending, may ultimately ameliorate any stress amplification (Chapter 3). Although genicular tissue is known to be stronger than other algal tissues (Chapter 1), the strength of fortified peripheral

genicular tissue is unknown and the forces to bend articulated fronds to failure have never been properly quantified.

In this study, I characterize the breaking strength of peripheral genicular tissue by applying known forces to *Calliarthron* fronds in bending, and I assess whether fronds are more likely to break in tension or in bending in the field. I characterize drag on articulated fronds in a novel high-speed water flume and predict the size to which fronds can grow in a given water velocity. I test laboratory predictions by measuring maximum water velocities and frond sizes in the field and propose that wave-induced drag forces may, indeed, be sufficient to limit the size of intertidal *Calliarthron*.

4.3. Materials & Methods

4.3.1. *Breakage of "bending" genicula*

Calliarthron fronds (N=34) were collected from the low-intertidal zone in a moderately wave-exposed surge channel at Hopkins Marine Station, Pacific Grove, CA. The field site was identical to that described in previous chapters. Branches were removed from each frond by cutting below the first dichotomy, and the remaining straight chains of segments were tested as follows. Individual fronds were gripped by the first few genicula in clamps and held horizontal (Figure 4-1A). The first 3-5 genicula of each frond, presumably susceptible to the most bending stresses, were (of necessity) held within the clamps and were not tested here (Figure 4-1A). To quantify the force to bend genicula to failure, a second clamp was secured near the tenth genicula and masses were hung, in 20g and 50g increments, from the clamp until fronds broke (Figure 4-1B).
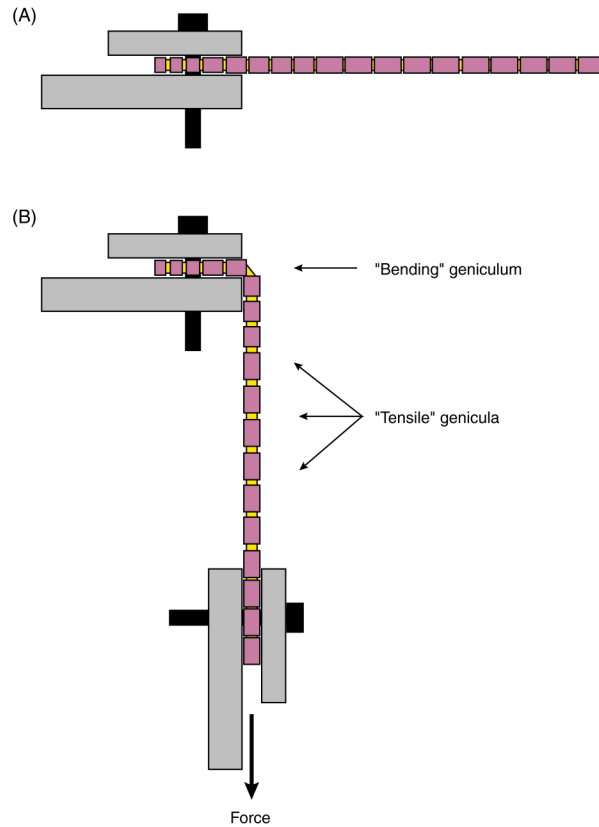
Figure 4-1. (A) *Calliarthron* segments were held horizontally between two clamps. Note that basal genicula, which are most susceptible to bending stresses in the field, were hidden within the clamps and not tested. (B) A second clamp was attached near the tenth intergeniculum. Force was applied by hanging weights from the second clamp.

Dimensions of broken genicula were quantified as described in Chapter 3 (see Figure 3-1). Genicula radii (r_1, r_2) and intergenicula radii (y) were measured with an ocular dial-micrometer. Genicular lengths (ω) and gap lengths ($\omega - 2x$) were measured in decalcified, long-sectioned genicula adjacent to broken genicula. Average length measurements were assumed for broken genicula. Intergenicular lip length (x) of broken genicula was estimated as half the difference between mean ω and mean gap length.
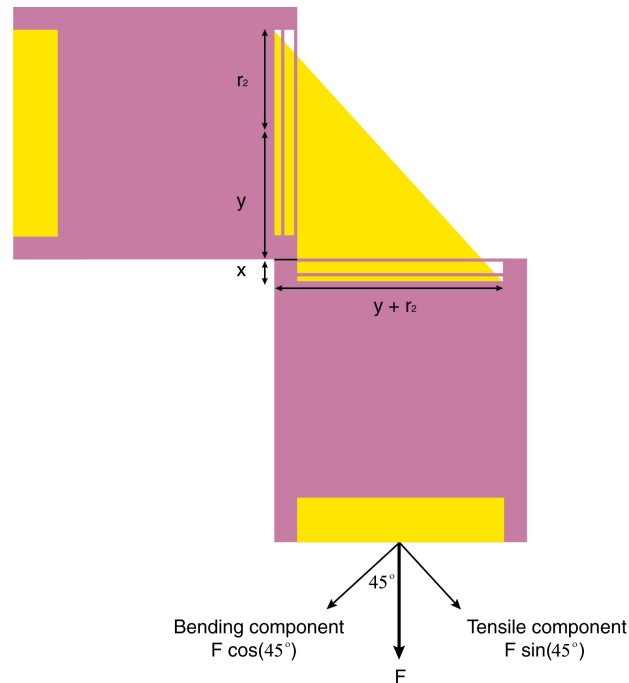
Figure 4-2. *Calliarthron* geniculum bent 90°. Note that intergenicula slipped to the outside edge of intergenicular lips.

All fronds bent 90° before breaking. "Bending" genicula assumed a triangular geometry between adjacent intergenicula (Figure 4-2), as predicted for cable-like genicula in the numerical model described in Chapter 3. Contrary to the simplified numerical model, contact of intergenicula adjacent to "bending" genicula was not stable, and intergenicula generally slipped to the outside edge of calcified lips (Figure 4-2).

"Bending" genicula were assumed to break when peripheral genicular tissue – the tissue that experiences the most strain and stress in bending – ruptured. Stress in peripheral tissue was calculated as the sum of tensile and bending stress components. Bending stress was assumed to reach a maximum value when genicula bent 90° and was computed by determining strain at the geniculum periphery (Figure 4-2). Strain was calculated from hypotenuse length:

$$\varepsilon_{bending} = \frac{\sqrt{(x + y + r_2)^2 + (y + r_2)^2}}{\omega} - 1 \qquad\qquad 4\text{-}2$$

Strain was used to calculate bending stress:

$$\sigma_{bending} = E_t\, \varepsilon_{bending} = E_t \left(\frac{\sqrt{(x + y + r_2)^2 + (y + r_2)^2}}{\omega} - 1 \right) \qquad 4\text{-}3$$

where E_t is tensile modulus, calculated to be 45.4 MN m^{-2} (see Ch. 3).

Tensile stress continued to increase with force after genicula bent 90° and was calculated from the tensile component of applied force (Figure 4-2):

$$\sigma_{tension} = \frac{F \sin\!\left(\dfrac{\phi}{2}\right)}{A} = \frac{F \sin(45°)}{\pi\, r_1\, r_2} = \frac{F\sqrt{2}}{2\pi\, r_1\, r_2} \qquad 4\text{-}4$$

where F is force, bending angle ϕ is 90°, and A is geniculum cross-sectional area, assumed to be elliptical.

Breaking stress in bending genicula was thus calculated as the sum of these components:

$$\sigma_{breaking} = E_t \left(\frac{\sqrt{(x + y + r_2)^2 + (y + r_2)^2}}{\omega} - 1 \right) + \frac{F\sqrt{2}}{2\pi\, r_1\, r_2} \qquad 4\text{-}5$$

4.3.2. *Breakage of "tensile" genicula*

During the bending experiment, "tensile" genicula sometimes broke before "bending" genicula (Figure 4-1B). Breaking stresses in "tensile" genicula were calculated by simply dividing force by geniculum cross-sectional area:

$$\sigma_{tension} = \frac{F}{\pi\, r_1\, r_2} \qquad\qquad 4\text{-}6$$

Note that this equation is equivalent to Eqn 4-4, when $\phi = 0$ for unbent "tensile" genicula.

Peripheral stresses were calculated for unbroken "bending" genicula using Eqn 4-5. Peripheral stresses in "bending" genicula and breaking stresses in "tensile" genicula were compared.

4.3.3. *Breakage of "bending" versus "tensile" genicula*

To generalize the likelihood of frond breakage in "bending" and "tensile" genicula, forces were estimated to break first genicula bent $90°$ and tenth genicula in tension, using dimensions of first and tenth genicula (N=10) measured in Chapter 3. First genicula were assumed to break when peripheral stress (Eqn 4-5) equaled the mean breaking stress determined in 4.3.1. Tenth genicula were assumed to break when tensile stress (Eqn 4-6) equaled the mean tensile breaking stress, determined to be 25.9 MN m^{-2} (see Chapter 1). Forces estimated to break first and tenth genicula in each frond were compared. Mean force to break *Calliarthron* fronds was calculated by averaging the weakest forces estimated to break first or tenth genicula, assuming that fronds in the intertidal zone will break at the weakest link.

4.3.4. *Drag force measurements*

To quantify the effect of frond size and growth on drag force, *Calliarthron* fronds (N=22) were collected from the field site and tested in a gravity-accelerated water flume (Figure 4-3). Untreated fronds were attached with cyano-acrylate glue to a custom force transducer in the water flume. Drag force was measured while fronds were struck with jets of water meant to mimic breaking waves. Water velocity was adjusted by varying the height of the valve in the water flume (Figure 4-3) and fronds were tested at 6.8 m s^{-1} (N=6), 10.0 m s^{-1} (N=10), and 11.6 m s^{-1} (N=6). Individual fronds were only tested at one flume velocity.
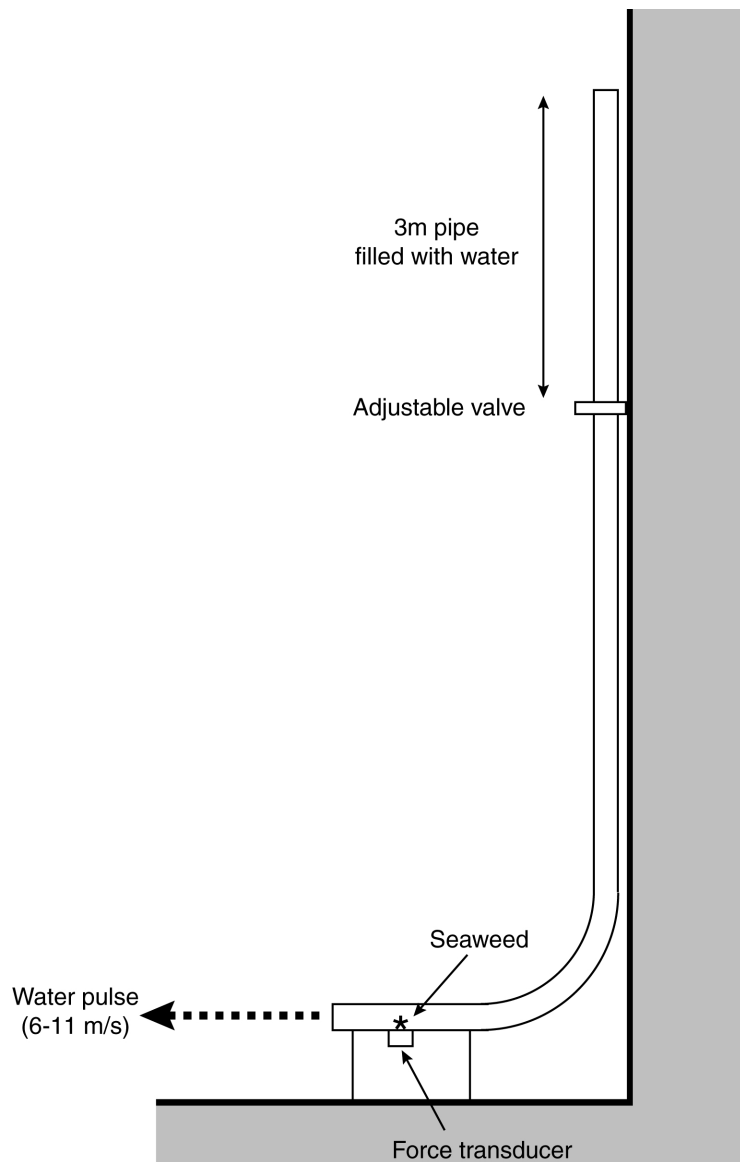
Figure 4-3. Gravity-accelerated water flume used to measure drag force on *Calliarthron* fronds. Valve height was adjusted to vary water velocity.

To explore changes in drag force over the lifetime of apically-growing *Calliarthron*, fronds were "de-grown" by sequentially removing apical branches and the resulting effect on drag force was quantified. Drag on whole fronds was measured, then apical branches of fronds were removed, and drag force was re-measured. Then sub-apical branches of fronds were removed, and drag force was re-measured. This process was repeated until all branches had been removed. Severed branches were digitally

photographed and planform areas were measured using an image analysis program (ImageJ, NIH). The correlation between frond planform area and drag force was plotted for fronds at all three water velocities, and one linear regression was fitted to all frond data for each velocity.

4.3.5. *Estimating drag coefficient, C_d*

Linear regressions fitted to drag-planform area data can be expressed as

$$F_{drag} = k \cdot A \qquad\qquad 4\text{-}7$$

where k is regression slope.

Combining Eqns 4-7 and 1-1 yields

$$k = \frac{1}{2}\rho U^2 C_d \qquad\qquad 4\text{-}8$$

Thus, drag coefficient can be estimated as

$$C_d = \frac{2k}{\rho U^2} \qquad\qquad 4\text{-}9$$

In this manner, C_d was estimated for *Calliarthron* at each water velocity in the water flume.

4.3.6. *Breakage predictions*

Fronds are expected to break in the field when drag force on fronds equals breaking force of genicula. This expectation can be represented as follows:

$$F_{break} = F_{drag} = \frac{1}{2}\rho U^2 A C_d \qquad\qquad 4\text{-}10$$

Rearranging this equation yields:

$$U = \sqrt{\frac{2F_{break}}{\rho A C_d}}$$ 4-11

Given breaking force (predicted in section 4.3.3) and drag coefficient (assumed to be constant at $U > 11.6$ m s^{-1}), we can use Eqn 4-11 to predict the maximum area to which fronds can grow in a given water velocity or, conversely, the minimum water velocity required to break fronds of a given size.

4.3.7. *Field measurements*

From November 2003 to November 2006, *Calliarthron* fronds were collected eight times from the intertidal field site described above. Collections typically consisted of 10-20 fronds and always involved searching for the largest available fronds. Fronds were digitally photographed and frond planform areas were measured using image analysis (ImageJ, NIH). Maximum frond size was recorded on each date over the three-year span.

From November 2005 to August 2006, water velocities were measured thirteen times at the field site. On 2 November 2005, three dynamometers (e.g., Bell and Denny 1994, Denny and Wethey 2001, Helmuth and Denny 2003) were installed at 0.0 ft tide height approximately 0.75 m apart across the field site. Dynamometers were first checked and reset on 4 November 2005 and were checked and reset during sufficiently low tides until 10 August 2006. The maximum water velocity recorded by any dynamometer was recorded on each date over the nine month span.

Field measurements were compared to breakage predictions to determine if drag forces in the field reached experimentally determined breaking forces of *Calliarthron* fronds.

4.4. Results

4.4.1. *Breaking strength of "bending" genicula*

Mean breaking strength of "bending" genicula was 120.7 ± 9.1 MN m^{-2} (mean $\pm$ 95%

C.I.) (Table 4-1). This value was used to estimate breakage in first genicula bent 90°.

Table 4-1. Breaking strength of peripheral tissue in genicula bent 90°.

Frond	Breaking force (N)	Breaking strength of peripheral tissue (MN m^{-2})
1	9.32	139.9
2	9.50	110.0
3	7.54	109.3
4	14.40	115.4
5	14.40	131.7
6	10.97	111.3
7	11.95	127.6
Mean		120.7

4.4.2. *Breaking strength of "tensile" genicula*

In two trials, "tensile" genicula broke before "bending" genicula. In one frond, the

breaking stress in the "tensile" geniculum was 30.2 MN m^{-2}, greater than the average

tensile breaking strength of *Calliarthron* (25.9 N m^{-2}), while the peripheral stress in

the "bending" geniculum was 120.9 MN m^{-2} (Table 4-2). In the second frond, stresses

in "tensile" and "bending" genicula were less than average breaking strengths (Table

4-2).

Table 4-2. Stresses in "bending" and "tensile" genicula, when "tensile" genicula broke first.

Frond	Breaking Force (N)	Peripheral stress in "bending" geniculum (MN m^{-2})	Breaking strength of "tensile" geniculum (MN m^{-2})
1	10.30	120.9	30.2
2	9.99	104.0	15.4

4.4.3. *Breakage of "bending" versus "tensile" genicula*

Given dimensions of first and tenth genicula, 90% of fronds were predicted to break initially at tenth genicula in tension, and 10% were predicted to break first at first genicula bent 90° (Table 4-3). On average, fronds were estimated to resist 41 N in bending and 22 N in tension. Mean force to break *Calliarthron* fronds was estimated to be 21 N.

Table 4-3. Comparison of forces predicted to break basal genicula in bending and tenth genicula in tension.

	Estimated force (N) to break:		
Frond	First geniculum bent 90°	Tenth geniculum in tension	Geniculum predicted to break first
1	52	18	Tenth
2	41	20	Tenth
3	46	21	Tenth
4	47	19	Tenth
5	63	16	Tenth
6	33	19	Tenth
7	29	16	Tenth
8	35	28	Tenth
9	44	35	Tenth
10	26	28	First
Mean	41	22	
Mean force to break frond	21		

4.4.4. *Drag force measurements and drag coefficient estimates*

For all water velocities, drag force increased linearly with frond planform area (Figure 4-4A, B). Linear regressions were significant for 6.8 m s^{-1} ($R^2 = 0.89$, $p < 0.01$), 10.0 m s^{-1} ($R^2 = 0.83$, $p < 0.01$), and 11.6 m s^{-1} ($R^2 = 0.77$, $p < 0.01$) water velocities. Slopes of drag-planform area regressions increased with increasing water velocity (Figure 4-4B) and are listed in Table 4-4. Drag coefficients (C_d) decreased with increasing water velocity (Table 4-4). Drag coefficient was calculated to be 0.017 at the maximum test velocity (11.6 m s^{-1}).
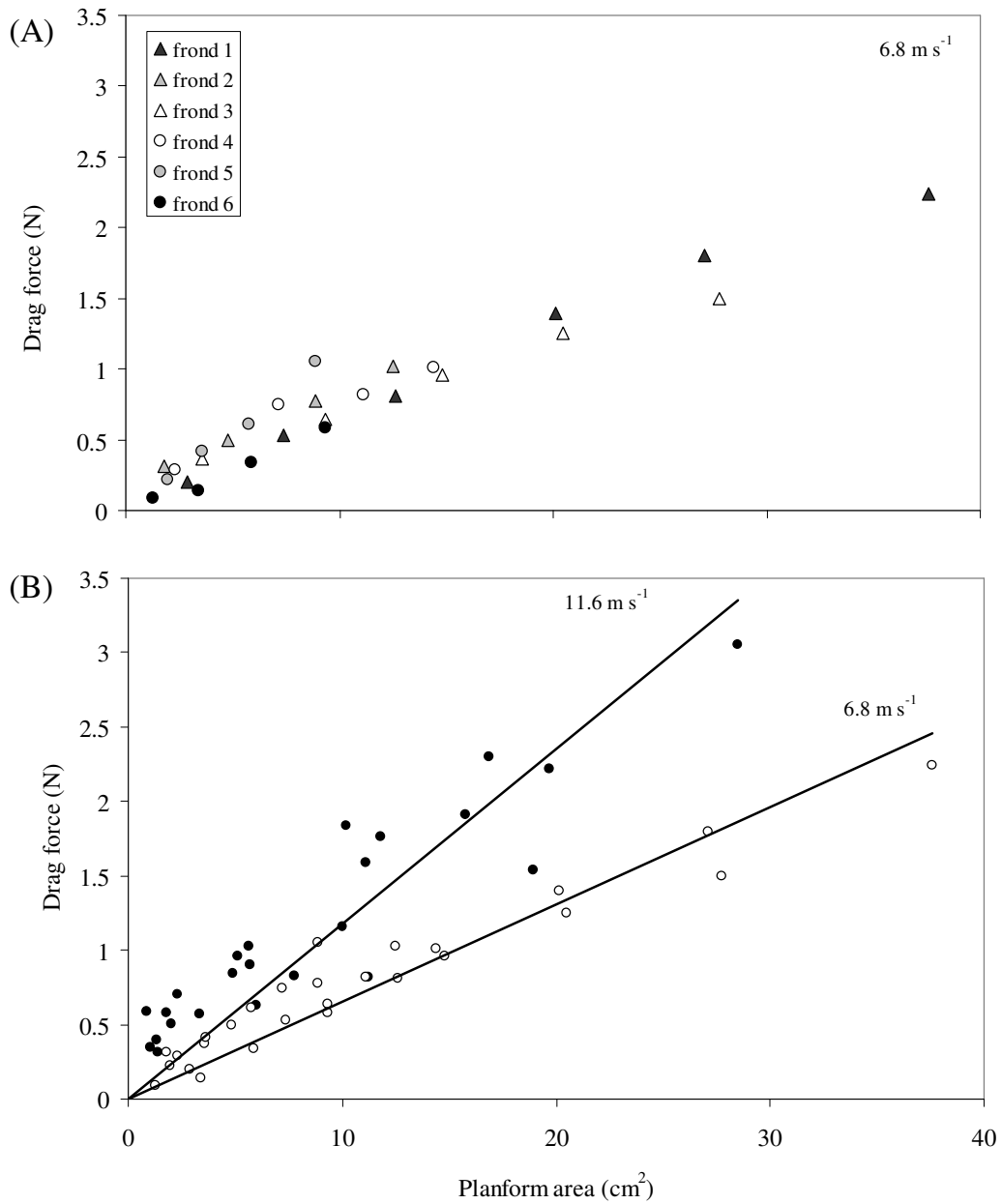
Figure 4-4. Effect of frond planform area on drag force, showing (A) variation among fronds tested at 6.8 m s^{-1} and (B) increasing regression slopes with increasing water velocity. Data are presented for all fronds at 6.8 m s^{-1} (white circles) and 11.6 m s^{-1} (black circles). Data collected at 10.0 m s^{-1} were excluded to clarify the second graph.

Table 4-4. Drag coefficients estimated from slopes of drag force/planform area regressions.

Water velocity (m s^{-1})	Regression slope	C_d estimate
6.8	653.8	0.028
10.0	1119.0	0.022
11.6	1178.2	0.017

4.4.5. *Breakage predictions and field validation*

Given a typical breaking force (21 N) and a minimum drag coefficient (0.017), *Calliarthron* fronds of given planform area were predicted to break at water velocities depicted in Figure 4-5, according to the equation:

$$U = 1.55A^{-0.5}$$

4-12

where *A* is planform area measured in m^2. Larger fronds were predicted to break at slower water velocities. Fronds smaller than 15 cm^2 are predicted to resist water velocities greater than 40 m s^{-1}.
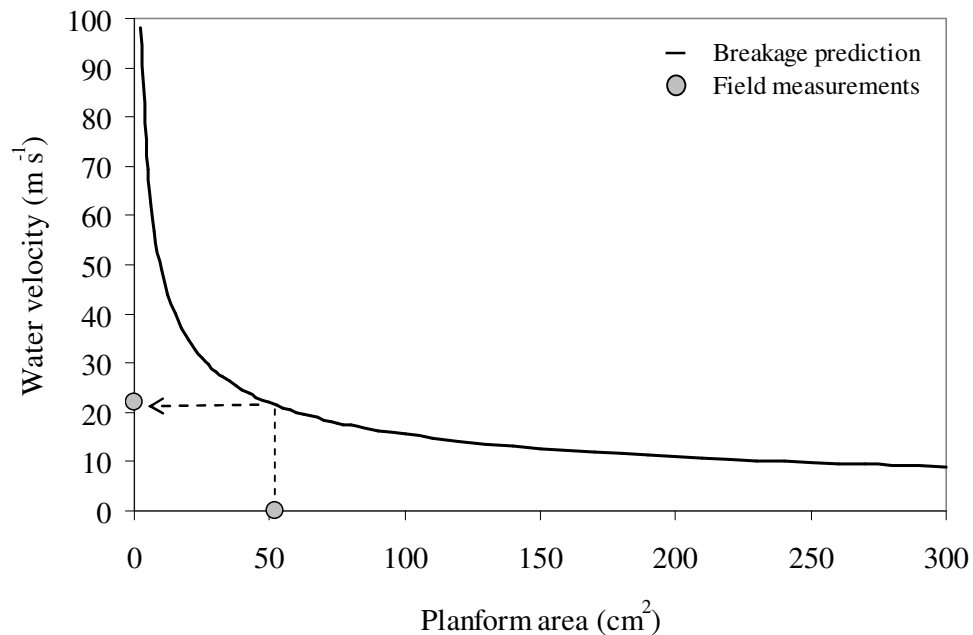
Figure 4-5. Water velocity predicted to break *Calliarthron* fronds of specific planform area (solid line). Field measurements (gray circles) match model predictions (see dotted lines).

The largest frond collected at the field site was 51.9 cm^2, and the fastest water velocity recorded was 22.1 m s^{-1} (Table 4-5 and Table 4-6). These field measurements correspond closely to breakage predictions (Figure 4-5).

Table 4-5. Maximum size of *Calliarthron* fronds collected on given dates.

Date	Maximum frond size (cm^2)
23-Nov-03	34.3
21-Jan-04	26.9
5-Jul-04	44.3
17-Jan-05	51.9
8-Feb-05	47.7
13-Dec-05	42.8
26-Jun-06	39.4
4-Nov-06	39.9
Maximum	51.9

Table 4-6. Maximum water velocities recorded by dynamometers at field site.

Date	Maximum water velocity (m s^{-1})
4-Nov-05	11.2
15-Nov-05	13.6
16-Nov-05	22.1
30-Nov-05	12.0
13-Dec-05	11.6
29-Dec-05	12.2
24-Feb-06	9.6
24-Mar-06	18.6
15-May-06	8.3
30-May-06	9.0
13-Jun-06	7.3
26-Jun-06	9.6
10-Aug-06	7.3
Maximum	22.1

4.5. Discussion

4.5.1. *Experimental limitations*

Basal genicula that connected *Calliarthron* fronds to encrusting bases were cut during frond collection, and genicula immediately distal to severed basal genicula were gripped within clamps during bending trials. Thus, because of collection and experimental protocols, the most basal genicula in *Calliarthron* fronds, which likely provide the most flexibility and experience the greatest bending stress in the field, could not be evaluated in this study. Instead, more distal genicula were tested and bent to failure. Basal genicula are morphologically adapted to resisting bending stresses (see Chapter 3), and dimensions of basal and distal genicula differ. Nevertheless, due to experimental limitations, data were collected for distal genicula and used to estimate forces to bend basal genicula to failure.

One major morphological difference between basal and distal genicula is the length of intergenicular lips. Distal genicula have significantly longer calcified lips (Chapter 3), partly due to less abrasion caused by bending adjacent intergenicula. When bent to failure, these genicula with long calcified lips often cracked, fracturing fronds at nearby intergenicula. Most fronds (74%) tested in the bending trials broke at intergenicula. However, seven fronds broke cleanly at "bending" genicula, providing sufficient data to calculate breaking strengths of genicula in bending and to predict forces to break basal genicula bent 90°. Ultimately, to groundtruth data presented here, future studies should test basal genicula directly by gripping the encrusting base of *Calliarthron* and bending intact fronds.

4.5.2. *Fortified against bending stresses*

Forces to break *Calliarthron* genicula in bending were surprisingly high; several fronds supported more than 1 kg of weight at 90° before breaking. Mean breaking strength in bending (120.7 MN m^{-2}) was nearly five-fold the mean breaking strength in tension (25.9 MN m^{-2}), a likely consequence of different cell wall composition in central and peripheral cells. Cell walls of peripheral cells are often twice as thick as central cells (Chapter 2) and contain unique compounds that may fortify them mechanically (Chapter 6). Breaking strength of peripheral genicular tissue exceeds breaking strengths of other algal tissues by more than an order of magnitude (see Chapter 1) and is comparable to that of terrestrial plant tissues, including tracheids (120 MN m^{-2}) (Wainwright et al. 1982) and non-woody fibers (e.g., coconut husk fiber: 137 N m^{-2}) (Munawar et al. 2007). The distinct chemical composition and cell wall structure that potentially underlie the unique mechanical properties of genicular cells are the subjects of Chapters 5 and 6.

4.5.3. *Breakage in bending or tension?*

Because of the high breaking strength of peripheral genicular tissue and the morphological adaptations of basal genicula to limit bending stress amplification

(Chapter 3), data presented here suggest that *Calliarthron* fronds are more likely to break in tension than in bending. In some cases, first genicula are predicted to resist more than twice the force in bending that tenth genicula can resist tension. Although the magnitude of forces to bend first genicula to failure needs verification, ultimately, I hypothesize that the conclusion will be the same. During the bending trials, "tensile" genicula broke twice before "bending" genicula, and in one of those fronds, stress in the "tensile" geniculum had clearly exceeded the average tensile strength of *Calliarthron* genicula.

In bending, stress is acutely amplified in the periphery of genicula, where it is expected to cause the most damage. Peripheral cell walls are robustly fortified, likely as a result of this selective pressure. However, in tension, stress is applied evenly across the tissue cross-section, and as a result, any flaw or weak link will lead to breakage (Currey and Taylor 1974). Given that the tensile strengths of calcified intergenicula (28.5 MN m^{-2}) and coral skeleton (25.6 MN m^{-2}) are similar (Chapter 1), there may not be a selective advantage to producing stronger genicular tissue (25.9 MN m^{-2}), if the calcium carbonate would ultimately fail first. Thus, *Calliarthron* may be well-adapted to resist bending stresses, but limited, in an evolutionary sense, in its capacity to resist tensile stresses.

4.5.4. *Environmentally-relevant drag coefficient*

This is the first study to report drag coefficients for an intertidal seaweed at high, environmentally-relevant water velocities. Drag coefficients reported here for *Calliarthron* are up to an order of magnitude lower than those measured for several other algae at slow water velocities (Carrington 1990, Dudgeon and Johnson 1992, Gaylord et al. 1994). Data suggest that drag coefficient continues to decrease as water velocity increases, contrary to the assumption that reconfiguration is a low-velocity phenomenon (Carrington 1990) and supporting non-linear extrapolation methods used in previous studies (Gaylord et al. 1994, Bell 1999). This emphasizes the importance of measuring drag at high water velocities to avoid, or at least improve, such

extrapolation. For example, Gaylord et al. (1994) extrapolated five-times beyond their data to generate drag predictions that the gravity-accelerated water flume could almost measure directly. The accuracy of their extrapolation awaits verification in the high-speed water flume. Reduction of projected area and branch reconfiguration both contribute to decreasing drag coefficient (Boller and Carrington 2006) and likely have absolute limits. Further experiments are being planned to separate these effects for flexible algae, including *Calliarthron*, at high velocities.

4.5.5. *Limits to frond size in the intertidal zone*

Forces estimated to break *Calliarthron* fronds in the field are corroborated by forces measured to break genicula in Chapter 1. An average *Calliarthron* frond can resist approximately 21 N of force before breaking – a substantial amount of force. For example, one large experimental frond (30 cm^2) experienced only 3 N of drag force at 11 m s^{-1}, far below the threshold breaking force. This suggests that *Calliarthron* may be able to support larger fronds in slower water velocities but may be size-limited when water velocities increase.

Indeed, data presented here suggest that the size of *Calliarthron* fronds may be limited by drag forces imposed by intertidal water velocities. According to the breakage model, the maximum water velocity measured at the field site (22.1 m s^{-1}) closely predicted the size of the largest *Calliarthron* frond (51.9 cm^2) expected to survive there. Admittedly, this model is an over-simplification. Intertidal water velocities vary widely over various spatial and temporal scales and are generally difficult to predict (Denny and Wethey 2001, Helmuth and Denny 2003, O'Donnell 2005). On any given date, dynamometer data were highly variable across the field site (maximum coefficient of variation, CV=55%), and forces recorded by the same meter sometimes doubled or tripled between dates. Ideally, experiments would measure water velocity immediately adjacent to intertidal fronds and monitor velocity and frond size concurrently. Nevertheless, the close correlation between maximum velocity and frond size across the field site suggests that growth may be limited by wave-induced

drag forces. Observations of larger fronds growing subtidally (K.A. Miller, *pers. obs*.) support this conclusion, but have yet to be properly quantified.

Chapter 5

TO TRANSFORM A CORALLINE:
CHANGES IN CELL WALL POLYSACCHARIDES DURING GENICULA DEVELOPMENT

5.1. Abstract

Corallinoid genicula are remarkable soft tissues that develop from previously calcified cells. While the morphological changes that occur during genicular development have been previously described, the chemical changes that accompany this transformation are not well understood. Past studies have examined differences in intergenicular and genicular cell walls using light and electron microscopy, but differences in chemical composition have never been investigated analytically. In this study, polysaccharides were extracted from genicular and intergenicular tissues that had been manually separated. Young and old tissues were compared to detect shifts in chemical composition with age. Older genicular tissue had twice the amount of cellulose as younger tissue, coinciding with the thickening of genicular cell walls and contributing to the strengthening of genicular tissue with age. Intergenicula contained xylogalactans with long xylose side chains, which may help define sites for calcium carbonate nucleation. In contrast, genicula contained highly methylated galactans with few xylose side chains, which may play a role in cell wall decalcification and allow for the compaction of polymers into elongated genicular cell walls. Changes in side chain substitutions may also help explain the unique mechanical properties of genicular tissue.

5.2. Introduction

Articulated coralline algae in the Corallinoid subfamily (Corallinaceae, Corallinoideae) develop flexible genicula by secondarily decalcifying cell walls of specific cells along their thalli (Johansen 1969a, Johansen 1974, Johansen 1981). Coralline decalcification is a well-regulated process that alters specific regions of genicular cell walls (Figure 5-1A-C), creating remarkable soft tissues from previously calcified cells. However, the striking transformation from calcified intergenicula (Figure 5-1D) to flexible genicula (Figure 5-1E) is not well-understood. Several
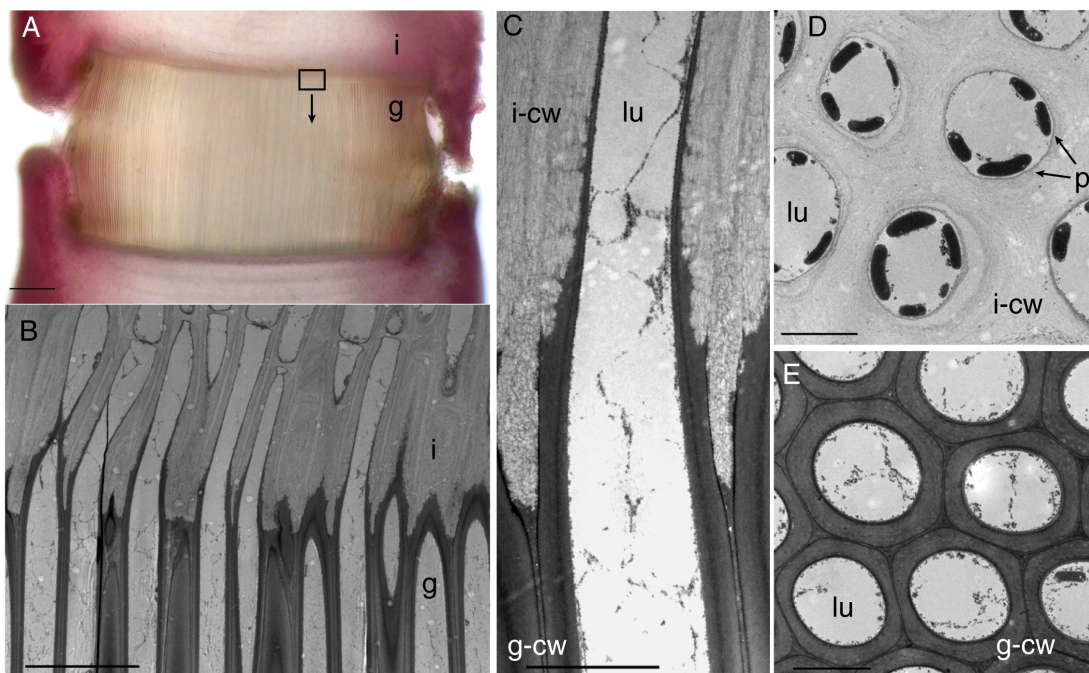
Figure 5-1. (A) Long-section of *Calliarthron* geniculum. Boxed area is geniculum-intergeniculum transition zone, magnified under TEM in (B). (C) TEM long-section of single cell at transition zone. (D) TEM cross-section of intergeniculum. (E) TEM cross-section of geniculum. Intergeniculum (i), geniculum (g), cellwall (cw), lumen (lu), and plastids (p). Scales A=200µm, B=20µm, C=5µm, D=5µm, E=5µm.

studies comparing intergenicular and genicular cell walls have noted major morphological differences, including dense fibrils of unknown composition found exclusively within genicula (e.g., Bailey and Bisalputra 1970, Borowitzka and Vesk 1978, 1979), and chemical differences based on histological stains (e.g., Yendo 1904, Johansen 1969a). Furthermore, experiments conducted on the articulated coralline *Calliarthron* have linked the great tissue strength of genicula (see Chapters 1 & 4) to

features of the cell wall (see Chapter 2). Unfortunately, chemical differences between genicular and intergenicular cell walls have never been investigated analytically.

Cell walls of red algae (class Florideophyceae) are broadly composed of (glyco)-proteins, skeletal polysaccharides, such as cellulose, and matrix polysaccharides typified by galactans with alternating 3-linked β-units and 4-linked α-units (e.g., Craigie 1990, Flores et al. 1997, Lechat et al. 2000) (Figure 5-2). Matrix polysaccharides can comprise 30-65% of the dry weight of red algal thalli (Kloareg and Quatrano 1988) and are often dominated by sulfated galactans, such as carrageenans, agarans, and DL-galactan hybrids (Usov 1992, Miller 1997, Stortz and Cerezo 2000). Cell wall polysaccharides are thought to play a significant role in seaweed physiology (Kloareg and Quatrano 1988). In particular, past studies have linked polysaccharide composition to algal mechanical properties (Carrington et al. 2001) and to calcium carbonate precipitation (e.g., Okazaki et al. 1984, Cabioch and

$\longrightarrow$ 3)–β–D-Galactose-(1 $\longrightarrow$ 4)-α-L-Galactose-(1 $\longrightarrow$
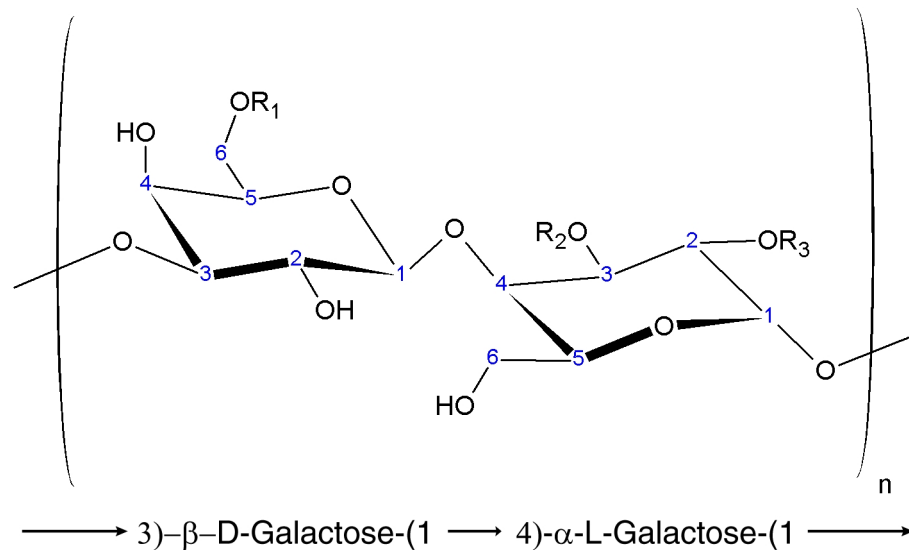
Figure 5-2. Basic alternating structure of galactan backbone in coralline algae (derived from Cases et al. 1994). (R_1=mostly xylose and sulfate, R_2=some sulfate and fewer methyl groups, R_3=some methyl and fewer sulfate groups)

Giraud 1986, Borowitzka 1987, Bilan and Usov 2001), suggesting that changes in genicular and intergenicular polysaccharides may help explain genicula biomechanics and regulation of calcification.

Coralline algae synthesize unique types of agarans called "corallinans" (Cases et al. 1994), which have β-D-xylopyranosyl, methoxyl, or sulfate groups attached to C-6 of the β-D-galactose units and methoxyl or sulfate groups attached to C-2 or C-3 of α-L-galactose units (Cases et al. 1994, Usov et al. 1997, Navarro and Stortz 2002) (Figure 5-2). Previous studies of coralline algal chemistry extracted polysaccharides from whole fronds, overlooking potential differences in genicular and intergenicular cell walls. Polysaccharide composition differs with tissue type and tissue age in several species of brown algae (Haug et al. 1974), suggesting that cell wall chemistry may also vary along coralline algal thalli.

In this study, I extract polysaccharides from *Calliarthron* genicula and intergenicula separately to explore changes in cell wall chemistry that occur during genicular development. I determine the chemical composition of young and old tissues to resolve changes in cell wall chemistry at a finer temporal scale and to examine the chemical basis for tissue strengthening in *Calliarthron* genicula. Differences in cell wall polysaccharides may help explain genicular material properties and contribute to our understanding of coralline calcification and decalcification.

5.3. Materials & Methods

5.3.1. *Sample collection*

Calliarthron fronds were collected from the low intertidal zone at various wave-exposed sites at Hopkins Marine Station, Pacific Grove, CA. As in Chapter 2, both young sprouts and old fronds were collected to explore general effects of age on intergenicular and genicular tissue. All fronds were inspected, and epiphytized or unhealthy branches were discarded. In a subset of fronds, genicula and intergenicula were separated using a razor

Figure 5-3. Intergenicula (left) and genicula (right) were separated for chemical analyses. Scale in millimeters.

blade and analyzed independently (Figure 5-3). To increase yields and generate mean carbohydrate composition, all experimental samples included pieces of multiple fronds.

5.3.2. *Polysaccharide extractions*

The extraction procedure is described elsewhere (Cases et al. 1994, Navarro and Stortz 2002). Briefly, ball-milled plants (15 g) and excised intergenicula (3 g) were each suspended in 90 mL of water and 1M HCl was added dropwise with mechanical stirring until no more CO_2 evolution was detected. Ball-milled genicula (~1 g) were suspended in water without HCl. Suspensions were stirred for 24 h at room temperature to extract soluble polysaccharides, and α-amylase was added to degrade floridean starch, the primary storage carbohydrate in red algae. Whole samples, containing both soluble polysaccharides and cellulosic material, were dialyzed (molecular weight limited to 6.0-8.0 kDa) and freeze-dried. This material was used to quantify the proportion of water-soluble cell wall polysaccharides to cellulose. Soluble polysaccharides were separated from cellulosic ones by redissolution in water and centrifugation. Supernatants and residues were freeze dried and analyzed separately.

5.3.3. *Chemical analysis*

Total sugar content was analyzed by phenol-sulfuric acid method (Dubois et al. 1956) without previous hydrolysis of the polysaccharide. To analyze sulfated galactans, alditol acetates were obtained by reductive hydrolysis and acetylation of the samples (Stevenson and Furneaux 1991). To analyze fibrillar polysaccharides, 1-3 mg of decalcified material was dissolved in 100% TFA (37 °C, 1 h), followed by dilution of the acid to 80%, heating at 100 °C for 1 h, and further dilution to 2 M (Morrison

1988); hydrolyzate was derivatized from the corresponding alditol acetates. For the linkage analysis, polysaccharides (3-6 mg) were converted into the corresponding triethylammonium salt (Stevenson and Furneaux 1991) and methylated according to Ciucanu and Kerek (1984) using finely powdered NaOH as base. The methylated samples were derivatized to the alditol acetates as described for the polysacharides. The linkage analysis was conducted by the Complex Carbohydrate Research Center (CCRC, Athens, Georgia, USA).

5.3.4. *Percent calcium carbonate*

To determine the proportion of *Calliarthron* fronds composed of $CaCO_3$, ten fronds were dried overnight at 50°C and weighed. Fronds were then decalcified thoroughly in 1N HCl, dried overnight, and re-weighed. Percent $CaCO_3$ was calculated from weight loss.

5.3.5. *Percent genicula*

To determine the proportion of *Calliarthron* fronds composed of genicula, 10-20 segments before the first dichotomy were isolated from four fronds. For each frond, segments were weighed intact, then genicula were removed and weighed separately. Difference in sample weight was used to calculate percent geniculum in dry frond mass. Dividing percent geniculum by (1 - fraction $CaCO_3$) (see section 5.3.4) yielded the proportion of uncalcified dry mass composed of genicula.

5.3.6. *Light and Transmission Electron Microscopy*

Calliarthron fronds were immersed in dilute fixative (1% glutaraldehyde, 1% formaldehyde, 98% filtered seawater) for 24 h then decalcified in 1 N HCl for 24 h. Genicula were excised completely by cutting through decalcified intergenicula. Samples were dehydrated with ethanol (25%, 50%, 75%: 2 hours each), infiltrated with Spurr's resin (Standard "Firm" recipe, 33%, 50%, 66%, 100%: 24 hours each), and cured overnight in a 70° C oven. For light microscopy, thin long-sections (4 µm)

were cut through genicula using a standard microtome (DuPont Instruments, Sorvall®, model MT2-B). For Transmission Electron Microscopy (TEM), ultra-thin sections were cut with a diamond knife (Diatome Ltd., Bienne, Switzerland) on a Leica Ultracut S (Leica Microsystems GmbH, Wetzlar), mounted on Formvar coated grids, and stained for 20 seconds in 3% Uranyl Acetate in 50% Acetone followed by 3 minutes in 0.2% Lead Citrate. Images were taken using a JEOL 1230 TEM (Jeol Ltd., Akishima, Tokyo, Japan) at 80kV using a Gatan peltier-cooled Bioscan camera (Gatan, Pleasanton, California).

5.3.7. *FT-IR microspectroscopy*

Fourier transform infrared spectra were recorded from the geniculum-intergeniculum transition zone in thin-sectioned young samples using a 510P Nicolet FT-IR spectrophotometer (Madison WI, USA). FT-IR absorption spectra were acquired at the infrared spectromicroscopy beamline 1.4.3 at the Advanced Light Source (ALS) in Berkeley, CA. Synchrotron Radiation (SR-FT-IR) was used as an external source for a Nicolet 760 FT-IR bench and Nic-PlanTM microscope with a computer-controlled x-y-z sample stage. The beamline allows light only between 400 and 10000 cm^{-1} to strike the sample with diffraction-limited (3-10 μm diameter) area and high brightness intensity (1.3 X 10^{-2} mW μm^{-2}) about ~150 times that of the terminal light source. 48-96 spectra were recorded at a spectral resolution of 4 cm^{-1} with 32-64 scans averaged. Major spectral differences in the geniculum-intergeniculum area map were analyzed using Principal Component Analysis (PCA) on all recorded spectra.

5.3.8. *NMR spectroscopy*

Ball-milled *Calliarthron* fronds (20-30 mg) were dissolved in 1:1 H_2O: D_2O solutions (0.5 mL), agitated 24 h at room temperature, and centrifuged. Proton decoupled 125 MHz ^{13}C NMR spectra were recorded on a spectrometer (Bruker AM-600, Germany) at room temperature, with external reference of tetramethylsilane (TMS). The

parameters were as follows: pulse angle 51.4°, acquisition time 0.56 s, relaxation delay 0.6 s, spectral width 29.4 kHz and scans 19,000-34,000. Chemical shifts were referenced to (δ 31.1 ppm).

5.4. Results

5.4.1. *Chemical analysis*

Extractions from whole *Calliarthron* fronds contained mainly galactose, high levels of 6-methyl galactose and xylose, and moderate amounts of 2-methyl galactose and mannose (Table 5-1). Galactose plus mono-O-methyl galactose and xylose units comprise 93.9% of the total sugar content of *Calliarthron*, similar to other coralline algae. Intergenicular polysaccharides were similar to whole-thalli polymers, but with higher amounts of 2-O-methyl galactose and xylose units. Young intergenicula were similar to old intergenicula, but with slightly increased 2-methyl galactose (Figure 5-4A). Unlike intergenicula, genicula had very high levels of 6-methyl galactose and low levels of xylose and 2-methyl galactose (Table 5-1). Old genicula had more 6-methyl galactose than young genicula (Figure 5-4B). No 3- or 4-methoxyl groups were detected on the galactose units in *Calliarthron* (Table 5-1).

Table 5-1. Composition of galactans from *Calliarthron* tissues, including comparison to other coralline species.

Coralline species	Monosaccharide composition (mol %)							
	Gal	2-*O*-Me-Gal	3-*O*-Me-Gal	4-*O*-Me-Gal	6-*O*-Me-Gal	Xyl	Man	Reference
Calliarthron cheilosporioides	61.8	6.2	-	-	10.3	15.6	4.5	*This study*
Genicula only	72.5	2.4	-	-	19.4	2.9	2.8	*This study*
Intergenicula only	55.8	11.3	-	-	7.1	20.7	5.1	*This study*
Bossiella orbigniana	45.3	11.5	5.0	-	9.4	25.2	3.6	Navarro & Stortz 2002
Corallina officinalis	51.1	14.6	3.6	2.2	1.5	24.8	2.2	Navarro & Stortz 2002
Corallina vancouveriensis	60.9	10.8	3.4	2.3	tr.	22.6	n.d.	Cases et al. 1992
Jania rubens	55.1	6.6	5.1	-	2.9	27.9	2.2	Navarro & Stortz 2002
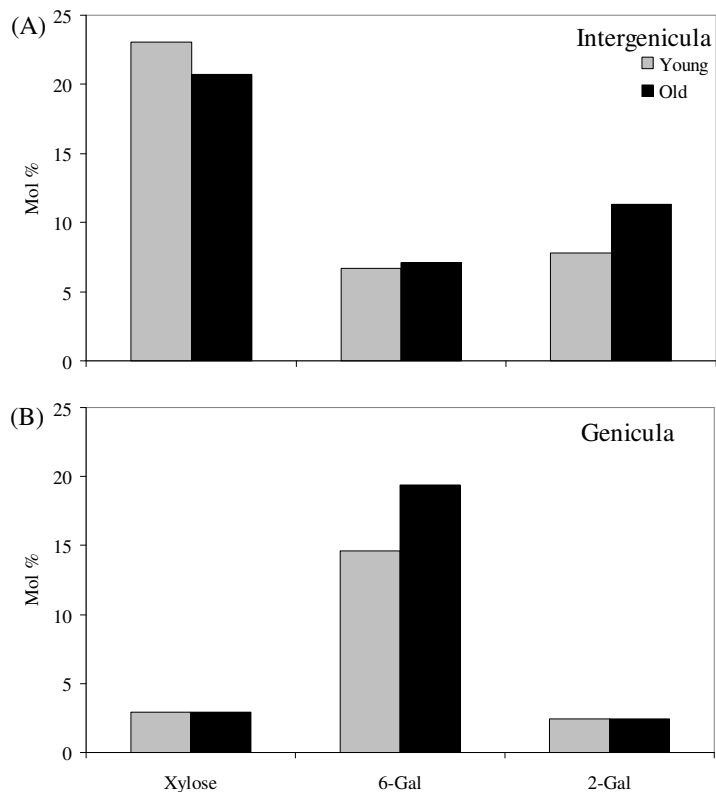
Figure 5-4. Differences in galactan side chains present in young (gray) and old (black) tissue of (A) intergenicula and (B) genicula.

5.4.2. *Dry weight proportions*

Old genicula contained 15% cellulose per dry weight, almost twice as much cellulose as young genicula (8.1%; Figure 5-5). Old and young intergenicula contained similar amounts of cellulose, approximately 13.8% of dry, decalcified weight.
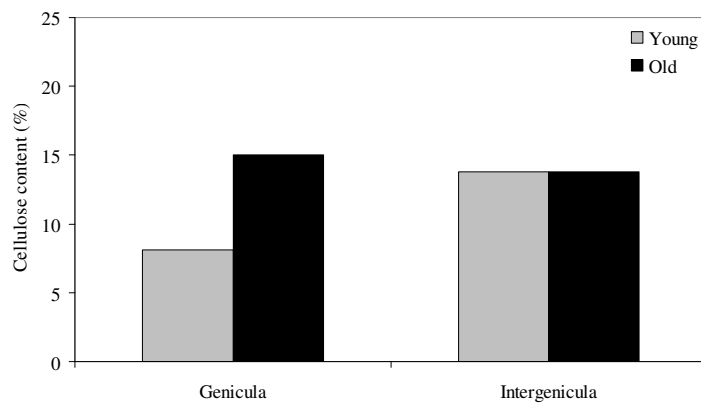
Figure 5-5. Cellulose content of young (gray) and old (black) tissue from genicula and intergenicula. Values are percent of dry, decalcified weight.
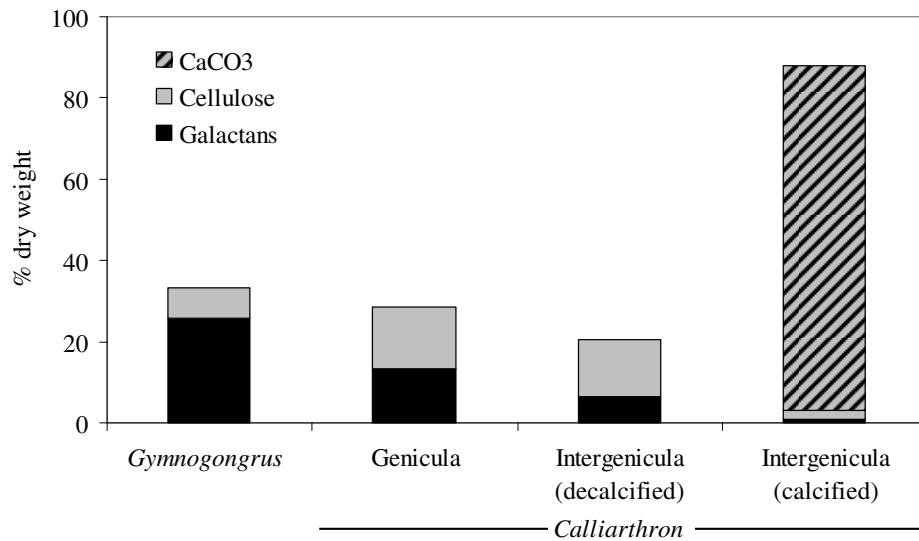
Figure 5-6. Comparison of polysaccharide content between the calcified seaweed *Calliarthron* and the fleshy seaweed *Gymnogongrus* (Estevez et al. 2007).

Genicula consisted of approximately 28.5% polysaccharide per dry weight, divided almost exactly in half by galactans (15%) and cellulose (13.5%) (Figure 5-6). Intergenicula consisted of 20.4% polysaccharide per dry decalcified weight, with fewer galactans (6.6%) than cellulose (13.8%) (Figure 5-6). Calcium carbonate comprised 84.7 ± 0.4% (mean ± 95% C.I.) of the dry weight of *Calliarthron* and dominated the cell wall of intergenicula (Figure 5-6). Overall, genicula comprised 3.3 ± 0.1% (mean ± 95% C.I.) of the dry calcified weight of *Calliarthron* fronds, but comprised approximately 21.8% of the dry decalcified weight (Figure 5-7).
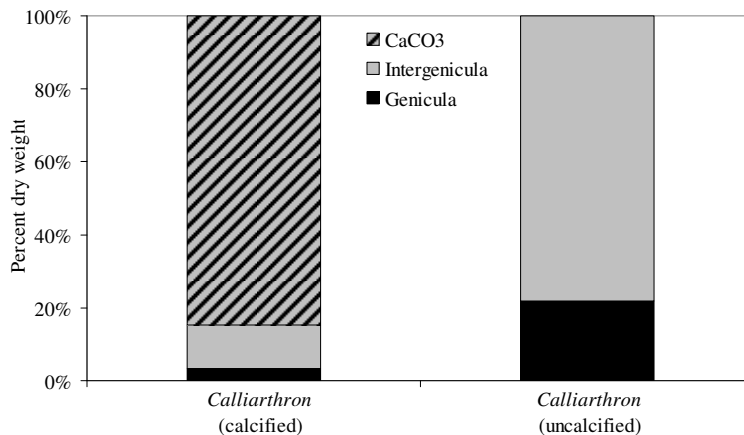
Figure 5-7. Percent dry weight of (A) calcified and (B) uncalcified *Calliarthron* fronds composed of genicula (black), intergenicula (gray), and $CaCO_3$ (striped).

5.4.3. *Linkage analysis*

Linkage analysis revealed high levels of 3-linked galactose (as 2,4,6-*O*-methyl galactose) and 4-linked galactose units (as 2,3,6-tri-*O*-methyl galactose) in *Calliarthron* genicula and relatively low levels of xylose with a 4-linked xylose : terminal xylose ratio of about 2:1 (Table 5-2). Most of the 6-*O*-methyl galactose detected in the sugar analysis (Table 5-1) was likely included in the 2,4,6-*O*-methyl galactose derivative.

Intergenicula had high levels of 3-linked galactose residues, but fewer 4-linked galactose units. In a similar way, most of the 2-*O*-methyl galactose detected in the sugar analysis (Table 5-1) are included in the 2,4,6-*O*-methyl galactose derivative. Intergenicula contained higher levels of xylose with a 4-linked xylose : terminal xylose ratio of about 3:1 (Table 5-2). Intergenicula had more 4-linked 6-substituted galactose residues than genicula, and both genicula and intergenicula had very low levels of 3-linked 6-substituted galactose units.

Table 5-2. Methylation linkage analysis of *Calliarthron* tissues, including comparison to two different coralline species. All values given as mol%.

Monosaccharide	Methylated product	*Calliarthron cheilosporioides*			*Corallina pilulifera*	*Corallina officinal.*
		Genicula	Intergenicula	Whole	Whole[a]	Whole[b]
Galactose						
t-Gal	2,3,4,6-*O*-Me	9.7	9.5	6	1	22
3-Gal	2,4,6-*O*-Me	33.4	24.2	18.9	4	16
4-Gal	2,3,6-O-Me	20.9	6.7	16.2	26	21
3,4-Gal	2,6-O-Me	2.5	1	1.9	4	5
2,4-Gal	3,6-O-Me	1.9	1	2.7	8	2
4,6-Gal	2,3-O-Me	2.1	5.8	5.5	1	-
3,6-Gal	2,4-O-Me	1	1	2.7	30	18
Xylose						
t-Xyl	2,3,4-*O*-Me-X	3.7	6.8	11.8	26	15
4-Xyl	2,3-*O*-Me-X	5.7	16.4	6.8	n.d.	n.d.

[a] Usov et al. 1997

[b] Cases et al. 1994

5.4.4. *FT-IR microspectroscopy*

In the FT-IR spectral analysis, the two principal components (PC1 and PC2; Figure 5-8) comprised approximately 90% of the variance in the spectral dataset. PC1 showed clear peak absorbances at 1380 cm^{-1}, corresponding to sulphate esters, and at 1258-1230 cm^{-1}, related to asymmetric stretching of sulphate bonds (Figure 5-8). Both bands associated with sulfate groups showed higher intensities in the genicula cells. PC1 also showed absorbances at 1650 cm^{-1} and 1540 cm^{-1}, corresponding to stretching of amide I bonds and bending of amide II bonds (Pelton and McLean 2000), respectively, primarily in intergenicula. PC2 showed absorbances at 1025, 1056, 1103, and 1159 cm^{-1}, corresponding to cellulose (Kakurakova et al. 2000) with higher intensities in intergenicula. The band at 1159 cm^{-1} could be assigned to the glycosidic C-O-C vibration of (1→4)-β-D-glucopiranosyl, whereas the peaks at 1056 and 1025 cm^{-1} could be associated with C-O-C and C-C bonds of the glucose rings, respectively (Kakuráková et al. 2000).
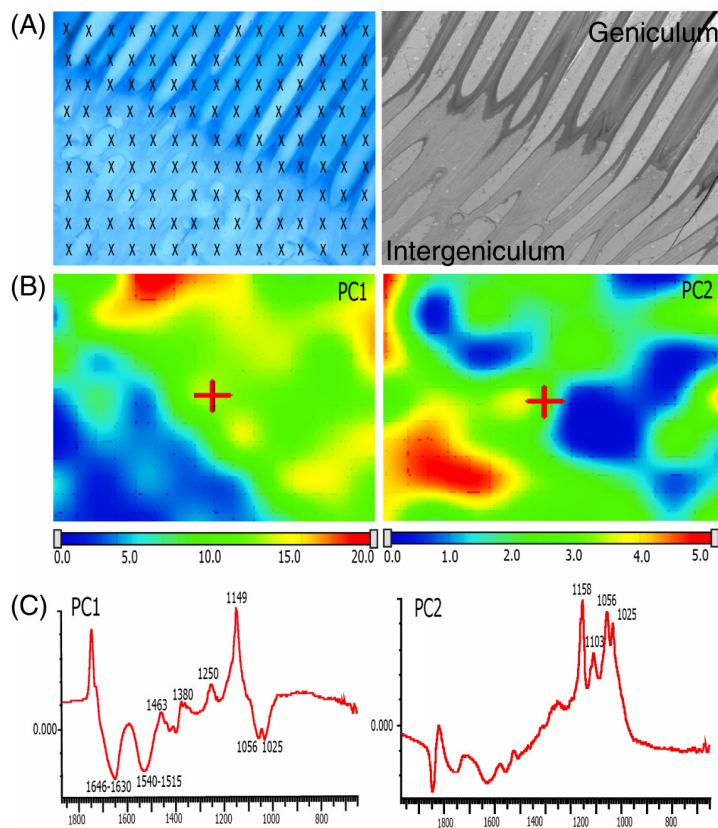
Figure 5-8. SR-FTIR spectromicroscopy data were collected at the intergeniculum-geniculum transition zone (A) and demonstrated clear spectral differences (B). Data were analyzed in terms of two principal components (C).

5.4.5. C^{13} NMR spectra

The C^{13} NMR spectrum of the water soluble galactans from *Calliarthron* is shown in Figure 5-9. Structural units in the galactan backbone were assigned (Table 5-3) and annotated (Figure 5-9) based on results from the sugar and linkage analyses (Table 5-1 and Table 5-2) and previous C^{13} NMR spectra of coralline algal galactans (Usov et al. 1997). The most evident signals corresponded to β-D-xylose units (104.3, 73.7, 76.4, 70.0, 65.8 ppm) linked to C-6 of either galactose unit (61.4-61.6 ppm) (Figure 5-9, Table 5-3). The ratio of D-galactose:L-galactose units was close to 1:1 according to the relative intensities of the anomeric signals in both spectra. β-D-galactose units were primarily substituted with 6-*O*-methyl groups (104.1 ppm) or were not substituted at all (103.3 ppm). L-galactose units were primarily not substituted (101.3 ppm) or substituted with 2-*O*-methyl groups (98.8 ppm). Infrequently, these units

were substituted with 2-sulfate groups (99.3 ppm). A signal corresponding to floridean starch was detected at 100.7 ppm.
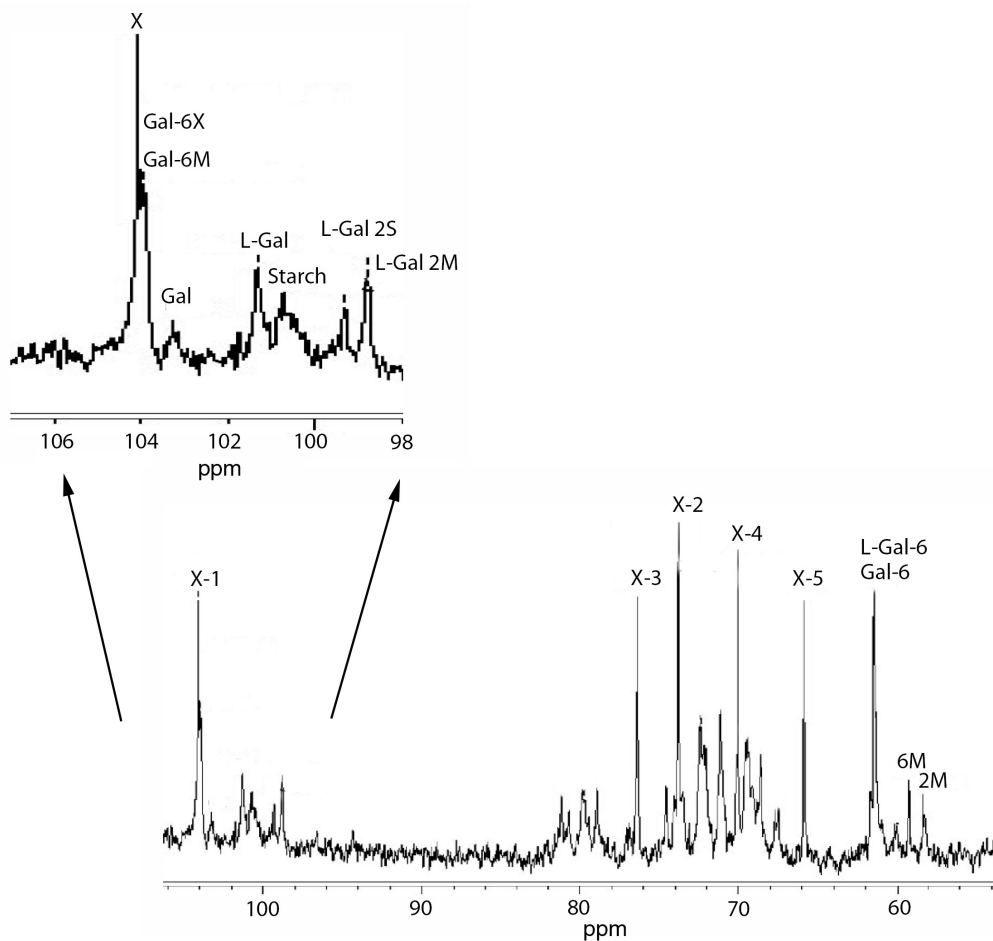
Figure 5-9. ^{13}C NMR spectrum of polysaccharides extracted from *Calliarthron*.

Table 5-3. Assignments (ppm) of ^{13}C NMR spectra for *Calliarthron*.

Residue	C-1	C-2	C-3	C-4	C-5	C-6
D-galactose units (G)						
G	103.3	71.1	81.2	69.4	74.6	61.4
G-**6M**	104.1	71.1	80.6-81.2	68.6	73.6	69
G-**6X**	104.1	71.1	80.6-81.2	~69.5	74.6	69.4
L-galactose units (LG)						
LG	101.3	69.4	70.4	79.8	72.4-72.0	61.6
LG-**2S**	99.3	78.9	67.8	77	71.6	61.4
LG-**2M**	98.8	79.1	69.4	79.5	72.4-72.0	61.4
t-Xyl	104.3	73.7	76.4	70	65.8	-
Floridean starch	100.7	71.9	78.4	78.2	72.4	62

5.5. Discussion

5.5.1. *Chemical differences between genicula and intergenicula*

This study identifies important differences in cell wall chemistry among *Calliarthron* genicula and intergenicula. Intergenicula contain high levels of xylose that likely form long side chains approximately 4-units in length (given the high methylated xylose ratio). Because intergenicula had very low levels of 3,6-linked galactose, linkage results suggest that these xylose side chains are rarely substituted on β-D-galactose, unlike sugars extracted from other corallinoids (Cases et al. 1994, Usov et al. 1997). Furthermore, intergenicula had surprisingly low levels of 4-linked galactose, suggesting that α-L-galactose units are rarely unsubstituted and may, instead, have xylose side chains. This conclusion is supported by high levels of 4,6-linked galactose in intergenicula, which suggests xylose side-chains may link to C-6 of α-L-galactose. This result is in sharp contrast to previous studies of coralline algae that demonstrated abundant single xylosyl substitutions on 3-linked β-D-galactose units (reflected by high 3-linked 6-substituted galactose content and only terminal xylosyl units, Table 5-2).

High levels of 3-linked galactose in *Calliarthron* intergenicula suggest unsubstituted β-D-galactose units or 2-*O*-methyl or 6-*O*-methyl substitutions, which were detected in moderate amounts (Table 5-1) and may have been included together in the 2,4,6-tri-*O*-methyl derivative detected in the methylation analysis signal (Table 5-2). Likewise, 4-linked galactose units in *Calliarthron* intergenicula suggest that some 2-*O*-methyl or 6-*O*-methyl groups may also occur on α-L-galactose. In contrast, *Corallina* species had higher levels of unsubstituted or 2-*O*-methylated α-L-galactose units (reflected in high 4-linked galactose, Table 5-2). In order to differentiate the exact position of methoxyl groups in *Calliarthron* polysaccharides, an ethylation analysis is currently under way.

Unlike intergenicula, *Calliarthron* genicula contained very little xylose that, when present, formed shorter side chains with an average length of 3 xylose. Instead,

genicula had very high levels of 6-*O*-methyl substitutions that continue to increase as fronds age. High levels of 3-linked galactose suggest that these methoxyl groups were found on C-6 of β-D-galactose. High levels of 4-linked galactose suggest that α-L-Galactose units are either unsubstituted or also highly methylated at C-6. Again, this differs from previous studies that found many 6-xylosyl and few 6-methyl substitutions in other genera (Table 5-1 and Table 5-2).
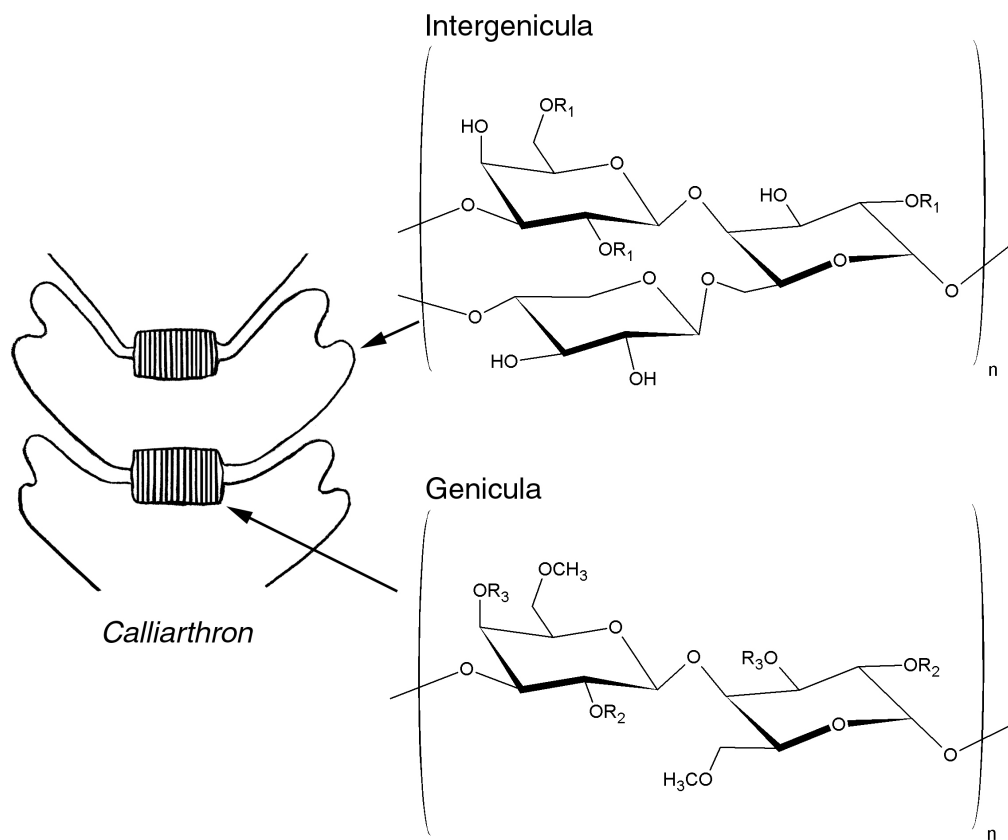
Figure 5-10. Predominant galactan composition of *Calliarthron* intergenicula and genicula. (R₁=some methyl groups, R₂=methyl or sulfate groups, R₃=some sulfate groups)

FT-IR data show higher levels of sulfate groups in genicula than in intergenicula. This is supported by slightly elevated levels of 3-linked 4-substituted or 4-linked 3-substituted galactose and 4-linked 2 substituted galactose in genicula, suggesting putative sulfate substitutions at C-2 and C-3 of α-L-galactose units and/or C-4 of β-D-galactose.

In sum, these data suggest that intergenicular cells produce xylogalactans with little methylation, while genicular cells biosynthesize highly methylated galactans with very few xylose side chains. This structural difference could be a consequence of high xylosyltransferase activity in intergenicula and low (or repressed) xylosyltransferase activity in genicula. It is also possible that putative methoxyl transferases block the C-6 of the α-L-galactose units before xylosyltransferases can add pentose sugars to the galactan backbone. In essence, 6-methyl groups in genicula cell walls replace the 6-xylosyl units present in the intergenicula cell walls. In addition, sulfate substitutions in genicular galactans may replace 2-methyl groups found in intergenicula, further suggesting differences in methoxyl transferase activity.

5.5.2. *Interpretation of previous studies*

Previous studies of polysaccharide chemistry in articulated coralline algae (e.g., Cases et al. 1992, 1994, Usov et al. 1997, Navarro and Stortz 2002) likely overlooked significant differences between genicula and intergenicula tissues. Data reported for other corallines are difficult to interpret because genicula are chemically distinct from intergenicula and comprise a significant proportion of the decalcified dry weights of articulated fronds (20% in *Calliarthron*). For example, high levels of 6-*O*-methyl groups in *Bossiella orbigniana* (Table 5-1) may specifically reflect similarities between *Calliarthron* and *Bossiella* genicula, perhaps related to the similar morphologies of these two species.

5.5.3. *Effect of polysaccharides on mechanical properties*

Without calcium carbonate, intergenicula and genicula synthesize comparable amounts of polysaccharide to other fleshy red algae, such as *Gymnogongrus*. However, *Calliarthron* produces more cellulose (1-8%) and less galactan than other red algae (Kloareg and Quatrano 1988). After an initial decline in cellulose content as cells transition from intergenicula to genicula (see Figure 5-5 and Figure 5-8), the

cellulose content of genicular cell walls doubles over time, coinciding with the thickening of genicular cell walls demonstrated in Chapter 2 (see Chapter 6 for further details about genicular cell wall elaboration). This increase in cellulose explains, at least in part, the increase in genicular tissue strength over time (Chapters 1 and 2). Chemical evidence of cellulose supports past observations of unknown fibrillar components in genicular cell walls (Borowitzka and Vesk 1978, 1979).

Differences in galactan substitution patterns among genicula and intergenicula likely affect the spacing and arrangement of adjacent molecules within coralline cell walls. For example, the lack of xylose side chains in genicular cells may allow for (or be the result of) compaction of polymers into elongating, thin genicular cell walls. Furthermore, replacing hydrophilic xylose groups with hydrophobic methoxyl groups may change the properties of polysaccharides within genicular cell walls. Changes in polysaccharide chemistry have been shown to affect mechanical properties of algal cells (Toole et al. 2002), and I plan to explore correlations between chemical composition and mechanical properties of genicular cell walls in the future.

5.5.4. *Effect of polysaccharides on calcification and decalcification*

Differences in galactan substitutions may be linked to calcification and decalcification in coralline algae.   Polysaccharide production can influence precipitation of calcium carbonate into coralline cell walls by generating sites for crystal nucleation, by attracting ions electrostatically, or by affecting the type of $CaCO_3$ isomorph deposited (Borowitzka 1977, Cabioch and Giraud 1986, Borowitzka 1987, Bilan and Usov 2001). Although the details are not well-understood, $CaCO_3$ crystals align precisely along an organic matrix (thought to be a protein-polysaccharide complex) within coralline cell walls (Borowitzka and Vesk 1978, Cabioch and Giraud 1986, Borowitzka 1987). It is reasonable to hypothesize that the highly-branched structure of xylogalactans (and higher protein content) of intergenicula may help define sites for calcium carbonate nucleation. Consequently, shifts in polysaccharide production may be directly linked to genicular decalcification. For example, Pueschel *et al.* (2005)

described an abundance of organic material secreted into coralline cross-walls during localized decalcification. Whether this material actively contributed to decalcification is an open question. Explorations into the genicular chemistry of articulated genera, such as *Metagoniolithon*, that have genicula which do not form via decalcification would lend insight to these patterns.

TO FORTIFY A CORALLINE:
SECONDARY CELL WALLS AND LIGNIN PRECURSORS IN *CALLIARTHRON* GENICULA

6.1. Abstract

Genicular tissue from the articulated coralline *Calliarthron* is stronger and stiffer than other algal tissues. Previous studies demonstrated that tissue strengthening results from thickening of genicular cell walls, but tissue stiffness is likely a consequence of distinct material composition. Stiff, thickened cell walls are characteristic of the vessel and fiber elements of terrestrial plant xylem, which produce secondary cell walls fortified with lignin. Electron microscopy revealed the presence of secondary cell walls in genicular cells that develop after cell elongation ceases. Mass spectrum analyses demonstrated that *Calliarthron* genicula contain three distinct monolignols, which polymerize to form P-, G-, and S-lignins in terrestrial plants. Secondary cell walls and monolignols are known only from terrestrial plant tissues and have never been described in marine algae. Lignin histochemistry corroborated mass spectra results, suggesting that G-monolignols are concentrated in secondary cell walls, while G- and S-monolignols may be present at lower levels in primary walls. Data presented here suggest the need to re-examine the evolutionary history of lignified cell walls. Developmental pathways for both secondary cell walls and monolignols may have evolved in the common ancestor of red and green algae more than 1 billion years ago or may have evolved convergently in coralline algae and land plants as adaptations to mechanical stress.

6.2. Introduction

Previous studies have demonstrated that joints, called genicula, play a critical role in the survival of articulated coralline algae by lending flexibility to calcified algal thalli, allowing them to bend and reconfigure to resist drag forces imposed by breaking waves (Chapters 1-4). Genicular tissue is much stronger than other algal tissues and even stronger than some terrestrial plant tissues, such as *Arabidopsis* stem (Figure 6-1A), perhaps due to the great quantity of supportive cell wall – up to 50% of tissue volume – in mature genicula (Chapter 2).
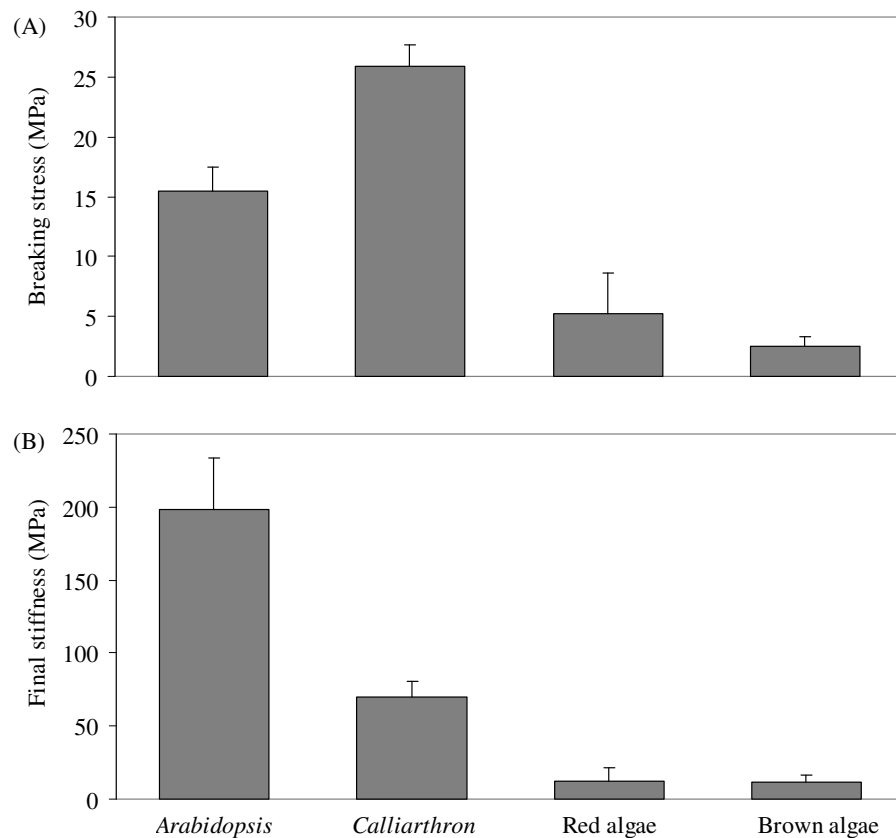
Figure 6-1. (A) Breaking stress and (B) final stiffness of *Arabidopsis* stems, *Calliarthron* genicula, and several red and brown algal tissues. Data are means ± 95% CI. See methods for analysis details.

Cell wall thickening in *Calliarthron* genicula occurs after genicula have fully formed (Chapter 2); that is, after cells have completely decalcified, been revealed by cortical dissolution, and ceased their approximately ten-fold elongation (Johansen 1969a, 1981). Thickening of cell walls following cell elongation is characteristic of

secondary cell wall formation in terrestrial xylem (Raven et al. 2003) and has not been described in other marine algal tissues, which are widely considered to have only primary walls (Kloareg and Quatrano 1988, Craigie 1990, Tsekos et al. 1993). Nevertheless, past studies have noted thick cell walls in genicula (Yendo 1904, Johansen 1969a, Johansen 1974, Borowitzka and Vesk 1978, Johansen 1981) and have linked wall thickness to distinct layers within genicular cell walls (Bailey and Bisalputra 1970, Borowitzka and Vesk 1979), but none has examined young and old genicula to document the development of layers within genicular cell walls.

In addition to the breaking stress of genicular tissue, the final stiffness (i.e., the tissue stiffness that immediately precedes breakage) is distinct from both terrestrial and algal tissues, assuming an intermediate value (Figure 6-1B). In general, marine algal tissues are quite compliant (i.e. have low tissues stiffness) (Hale 2001), possibly resulting from high amounts of matrix polysaccharides relative to skeletal components in their cell walls (McCandless and Craigie 1979, Kloareg and Quatrano 1988). Conversely, terrestrial tissues, such as xylem, are much stiffer due in part to the presence of lignin, a complex racemic-branched heteropolymer that cross-links other cell wall components, such as cellulose microfibrils, in secondary cell walls (Wainwright et al. 1982). By providing rigidity to ancestral tracheids, preventing the collapse of conductive vessels, and helping plants grow erect in air without toppling, lignification of secondary cell walls is widely considered to have been a key innovation in the evolution of terrestrial plants from aquatic ancestors some 475 million years ago (Kendrick and Crane 1997, Friedman and Cook 2000, Boyce et al. 2004, Peter and Neale 2004).

Lignins can be derived from three types of monolignols: p-coumaryl, coniferyl, and sinapyl alcohols, comprising p-coumaryl "P"-lignin, guaiacyl "G"-lignin, and sinapyl "S"-lignin, respectively (Lewis 1999, Peter and Neale 2004). P-lignin and G-lignin, considered to be ancestrally conserved forms of lignin, are found in both angiosperms and gymnosperms (Peter and Neale 2004). S-lignin, however, is derived from the G-lignin pathway and has been found only in angiosperms (Peter and Neale 2004). All

lignins are thought to be terrestrial in origin and have never been found in non-vascular organisms, such as aquatic algae (Ragan 1984, Lewis 1999, Friedman and Cook 2000, Boyce et al. 2004, Peter and Neale 2004).

Given the well-documented thickening of *Calliarthron* genicular cell walls (Chapter 2) and the unique material properties of genicula (Figure 6-1), I hypothesized that *Calliarthron* genicula have lignified secondary cell walls. In this study, I use transmission electron microscopy on young and old tissue to carefully describe the development and structure of genicular cell walls, and I employ histological stains and chemical techniques to detect monolignols within genicular tissue.

6.3. Materials & Methods

6.3.1. *Comparison of mechanical properties*

All mechanical data presented here were extracted from previous studies. Breaking stresses were obtained for *Arabidopsis* stems (Jones et al. 2001), *Calliarthron* genicula (Chapter 1), and several red (N=11) and brown (N=18) algal tissues (see species list below).

Final stiffness data were collected for *Calliarthron* genicula by re-analyzing stress-strain curves generated in Chapter 3 (N=15). Two linear regressions were fitted to J-shaped data at low and high strains from each geniculum. by incrementally adding datapoints to the first linear regression and removing datapoints from the second regression to maximize R^2 fit of both lines. Final stiffness (i.e., stiffness at high strains) was calculated as the slope of the second regression.

Final stiffness data were also obtained for *Arabidopsis* stems (Koehler and Spatz 2002) and several red (N=10) and brown (N=16) algal tissues (see species list below).

Data were collected for the following red algae (all data were collected in tension and asterisks indicate that no stiffness data were available): *Chondracanthus harveyanus*

(Hale 2001), *Chondracanthus exasperatus* (Koehl 2000), *Chondrus crispus* (Carrington et al. 2001), *Endocladia muricata* (Hale 2001), *Gracilariopsis lemaneiformis* (Hale 2001), *Mastocarpus papillatus* (Kitzes and Denny 2005)*, *Mastocarpus stellatus* (Dudgeon and Johnson 1992), *Mazzaella flaccida* (Hale 2001), *Nemalion helminthoides* (Hale 2001), *Porphyra occidentalis* (Hale 2001), and *Prionitis lanceolata* (Hale 2001).

Data were collected for the following brown algae (all data were collected in tension and asterisks indicate that no stiffness data were available): *Alaria marginata* (Hale 2001), *Desmarestia ligulata* (Hale 2001), *Dictyoneuropsis reticulate* (Hale 2001), *Durvillaea Antarctica* (Harder et al. 2006), *Durvillaea willana* (Harder et al. 2006)*, *Egregia menziesii* (Hale 2001), *Eisenia arborea* (DeWreede et al. 1992)*, *Fucus distichus* (Hale 2001), *Hedophyllum sessile* (Armstrong 1987), *Hesperophycus californicus* (Hale 2001), *Laminaria digitata* (Harder et al. 2006), *Laminaria hyperborea* (Harder et al. 2006), *Lessonia nigrescens* (Koehl 1986)*, *Macrocystis pyrifera* (Hale 2001), *Nereocystis luetkeana* (Johnson and Koehl 1994), *Silvetia compressa* (Hale 2001), *Postelsia palmaeformis* (Holbrook et al. 1991), and *Pterygophora californica* (Biedka et al. 1987).

6.3.2. *Sample collection.*

Calliarthron cheilosporioides were collected from the wave-exposed, low intertidal zone at Hopkins Marine Station, Pacific Grove, CA.

6.3.3. *Sample preparation.*

Calliarthron thalli were fixed at 4° C in 1% formaldehyde: 1% glutaraldehyde: 98% seawater and decalcified in 1N HCl. Genicula were dissected from fronds, dehydrated through an ethanol series, and embedded with Spurr's low viscosity resin, as described in Chapter 2. *Arabidopsis* stem sections were prepared and viewed as described by Turner and Somerville (1997).

6.3.4. *Transmission electron microscopy.*

Ultra-thin sections were cut with a diamond knife (Diatome Ltd., Bienne, Switzerland) on a Leica Ultracut S (Leica Microsystems GmbH, Wetzlar), mounted on Formvar coated grids, and stained for 20 seconds in 3% uranyl acetate in 50% acetone followed by 3 minutes in 0.2% lead citrate. Images were taken using a JEOL 1230 TEM (Jeol Ltd., Akishima, Tokyo, Japan) at 80kV using a Gatan peltier-cooled Bioscan camera (Gatan, Pleasanton, California).

6.3.5. *Monolignol analysis.*

Calliarthron genicula and intergenicula were separated from one another, as described in Chapter 5. Whole fronds and isolated genicular and intergenicular tissue were ball milled and extracted with ethanol, acetone, and chloroform for removing the low molecular weight soluble components. Material was de-calcified with diluted HCl, and incubated in water (X2) to extract the water-soluble polysaccharides. The residue obtained was treated with crude cellulases (Cellulysin, Calbiochem). Samples were then extracted with 96:4 dioxane/water (Bjorkman 1954). Derivatization followed by reductive cleavage (DFRC method), release and quantification of acetylated monolignols by reductive cleavage of aryl ethers was performed as described previously (Lu and Ralph 1999). Briefly, for GC/MS analysis, 5-10 mg of substrates were used for DFRC. AcBr treatment products were separated on normal-phase preparative (2-mm) TLC plates (Alltech, Deerfield, IL) using $CHCl_3$/EtOAc (20:1) as solvent.

6.3.6. *Monolignol histochemistry*

In order to localize monolignols, tissues were dyed with Maule reagent, Phloroglucinol-HCl, and acriflavine, three histological stains commonly used to detect lignins in terrestrial plant xylems (Lewis and Yamamoto 1990, Jones et al. 2001, Christiernin et al. 2005, Patten et al. 2005). Maule reagent differentiates S-lignins (red reaction) from G-lignins (orange-brown reaction), Phloroglucinol-HCl reacts specifically with G-lignins, and acriflavine causes generic lignins to fluoresce.

Semi-thin sections (4 µm) were cut with glass knives on a microtome (DuPont Instruments, Sorvall®, model MT2-B) and mounted on glass slides. Sections were stained with Maule and Phloroglucinol-HCl reagents according to Krishnamurthy (1999). Briefly, Maule staining was performed by first incubating sections in 1% $KMnO_4$, and after 10 min, sections were washed with water, and acidified with 2% HCl for 1 min, washed again, and then incubated in $NaHCO_3$. For Phloroglucinol-HCl staining, cross sections were placed in 1% Phloroglucinol in ethanol:water (7:3) with 20% HCl. Slides were viewed with a compound microscope (Leitz DMRB, Leica, Deerfield, IL). 1% Acriflavine was applied on the cross sections and fluorescence was followed at 488 nm for emission and 522/520 nm for excitation in the confocal microscope (see LSCM).

6.3.7. *Laser Scanning Confocal Microscopy (LSCM).*

Confocal imaging was performed using an MRC 1024 laser scanning confocal head (Bio-Rad, Hercules, CA) mounted on a Diaphot 200 inverted microscope (Nikon, Tokyo, Japan), a Zeiss 510 laser scanning confocal microscope, and a Leica TCS SP2 AOBS. The objectives used were a 60 X Nikon PlanApo water immersion (WI) 1.2 numerical aperture; Technical Instruments, San Francisco), a 40X Nikon PlanApo WI 0.9 NA, and a HCX PL APO 63X/1.2 W Corr/0.17 Lbd. Bl. objective. The samples incubated with acriflavine were excited with two lasers (Ar/Kr and He/Cd) at 488 nm and 522/520 nm. All images were processed with Adobe Photoshop 7.0 (Adobe Systems, Mountain View, CA).

6.4. Results

6.4.1. *Transmission electron microscopy*

Transmission electron micrographs revealed the presence of secondary cell walls in *Calliarthron* genicular cells. Immature cells had thick primary walls and negligible secondary walls (Figure 6-2A,B). However, mature genicular cells had distinct

secondary walls that developed along the inner surface of primary walls (Figure 6-2C,D). Unlike primary walls, secondary cell walls were striated (Figure 6-2D), suggesting differences in composition or mode of deposition. Mature genicular cells resembled multi-layered fiber cells from *Arabidopsis* xylem (Figure 6-2E). Calcified cell walls in intergenicula had only primary walls (Figure 6-2F). The distal ends of genicular cells remain calcified, connected to adjacent intergenicular cells via pit connections (Figure 6-2G). Pit plugs were found only on the geniculum side of geniculum-intergeniculum pit connections (Figure 6-2G).
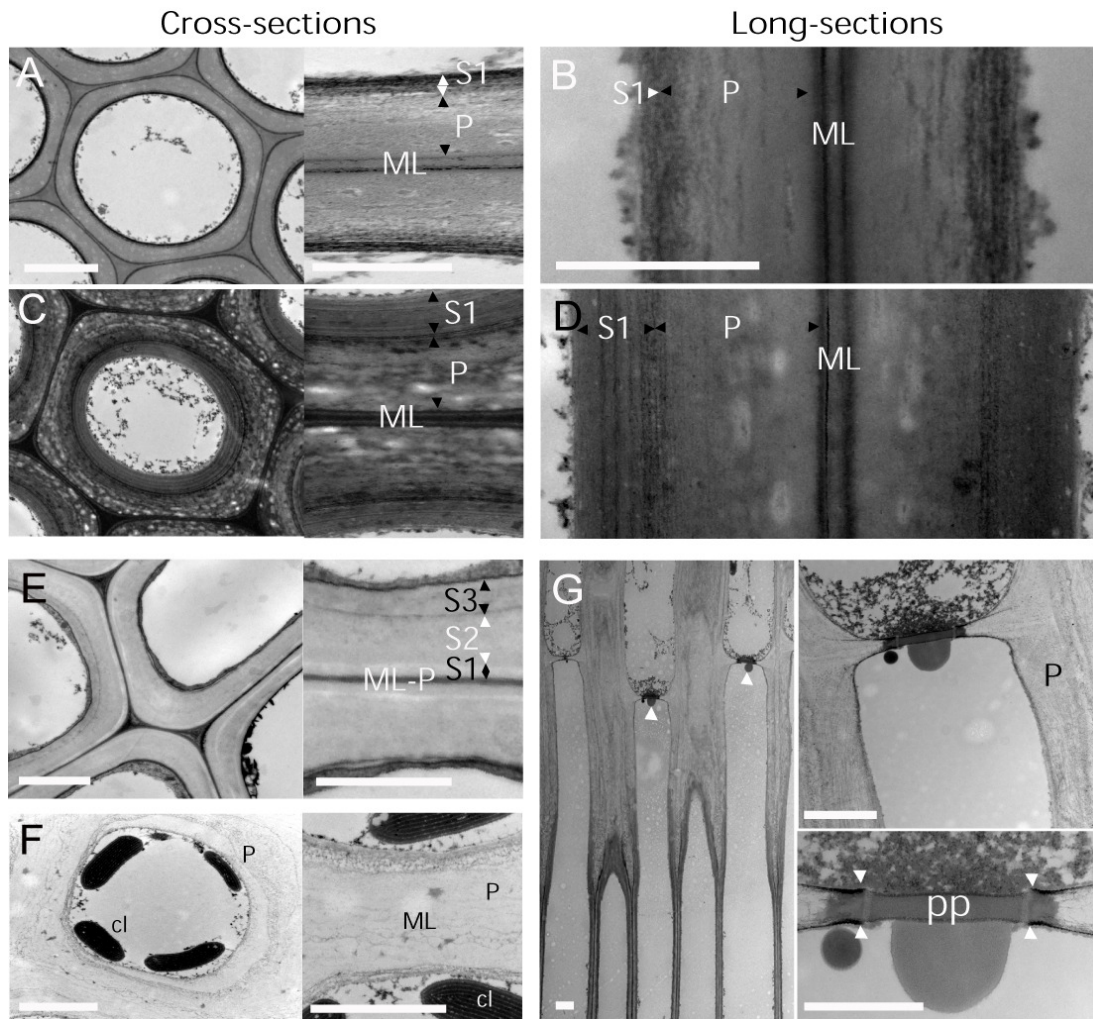
Figure 6-2. Ultra-structure of *Calliarthron* genicular cell wall with comparisons to intergenicula and *Arabidopsis* xylem. Immature genicular cells (A, B) have distinct primary walls, while mature genicular cells (C, D) develop secondary cell walls, resembling fiber cells from *Arabidopsis* xylem (E). Intergenicular cells (F) have calcified primary cell walls. The distal ends of genicular cells remain calcified, connecting to intergenicula cells via pit connections (G). P=primary wall, S1-S3=secondary cell wall layers, cl=chloroplast, ML=middle lamella, pp=pit plug. Scale bars=2 μm.

6.4.2. *DFRC monolignols*

Mass spectrum analysis confirmed that *Calliarthron* fronds contain three types of monolignols (Figure 6-3). Total ion and mass selected chromatograms indicated that both genicula and intergenicula possess all three monolignols (Figure 6-4).

(A) Synthetic monolignols
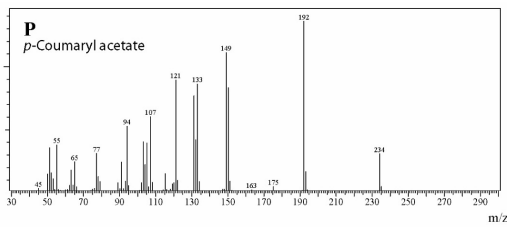
(B) *Calliarthron cheilosporioides*
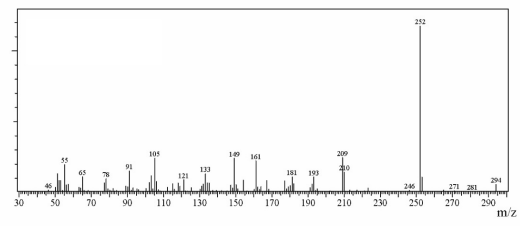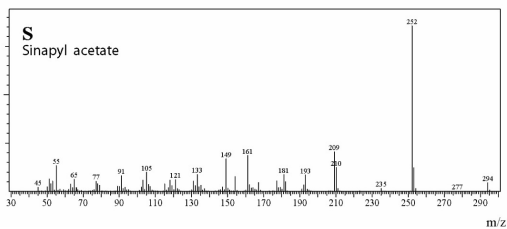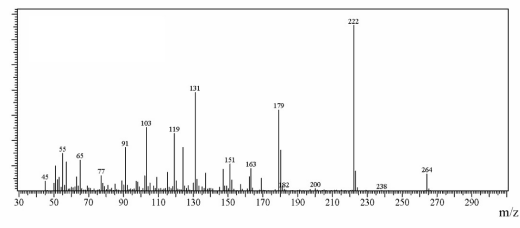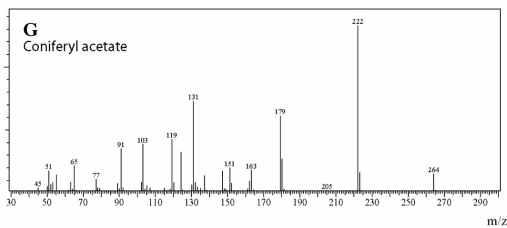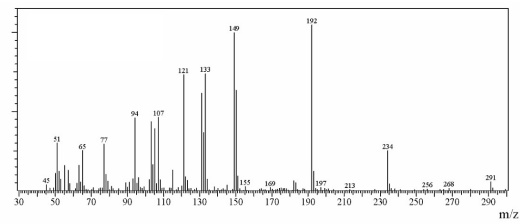
Figure 6-3. Mass spectra of (A) synthetic monolignols and (B) DFRC monolignols derived from *Calliarthron*.
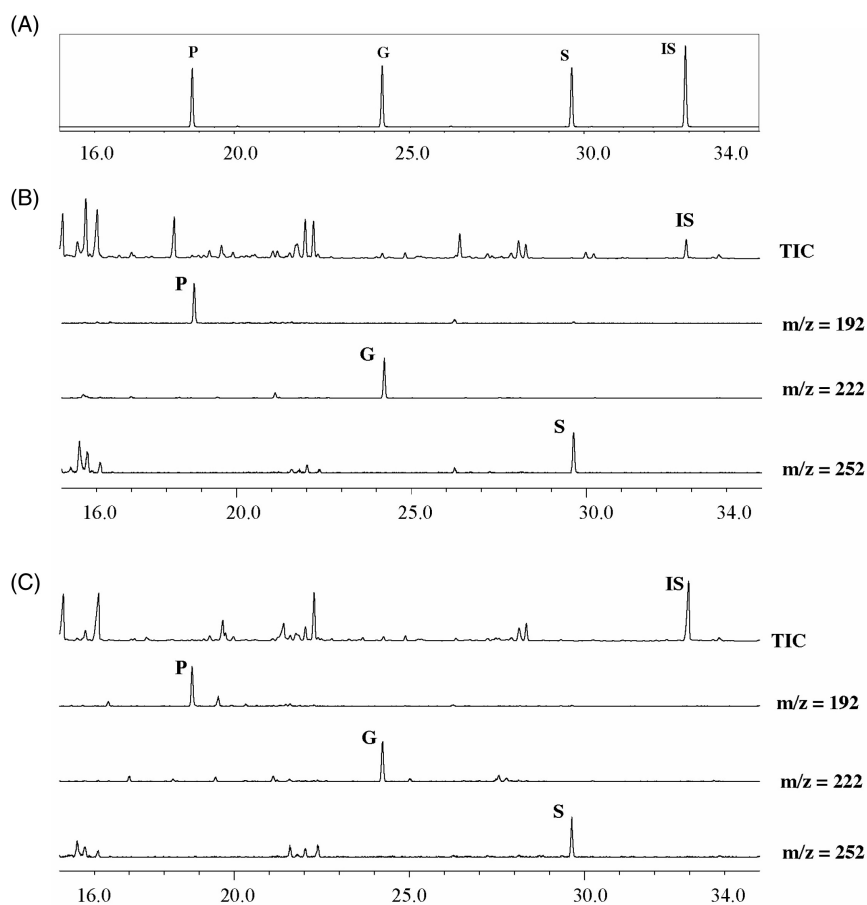
Figure 6-4. Total ion and mass selected chromatograms of (A) synthetic monolignols and DFRC monolignols derived from (B) intergenicula and (C) genicula.

6.4.3. *Histochemistry*

All histochemical stains reacted with genicular cell walls, and none reacted with intergenicular cell walls (Figure 6-5). Maule stained primary cell walls of genicula weak orange-brown (Figure 6-5b) and secondary cell walls dark brown (Figure 6-5c), similar to protoxylem in *Arabidopsis* (Figure 6-5e). Phloroglucinol-HCl did not react with primary walls of genicula (Figure 6-5g), but stained secondary walls dark red (Figure 6-5h), as in protoxylem of *Arabidopsis* (Figure 6-5j). Acriflavine stimulated both primary and secondary cell walls to fluoresce, but at varying intensity (Figure 6-5k-m). Brightly fluorescent secondary cell walls (Figure 6-5m) suggest levels of lignin expression similar to *Arabidopsis* xylem (Figure 6-5o).
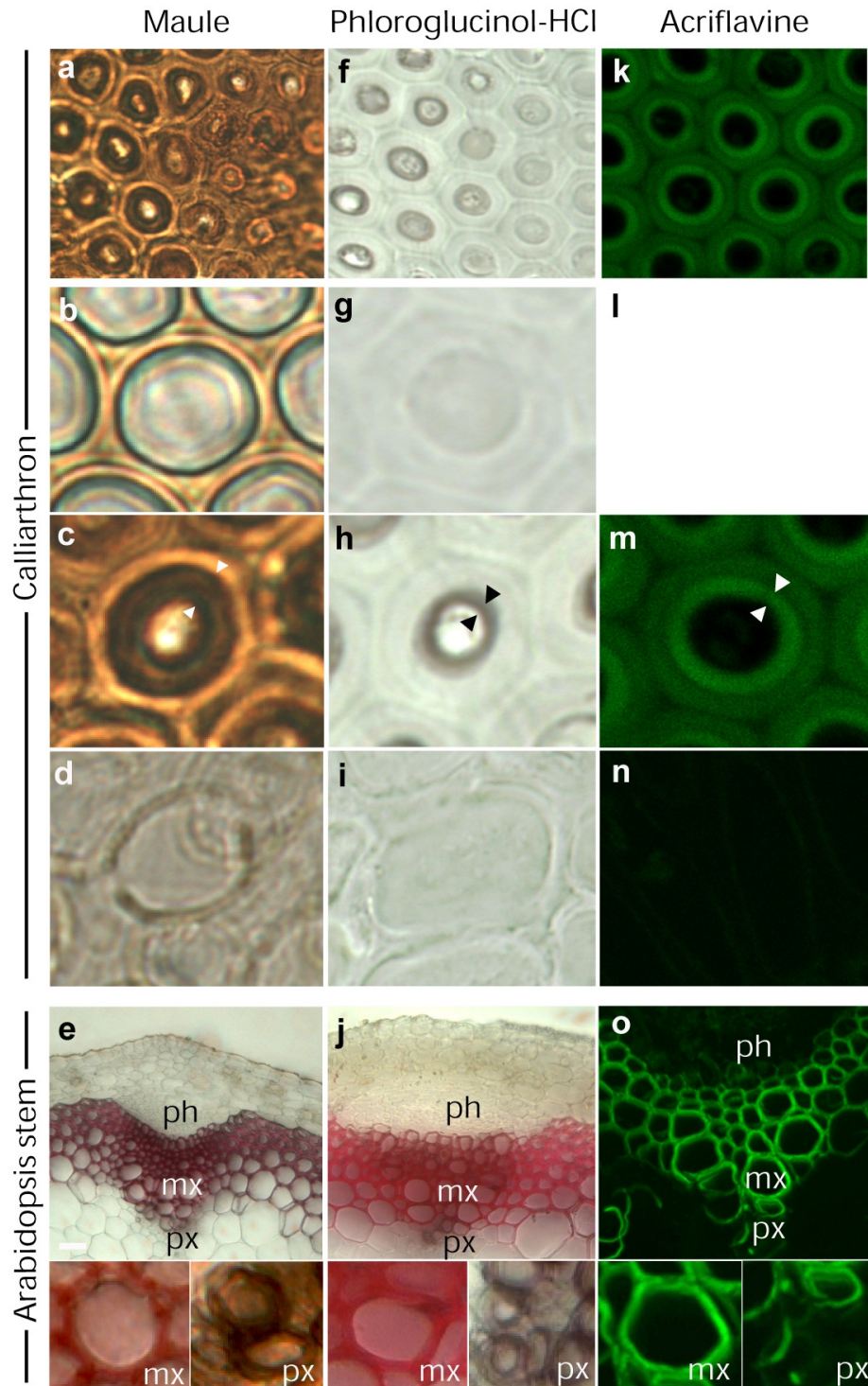
Figure 6-5. Maule (a-e), Phloroglucinol-HCl (f-j), and acriflavine (k-o) stains applied to *Calliarthron* and *Arabidopsis* tissues. *Calliarthron* tissues are young genicula (b,g,l), old genicula (c,h,m), and intergenicula (d,i,n). ph=phloem, mx=metaxylem, px=protoxylem.

6.5. Discussion

6.5.1. *Secondary cell walls*

TEM micrographs illustrate that the thickening of genicular cell walls in *Calliarthron* (Chapter 2) is a consequence of secondary cell wall development. This is the first documentation of secondary cell walls in red algae. The production of secondary walls is distinct from the well-described expansion of primary walls that occurs as genicula initially decalcify and elongate (Borowitzka and Vesk 1978, Borowitzka and Vesk 1979, Johansen 1981). In *Calliarthron*, secondary walls can be nearly 1 μm thick, and fully developed genicular cells bear striking resemblance to vessel and fiber elements in xylems of terrestrial angiosperms, such as *Arabidopsis*. However, while tracheid walls gain most of their thickness from layers of secondary cell walls, genicular cells benefit from near-equally thick primary and secondary walls.

6.5.2. *Lignin monomers*

DFRC analyses suggest that cell walls in *Calliarthron* contain hydroxycinnamyl monolignols that comprise lignin in terrestrial plant tissues. *Calliarthron* contains p-coumaryl and coniferyl units, derived from P-lignin and G-lignin in gymnosperms, as well as sinapyl units, derived from S-lignin in angiosperms. Whether these monolignols polymerize to form terrestrial lignins or novel polymers is unknown, but the presence of all three monolignols in genicula is striking.

Genicular tissue reacted positively with three different histological stains, which are generally considered diagnostic for lignins in terrestrial plants (e.g., Lewis and Yamamoto 1990, Jones et al. 2001, Christiernin et al. 2005, Patten et al. 2005). Maule reagent and Phloroglucinol-HCl both stained secondary cell walls brownish-black, suggesting the presence of G-monolignols. Maule reagent also stained young genicula yellowish-orange, suggesting that G- or S-monolignols may be present at low levels in primary cell walls. These conclusions were corroborated with acriflavine, which indicated high levels of monolignols in secondary cell walls and lower levels of

monolignols in primary cell walls based on fluorescence intensity. NMR analyses are currently underway to verify that these histological stains are labeling true lignins.

DFRC monomers were detected in both *Calliarthron* genicula and intergenicula, but histological stains did not react with intergenicula tissue. One explanation is that monolignols may be synthesized in both tissues but mobilize and polymerize specifically in genicular cells, as monolignol biosynthesis and lignin polymerization are spatially separated in terrestrial xylem (Lewis 1999). Genicular cells remain connected to intergenicular cells via pit connections, and translocation of monolignols from intergenicula to genicula is hypothetically possible.

6.5.3. *Evolutionary significance*

Monolignols and secondary cell walls likely confer unique mechanical properties to geniculate fronds living in the wave-swept intertidal zone. The intermediate stiffness of genicular tissue may result from the unique combination of lignin-like polymers cross-linking red algal polysaccharides. Genicular stiffness may help articulated fronds maintain an upright posture (see Chapter 3) to maximize access to light or to raise reproductive structures off the substratum, away from grazing herbivores (e.g., Padilla 1984). Furthermore, peripheral genicular cells have the thickest (Chapter 2) and most developed secondary cell walls, ideally positioned to limit bending stresses (Chapter 4), like the arrangement of thick-walled cells within stems of early fossilized land plants (Kendrick and Edwards 1988, Niklas 1992).

Although selective pressures in the marine environment differ from those on land, the wind-induced drag forces that presumably contributed to the evolution of wood in terrestrial plants are mirrored by flow-induced drag forces on aquatic algae. On land, xylem lends mechanical support to erect stems (Kendrick and Crane 1997, Friedman and Cook 2000, Boyce et al. 2004, Peter and Neale 2004), and in water, genicula provide mechanical support to *Calliarthron* fronds (Chapters 1-4). Data presented here suggest that secondary cell walls and monolignols may have evolved

convergently in both environments in response to mechanical stresses. Previous studies have supported this hypothesis by demonstrating the presence of mechanical on/off switches for lignin expression. For example, plants grown in microgravity synthesized less lignin (Cowles et al. 1984), and plants grown in hypergravity synthesized more lignin (Tamaoki et al. 2006) – including aquatic angiosperms that normally lack lignin altogether (Chen et al. 1980). Given this correlation, it is surprising that other wave-battered algae lack lignin (Ragan 1984, Lewis 1999), although few intertidal taxa have been investigated using modern techniques.

The discovery of "lignified" secondary cell walls in red algae would have major evolutionary implications. Contrary to the current paradigm of a terrestrial origin of monolignols, data presented here suggest that relevant developmental pathways may be highly conserved, evolving prior to the divergence of red and green algae more than 1 billion years ago (Saunders and Hommersand 2004). Whether other red and green seaweeds possess developmental machinery for monolignols is an open question. Previous studies have identified genes involved in the synthesis of terrestrial lignins (Peter and Neale 2004), and one logical next step will be to search for homologous genes in *Calliarthron*. Lignin genes may be present, but silenced, in green algal ancestors of land plants.

Genicular cells in *Calliarthron* lose organelles and cytoplasm throughout their ontogeny (Johansen 1969a), similar to the programmed death of tracheids in terrestrial xylem. While degradation of cellular contents facilitates hydraulic transport in xylem (Raven 1993), loss of organelles and cytoplasm in genicula may simply be a byproduct of cell wall thickening, since aquatic algae have little need for hydraulic transport. Nevertheless, nutrient translocation has been documented in *Calliarthron* (LaVelle 1979), and G-lignin, which seals the cell walls of vessel elements to facilitate transport (Friedman and Cook 2000, Boyce et al. 2004, Peter and Neale 2004), is found in the secondary cell walls of genicula, where it could play a similar role. Convergent evolution of cell structure and development of *Calliarthron* genicula and terrestrial xylem may shed light on the early evolution of land plants, as nutrient and

hydraulic transport may be exaptations of structures that initially evolved for biomechanical support.

APPENDIX 1

MATLAB scripts used in Chapter 3 to calculate articulated frond deflections and stress amplifications.

Articulated_bend.m

% calculates deflection of an articulated frond and stress amplification in genicula

```
clear

D=input('Measurement file: ', 's');          % inputs text file of geniculum dimensions
force=input('Applied Force (N): ');

dimension=dlmread(D,'\t');
gen=size(dimension,1);                        % number of genicula

Et =45.4E6;                                   % tensile modulus
Ec = Et/4;                                     % compressive modulus

w=zeros(gen,1);
x=zeros(gen,1);
y=zeros(gen,1);
r1=zeros(gen,1);
r2=zeros(gen,1);
intergen=zeros(gen,1);
neut=zeros(gen,1);
B=zeros(gen,1);
It=zeros(gen,1);
Ic=zeros(gen,1);
pretouchmomentline =zeros(gen,2);
posttouchmomentline =zeros(gen,2);

for i=1:gen
    w(i)=dimension(i,1);                       % lengths of genicula
    x(i)=dimension(i,2) ;                      % height of intergen lips
    y(i)=dimension(i,3) ;                      % radii of intergenicula
    r1(i)=dimension(i,4)    ;                  % long radii of genicula
    r2(i)=dimension(i,5);                      % short (bending) radii of genicula
    intergen(i)=dimension(i,6) + w(i)-2*x(i);  % lengths of intergenicula minus gap
    neut(i)=neutralsurface(r2(i),Et,Ec);       % computes neutral axis location
    B(i)= asin((w(i)-2*x(i))/(2*(neut(i)+y(i)))); % angle when intergen touch
    It(i)=Itension(r1(i),r2(i),neut(i));       % 2nd moment of area, tension
    Ic(i)=Icompression(r1(i),r2(i),neut(i));   % 2nd moment of area, compression
pretouchmomentline(i,:)=estimate_pretouch(w(i),x(i),y(i),r1(i),r2(i),B(i),neut(i),Et,E
c);
```

```
posttouchmomentline(i,:)=estimate_posttouch(w(i),x(i),y(i),r1(i),r2(i),B(i),neut(i),Et,
Ec);
end;

height=zeros(gen,1);                         % Use frond height to scale figure
height(1)=intergen(1);
for i=2:gen
   height(i)=height(i-1)+intergen(i);
end;

figure;
hold on;
axis([0,height(gen),0,height(gen)]);

phi=zeros(gen+1,1);
ylever=zeros(gen+1,1);
Moment=zeros(gen+1,1);
position=zeros(gen+1,2);
sumangle=zeros(gen+1,1);

position(1,1)=0;                             % starting position of articulated frond
position(1,2)=0;
for i=2:gen+1
   position(i,1)=0;
   position(i,2)=height(i-1);
end;

for F = 0:0.01:force

   k=0;

   for cycle = 1:20                          % cycle frond at each sub-force

      for g=1:gen
         for i=1:gen
            sumangle(i)=0;
            for j = 1: i
               sumangle(i) = sumangle(i) + phi(j);   % sum angles to current geniculum
            end;
         end;

         for i=1:gen
            if sumangle(i) >= pi/2            % determine where frond bends 90 degrees
               if k ==0;
                  k=i;
               end;
```

```
        end;
        if k ~= 0
            for p=k:gen
                sumangle(p) = pi/2;              % then set all distal angles to 90 degrees
            end;
        end;
    end;

    ylever(g) = 0;

    for i = g:gen                                % calculate new lever arm
        ylever(g) = ylever(g) + intergen(i) * cos(sumangle(i));
    end;

    Moment(g)= F*cos(phi(g)/2)*ylever(g);        % calculate external moment

    if Moment(g) < 0
        Moment(g) = 0;
    end

    if phi(g) <= (2*B(g))                        % before intergenicula touch
        phi(g)=pretouchmomentline(g,1)*Moment(g)+pretouchmomentline(g,2);
    else                                         % after intergenicula touch
        phi(g)=posttouchmomentline(g,1)*Moment(g)+posttouchmomentline(g,2);
    end;

    if phi(g) > pi/2
        phi(g) = pi/2;
    end;

    end;
end;

for i=1:gen+1
    if i==1
        position(1,1)=0;
        position(1,2)=0;
    else
        position(i,1)= position(i-1,1) + (intergen(i-1) * sin(sumangle(i-1)));
        position(i,2)= position(i-1,2) + (intergen(i-1) * cos(sumangle(i-1)));
    end;
end;
end;

for i=1:gen+1
    if i==1
```

```
      position(1,1)=0;
      position(1,2)=0;
   else
      position(i,1)= position(i-1,1) + (intergen(i-1) * sin(sumangle(i-1)));
      position(i,2)= position(i-1,2) + (intergen(i-1) * cos(sumangle(i-1)));
   end;
end;

plot(position(:,1),position(:,2),'bo-');

z=1;                        % geniculum index to calculate stress (default first geniculum)

while z ~= 0
   z = input('Enter geniculum number: ');

   if z == 0
      break
   end;

   if z == 1
      if sumangle(z) > 2*B(z)
         Bending=Et* [2*cos(pi/2-B(z))*(r2(z)-neut(z))/(w(z)-2*x(z)) +
                       (2*(y(z) + r2(z))*sin(sumangle(z)/2 - B(z)))/(w(z)-2*x(z)) - 1];
      else
         Bending=Et * [2* cos(pi/2 - sumangle(z)/2)*(r2(z)-neut(z))/(w(z)-2*x(z))];
      end;
   end;

   if z ~= 1
      if sumangle(z)-sumangle(z-1) > 2*B(z)
         Bending=Et* [2*cos(pi/2-B(z))*(r2(z)-neut(z))/(w(z)-2*x(z)) +
                       (2*(y(z) + r2(z))*sin((sumangle(z)-sumangle(z-1))/2 - B(z))) /
                       (w(z)-2*x(z)) - 1];
      else
         Bending=Et*[2* cos(pi/2 - (sumangle(z)-sumangle(z-1))/2) *
                       (r2(z)-neut(z))/(w(z)-2*x(z))];
      end;
   end;

   Tension=force*sin(sumangle(z)/2) / (pi*r1(z)*r2(z));
   Total = Tension + Bending;
end;
```

neutralsurface.m

% Solves for the location of the neutral axis in the cross-section of an elliptical geniculum, using equation from Gaylord (1997), p. 414

```
function neut=neutralsurface(r, Et, Ec);

y=0;                                    % Starting condition, center of ellipse
dy=0.0000001;

while y < r

    D= (Et-Ec)*(((r^2-y^2)^1.5)/3 + y*r^2/2*asin(y/r) + y^2/2*sqrt(r^2-y^2)) –
        (Et+Ec)*y*r^2*pi/4;

    if D < 0
       break;
    else
       y=y+dy;
    end;

end;

neut = y-dy;
```

Itension.m

% Calculates the 2nd moment of area in tension (It), using equation from Gaylord (1997), p. 415

```
function It = Itension(r1, r2, neut);

y=neut;                                 % for simplicity here

It = 2*r1/r2*(-(y^2*r2^2/2*asin(y/r2)+3*y^3/4*sqrt(r2^2-y^2)+2*y/3*(r2^2-
y^2)^1.5+r2^4/8*asin(y/r2)-r2^2*y/8*sqrt(r2^2-y^2))+(y^2*r2^2*pi/4+r2^4*pi/16));
```

Icompression.m

% Calculates the 2nd moment of area in compression (Ic), using equation from
Gaylord (1997), p. 415

```
function Ic = Icompression(r1, r2, neut);

y=neut;                                 % for simplicity here

Ic = 2*r1/r2*((y^2*r2^2/2*asin(y/r2)+3*y^3/4*sqrt(r2^2-y^2)+2*y/3*(r2^2-
y^2)^1.5+r2^4/8*asin(y/r2)-r2^2*y/8*sqrt(r2^2-y^2))+(y^2*r2^2*pi/4+r2^4*pi/16));
```

estimate_pretouch.m

*% Numerically estimates the moment required to bend a joint phi degrees **before***
intergenicula touch. Outputs least-squares fit line to predict phi, given any moment

```
function momentline=estimate_pretouch(w,x,y,r1,r2,B,neut,Et,Ec);

totalmom=zeros(3);
mom=zeros(3);

testphi(1)=0.4;                         % three arbitrary phi to determine moment
testphi(2)=0.8;                              and fit least-squares regression
testphi(3)=1;

dt=.01;

for i=1:3

  t=-pi/2;                              % theta around geniculum center
  maxt=pi/2;

  while t<=maxt

    strain = 2* cos(pi/2 - testphi(i)/2)*(r2*sin(t)-neut)/(w-2*x);

    if strain >= 0
       E=Et;                           % positive strain: tensile modulus
    else
       E=Ec;                           % negative strain: compressive modulus
    end;

    mom(i)=(r2*sin(t)-neut)*strain*E*2*r1*r2*(cos(t))^2*dt;
```

```matlab
      totalmom(i)=totalmom(i)+mom(i);
      t=t+dt;
   end;

   M(1,i)=totalmom(i);                        % create matrix of data points
   M(2,i)=testphi(i);
end;

momentline=polyfit(M(1,:),M(2,:),1);         % fit line to data points for output
```

estimate_posttouch.m

*% Numerically estimates the moment required to bend a joint phi degrees **after**
intergenicula touch. Outputs least-squares fit line to predict phi, given any moment*

```matlab
function momentline=estimate_posttouch(w,x,y,r1,r2,B,neut,Et,Ec);

totalmom=zeros(3);
mom=zeros(3);

testphi(1)=0.4;                              % three arbitrary phi to determine moment
testphi(2)=0.8;                                  and fit least squares regression
testphi(3)=1;

dt=.01;

for i=1:3

   t=-pi/2;                                  % theta around geniculum center
   maxt=pi/2;

   while t<=maxt

      strain=2*cos(pi/2-B)*(r2*sin(t)-neut)/(w-2*x) +
             (2*(y + r2*sin(t))*sin(testphi(i)/2 - B))/(w-2*x) - 1;

      if strain >= 0
         E=Et;                               % positive strain: tensile modulus
      else
         E=Ec;                               % negative strain: compressive modulus
      end;

      mom(i)=(y+r2*sin(t))*strain*E*2*r1*r2*(cos(t))^2*dt;
      totalmom(i)=totalmom(i)+mom(i);
```

```
      t=t+dt;
  end;

  M(1,i)=totalmom(i);                  % create matrix of data points
  M(2,i)=testphi(i);
end;

momentline=polyfit(M(1,:),M(2,:),1);   % fit line to data points for output
```

REFERENCES

Abbott, I. A. & Hollenberg, G. J. 1976. *Marine Algae of California*. Stanford University Press, Stanford, CA, 827 pp.

Alexander, R. M. 1981. Factors of safety in the structure of animals. *Sci. Prog.* 67: 109-130.

Armstrong, S. L. 1987. Mechanical properties of the tissues of the brown alga *Hedophyllum sessile* (C. Ag.) Setchell: variability with habitat. *J. Exp. Mar. Biol. Ecol.* 114: 143-151.

Bailey, A. & Bisalputra, T. 1970. A preliminary account of the application of thin-sectioning, freeze-etching, and scanning electron microscopy to the study of coralline algae. *Phycologia* 9(1): 83-101.

Bailey, J. C. & Chapman, R. L. 1998. A phylogenetic study of the corallinales (Rhodophyta) based on nuclear small-subunit rRNA gene sequences. *J. Phycol.* 34: 692-705.

Bailey, J. C., Gabel, J. E. & Freshwater, D. W. 2004. Nuclear 18S rRNA gene sequence analysis indicate that the Mastophoroideae (Corallinaceae, Rhodophyta) is a polyphyletic taxon. *Phycologia* 43(1): 3-12.

Bell, E. C. 1999. Applying flow tank measurements to the surf zone: predicting dislodgment of the Gigartinaceae. *Phycological Research* 47: 159-166.

Bell, E. C. & Denny, M. W. 1994. Quantifying "wave exposure": a simple device for recording maximum velocity and results of its use at several field sites. *J. Exp. Mar. Biol. Ecol.* 181: 9-29.

Biedka, R. F., Gosline, J. M. & DeWreede, R. E. 1987. Biomechanical analysis of wave-induced mortality in the marine alga *Pterygophora californica. Mar. Ecol. Prog. Ser.* 36: 163-170.

Bilan, M. I. & Usov, A. I. 2001. Polysaccharides of calcareous algae and their effect on the calcification process. *Russian Journal of Bioorganic Chemistry* 27(1): 2-16.

Bjorkman, A. 1954. Isolation of lignin from finely divided wood with neutral solvents. *Nature* 174: 1057-1058.

Blanchette, C. A. 1997. Size and survival of intertidal plants in response to wave action: a case study with *Fucus gardneri*. *Ecology* 78(5): 1563-1578.

Boller, M. L. & Carrington, E. 2006. The hydrodynamic effects of shape and size change during reconfiguration of a flexible macroalga. *J. Exp. Biol.* 209: 1894-1903.

Boller, M. L., Swain, T. D. & Lasker, H. R. 2002. Skeletal morphology and material properties of a fragmenting gorgonian coral. *Mar. Ecol. Prog. Ser.* 228: 131-141.

Borowitzka, M. A. 1977. Algal calcification. *Oceanogr. Mar. Biol. Ann. Rev.* 15: 189-223.

Borowitzka, M. A. 1982. Morphological and cytological aspects of algal calcification. *Int. Rev. Cytol.* 74: 127-162.

Borowitzka, M. A. 1987. Calcification in algae: mechanisms and the role of metabolism. *CRC Critical Reviews in Plant Sciences* 6(1): 1-45.

Borowitzka, M. A. & Vesk, M. 1978. Ultrastructure of the Corallinaceae (Rhodophyta). I. The vegetative cells of *Corallina officinalis* and *C. cuvierii*. *Mar. Biol.* 46: 295-304.

Borowitzka, M. A. & Vesk, M. 1979. Ultrastructure of the Corallinaceae (Rhodophyta) II. Vegetative cells of Lithothrix aspergillum. *J. Phycol.* 15: 146-153.

Boyce, C. K., Zwieniecki, M. A., Cody, G. D., Jacobsen, C., Wirick, S., Knoll, A. H. & Holbrook, N. M. 2004. Evolution of xylem lignification and hydrogel transport regulation. *Proc. Natl. Acad. Sci.* 101(50): 17555-17558.

Cabioch, J. & Giraud, G. 1986. Structural aspects of biomineralization in the coralline algae (calcified Rhodophyceae). *In* Leadbeater, B. S. C.&Riding, R. [Eds.] *Biomineralization in Lower Plants and Animals.* Clarendon Press, Oxford, pp.

Carrington, E. 1990. Drag and dislodgement of an intertidal macroalga: consequences of morphological variation in *Mastocarpus papillatus* Kutzing. *J. Exp. Mar. Biol. Ecol.* 139: 185-200.

Carrington, E., Grace, S. P. & Chopin, T. 2001. Life history phases and the biomechanical properties of the red alga *Chondrus crispus* (Rhodophyta). *J. Phycol.* 37: 699-704.

Cases, M. R., Stortz, C. A. & Cerezo, A. S. 1992. Methylated, sulphated xylogalactans from the the red seaweed *Corallina officinalis*. *Phytochemistry* 31(11): 3897-3900.

Cases, M. R., Stortz, C. A. & Cerezo, A. S. 1994. Structure of the 'corallinans' - sulfated xylogalactans from *Corallina officinalis*. *Int. J. Biol. Macromol.* 16(2): 93-97.

Chen, N., Siegel, S. M. & Siegel, B. L. 1980. Gravity and land plant evolution: experimental induction of lignification by simulated hypergravity and water stress. *Life Sci. Space Res.* 18: 193-198.

Christiernin, M., Ohlsson, A. B., Berglund, T. & Henriksson, G. 2005. Lignin isolated from primary walls of hybrid aspen cell cultures indicates significant differences in lignin structure between primary and secondary wall. *Plant Physiol. Biochem.* 43: 777-785.

Ciucanu, I. & Kerek, K. 1984. A simple and rapid method for the permethylation of carbohydrates. *Carbohydr. Res.* 134: 209-217.

Cowles, J. R., Scheld, H. W., Lemay, R. & Peterson, C. 1984. Growth and lignification in seedlings exposed to eight days of microgravity. *Ann. Bot.* 54: 33-48.

Craigie, J. S. 1990. Cell walls. *In* Cole, K. M.&Sheath, R. G. [Eds.] *Biology of the Red Algae.* Cambridge University Press, Cambridge, pp. 221-257.

Currey, J. D. 1980. Mechanical properties of mollusc shell. *Symp. Soc. Exp. Biol.* 34: 75-78.

Currey, J. D. & Taylor, J. D. 1974. The mechanical behavior of some molluscan hard tissues. *J. Zool.* 173: 395-406.

Delf, E. M. 1932. Experiments with the stipes of *Fucus* and *Laminaria*. *J. Exp. Biol.* 9: 300-313.

Denny, M. W. 1988. *Biology and mechanics of the wave-swept environment*. Princeton University Press, Princeton, New Jersey, USA, pp.

Denny, M. W. 1994. Extreme drag forces and the survival of wind- and water-swept organisms. *J. Exp. Biol.* 194: 97-115.

Denny, M. W. 1999. Are there mechanical limits to size in wave-swept organisms? *J. Exp. Biol.* 202: 3463-3467.

Denny, M. W., Brown, V., Carrington, E., Kraemer, G. P. & Miller, A. 1989. Fracture mechanics and the survival of wave-swept macroalgae. *J. Exp. Mar. Biol. Ecol.* 127: 211-228.

Denny, M. W., Daniel, T. L. & Koehl, M. A. R. 1985. Mechanical limits to size in wave-swept organisms. *Ecol. Monogr.* 55(1): 69-102.

Denny, M. W. & Gaylord, B. 2002. The mechanics of wave-swept algae. *J. Exp. Biol.* 205: 1355-1362.

Denny, M. W., Gaylord, B., Helmuth, B. & Daniel, T. L. 1998. The menace of momentum: dynamic forces on flexible organisms. *Limnol. Oceanogr.* 43(5): 955-968.

Denny, M. W., Gaylord, B. P. & Cowen, E. A. 1997. Flow and flexibility II. The roles of size and shape in determining wave forces on the bull kelp *Nereocystis luetkeana*. *J. Exp. Biol.* 200: 3165-3183.

Denny, M. W., Miller, L. P., Stokes, M. D., Hunt, L. J. H. & Helmuth, B. S. T. 2003. Extreme water velocities: Topographical amplification of wave-induced flow in the surf zone of rocky shores. *Limnol. Oceanogr.* 48(1): 1-8.

Denny, M. W. & Wethey, D. 2001. Physical processes that generate patterns in marine communities. *In* Bertness, M. D., Gaines, S.&Hay, M. E. [Eds.] *Marine Community Ecology.* Sinauer Associates, Sunderland, MA, pp.

DeWreede, R. E., Ewanchuk, P. & Shaughnessy, F. J. 1992. Wounding, healing and survivorship in three kelp species. *Mar. Ecol. Prog. Ser.* 82: 259-266.

Dolan, S. 2001. The use of medullary unit patterns of intergenicula and genicula in the taxonomy of *Amphiroa* (Corallinaceae, Rhodophyta). *Eur. J. Phycol.* 36: 397-407.

Dubois, M., Gilles, K. A., Hamilton, J. K., Rebers, P. A. & Smith, F. 1956. Calorimetric method of determination of sugars and related substances. *Anal. Chem.* 28: 350-356.

Ducker, S. C. 1979. The genus *Metagoniolithon* Weber-van Bosse (Corallinaceae, Rhodophyta). *Aust. J. Bot.* 27(1): 67-101.

Dudgeon, S. R. & Johnson, A. S. 1992. Thick vs. thin: thallus morphology and tissue mechanics influence differential drag and dislodgement of two co-dominant seaweeds. *J. Exp. Mar. Biol. Ecol.* 165: 23-43.

Duggins, D. O., Eckman, J., E., Siddon, C. E. & Klinger, T. 2003. Population, morphometric and biomechanical studies of three understory kelps along a hydrodynamic gradient. *Mar. Ecol. Prog. Ser.* 265: 57-76.

Endler, J. A. 1986. *Natural Selection in the Wild*. Princeton University Press, Princeton, NJ, 336 pp.

Estevez, J., Cerezo, A. S. & Ciancia, M. 2007. Is there a true separation between agarophytes and carrageenophytes? The sulfated galactans from *Gymnogongrus torulosus. Phytochemistry* (*in review*).

Etnier, S. A. 2001. Flexural and torsional stiffness in multi-jointed biological beams. *Biol. Bull.* 200: 1-8.

Flores, M. L., Stortz, C. A., Rodriguez, M. C. & Cerezo, A. S. 1997. Studies on the skeletal cell wall and cuticle of the cystocarpic stage of the red seaweeds *Iridaea undulosa. Bot. Marina* 40: 411-419.

Friedland, M. T. & Denny, M. W. 1995. Surviving hydrodynamic forces in a wave-swept environment: consequences of morphology in the feather boa kelp, *Egregia menziesii* (Turner). *J. Exp. Mar. Biol. Ecol.* 190: 109-133.

Friedman, W. E. & Cook, M. E. 2000. The origin and early evolution of tracheids in vascular plants: integration of palaeobotanical and neobotanical data. *Phil. Trans. R. Soc. Lond. B* 355: 857-868.

Ganeson, E. K. 1971. Studies on the morphologie and reproduction of the articulated corallines - VI. *Metagoniolithon* Weber van Bosse. *Rev. Algol.* 10: 248-256.

Gaylord, B. 1997. *Consequences of wave-induced water motion to nearshore macroalgae.* PhD Thesis, Stanford University, Stanford, CA, USA.

Gaylord, B. 2000. Biological implications of surf-zone flow complexity. *Limnol. Oceanogr.* 45(1): 174-188.

Gaylord, B., Blanchette, C. A. & Denny, M. W. 1994. Mechanical consequences of size in wave-swept algae. *Ecol. Monogr.* 64(3): 287-313.

Gaylord, B. & Denny, M. W. 1997. Flow and flexibility I. Effects of size, shape and stiffness in determining wave forces on the stipitate kelps *Eisenia arborea* and *Pterygophora californica. J. Exp. Biol.* 200: 3141-3164.

Gaylord, B., Hale, B. B. & Denny, M. W. 2001. Consequences of transient fluid forces for compliant benthic organisms. *J. Exp. Biol.* 204: 1347-1360.

Gerard, V. A. & Mann, K. H. 1979. Growth and production of *Laminaria longicruris* (Phaeophyta) populations exposed to different intensities of water movement. *J. Phycol.* 15: 33-41.

Gordon, J. E. 1978. *Structures: or Why things don't fall down*. Penguin Books, Harmondsworth, 395 pp.

Graham, L. E. & Wilcox, L. W. 2000. *Algae*. Prentice-Hall, Inc., Upper Saddle River, NJ, 640 pp.

Hale, B. 2001. *Macroalgal Materials: Foiling Fracture and Fatigue from Fluid Forces*. PhD Thesis, Stanford University, Stanford, CA, USA.

Harder, D., Hurd, C. & Speck, T. 2006. Comparison of mechanical properties of four large, wave-exposed seaweeds. *Am. J. Bot.* 93(10): 1426-1322.

Harder, D., Speck, O., Hurd, C. & Speck, T. 2004. Reconfiguration as a prerequisite for survival in highly unstable flow-dominated environments. *J. Plant Growth Regul.* 23: 98-107.

Haug, A., Larsen, B. & Smidsrod, O. 1974. Uronic acid sequence in alginate from different sources. *Carbohydr. Res.* 32: 217-225.

Helmuth, B. & Denny, M. W. 2003. Predicting wave exposure in the rocky intertidal zone: Do bigger waves always lead to larger forces? *Limnol. Oceanogr.* 48(3): 1338-1345.

Highsmith, R. C. 1982. Reproduction by fragmentation in corals. *Mar. Ecol. Prog. Ser.* 7: 207-226.

Holbrook, N. M., Denny, M. W. & Koehl, M. A. R. 1991. Intertidal "trees": consequences of aggregation on the mechanical and photosynthetic properties of sea-palms *Postelsia palmaeformis* Ruprecht. *J. Exp. Mar. Biol. Ecol.* 146: 39-67.

Huisman, J. M. 2000. *Marine Plants of Australia*. University of West Australia Press, Nedlands, Western Australia, 300 pp.

Hurd, C. 2000. Water motion, marine macroalgal physiology, and production. *J. Phycol.* 36: 453-472.

Johansen, H. W. 1969a. Morphology and systematics of coralline algae with special reference to *Calliarthron*. *University of California Publications in Botany* 49: 1-98.

Johansen, H. W. 1969b. Patterns of genicular development in *Amphiroa* (Corallinaceae). *J. Phycol.* 5(2): 118-123.

Johansen, H. W. 1974. Articulated coralline algae. *Oceanogr. Mar. Biol. Ann. Rev.* 12: 77-127.

Johansen, H. W. 1981. *Coralline Algae, A First Synthesis*. CRC Press, Inc., Boca Raton, 239 pp.

Johansen, H. W. & Austin, L. F. 1970. Growth rates in the articulated coralline *Calliarthron* (Rhodophyta). *Can. J. Bot.* 48(1): 125-132.

Johnson, A. S. & Koehl, M. A. R. 1994. Maintenance of dynamic strain similarity and environmental stress factor in different flow habitats: thallus allometry and material properties of a giant kelp. *J. Exp. Biol.* 195: 381-410.

Johnson, J. H. 1961. *Limestone-Building Algae and Algal Limestones*. Colorado School of Mines, Boulder, 297 pp.

Jones, L., Ennos, A. R. & Turner, S. R. 2001. Cloning and characterization of *irregular xylem4* (*irx4*): a severely lignin-deficient mutant of *Arabidopsis*. *Plant J.* 26(2): 205-216.

Kakurakova, M., Capek, P., Sasinkova, V., Wellner, N. & Ebringerova, A. 2000. FT-IR study of plant cell wall model compounds: pectic polysaccharides and hemicelluloses. *Carb. Poly.* 43: 195-203.

Kendrick, P. & Crane, P. R. 1997. The origin and early evolution of plants on land. *Nature* 389: 33-39.

Kendrick, P. & Edwards, D. 1988. The anatomy of lower Devonian *Gosslingia breconensis* Heard based on pyritized axes, with some comments on the permineralization process. *Bot. J. Linn. Soc.* 97(2): 95-123.

Kitzes, J. A. & Denny, M. W. 2005. Red algae respond to waves: morphological and mechanical variation in *Mastocarpus papillatus* along a gradient of force. *Biol. Bull.* 208: 114-119.

Klinger, T. & DeWreede, R. E. 1988. Stipe rings, age, and size in populations of *Laminaria setchellii* Silva (Laminariales, Phaeophyta) in British Columbia, Canada. *Phycologia* 27(2): 234-240.

Kloareg, B. & Quatrano, R. S. 1988. Structure of the cell wall of marine algae and ecophysiological functions of the matrix polysaccharides. *Oceanogr. Mar. Biol. Ann. Rev.* 26: 259-315.

Koehl, M. A. R. 1984. How do benthic organisms withstand moving water? *Am. Zool.* 24: 57-70.

Koehl, M. A. R. 1986. Seaweeds in moving water: form and mechanical function. *In* Givnish, T. J. [Ed.] *On the Economy of Plant Form and Function.* Cambridge University Press, London, pp. 603-634.

Koehl, M. A. R. 1998. The quirks of jerks. *Nature* 396: 621-623.

Koehl, M. A. R. 2000. Mechanical design and hydrodynamics of blade-like algae: *Chondracanthus exasperatus*. *In* Spatz, H. C.&Speck, T. [Eds.] *Third International Plant Biomechanics Conference.* Thieme Verlag, Stuttgart, pp.

Koehl, M. A. R. & Wainwright, S. A. 1977. Mechanical adaptations of a giant kelp. *Limnol. Oceanogr.* 22(6): 1067-1071.

Koehler, L. & Spatz, H. C. 2002. Micromechanics of plant tissues beyond the linear-elastic range. *Planta* 215: 33-40.

Kogame, Y. & Kawai, H. 1996. Development of the intercalary meristem in *Chorda filum* (Laminariales, Phaeophyceae) and other primitive Laminariales. *Phycological Research* 44: 247-260.

Kraemer, G. P. & Chapman, D. J. 1991. Biomechanics and alginic acid composition during hydrodynamic adaptation by *Egregia menziesii* (Phaeophyta) juveniles. *J. Phycol.* 27: 47-53.

Krishnamurthy, K. V. 1999. Transmission electron microscopic cytochemistry. *In* Krishnamurthy, K. V. [Ed.] *Methods in Cell Wall Cytochemistry.* CRC Press, 177-226.

LaVelle, J. M. 1979. Translocation in *Calliarthron tuberculosum* and its role in the light-enhancement of calcification. *Mar. Biol.* 55: 37-44.

Lechat, H., Amat, M., Mazoyer, J., Buleon, A. & Lahaye, M. 2000. Structure and distribution of glucomannan and sulfated glucan in the cell walls of the red alga *Kappaphycus alvarezii* (Gigartinales, Rhodophyta). *J. Phycol.* 36: 891-902.

Lewis, N. G. 1999. A 20th century roller coaster ride: a short account of lignification. *Current Opinion in Plant Biology* 2(2): 153-162.

Lewis, N. G. & Yamamoto, E. 1990. Lignin: occurrence, biogenesis and biodegradation. *Ann. Rev. Plant Phys. Plant Mol. Biol.* 41: 455-496.

Littler, D. S. & Littler, M. M. 2003. *South Pacific Reef Plants*. OffShore Graphics, Inc., Washington, D.C., USA, 332 pp.

Lu, F. & Ralph, J. 1999. Detection and determination of p-coumarylated units in lignin. *J Agric Food Chem* 47(5): 1988-1992.

McCandless, E. L. & Craigie, J. S. 1979. Sulfated polysaccharides in red and brown algae. *Ann. Rev. Plant Physio.* 30: 41-53.

Miller, I. J. 1997. The chemotaxonomic significance of the water-soluble red algal polysaccharides. *Recent Res. Devel. in Phytochem.* 1: 531-565.

Milligan, K. L. D. & DeWreede, R. E. 2004. Morphological variations do not effectively reduce drag forces at high wave-exposure for the macroalgal species, *Hedophyllum sessile* (Laminariales, Phaeophyta). *Phycologia* 43(3): 236-244.

Morrison, I. M. 1988. Hydrolysis of plant cell walls with trifluoroacetic acid. *Phytochemistry* 27: 1097-1100.

Munawar, S. S., Umemura, K. & Kawai, S. 2007. Characterization of the morphological, physical, and mechanical properties of seven nonwood plant fiber bundles. *J. Wood Sci.* 53: 108-113.

Navarro, D. A. & Stortz, C. A. 2002. Isolation of xylogalactans frlom the Corallinales: influence of the extraction method on yields and compositions. *Carb. Poly.* 49: 57-62.

Niklas, K. J. 1992. *Plant biomechanics: an engineering approach to plant form and function*. University of Chicago Press, Chicago, 607 pp.

O'Donnell, M. 2005. *Habitats and Hydrodynamics on Wave-Swept Rocky Shores*. PhD Thesis, Stanford University, Stanford, CA, USA.

Okazaki, M., Shiroto, C. & Furuya, K. 1984. Relationship between the location of polyuronides and calcification sites in the calcareous red algae *Serraticardia maxima* and *Lithothamnion japonica* (Rhodophyta, Corallinaceae). *Jap. J. Phycol.* 32: 364-372.

Padilla, D. K. 1984. The importance of form: differences in competitive ability, resistance to consumers and environmental stress in an assemblage of coralline algae. *J. Exp. Mar. Biol. Ecol.* 79: 105-127.

Padilla, D. K. 1993. Rip stop in marine algae: minimizing the consequences of herbivore damage. *Evol. Ecol.* 7: 634-644.

Patten, A. M., Cardenas, C. L., Cochrane, F. C., Laskar, D. D., Bedgar, D. L., Davin, L. B. & Lewis, N. G. 2005. Reassessment of effects on lignification and vascular development in the *irx4 Arabidopsis* mutant. *Phytochemistry* 66: 2092-2107.

Pelton, J. T. & McLean, L. R. 2000. Spectroscopic methods for analysis of protein secondary structure. *Anal. Biochem.* 277: 167-176.

Peter, G. & Neale, D. 2004. Molecular basis for the evolution of xylem lignification. *Current Opinion in Plant Biology* 7: 737-742.

Pratt, M. C. & Johnson, A. S. 2002. Strength, drag, and dislodgement of two competing intertidal algae from two wave exposures and four seasons. *J. Exp. Mar. Biol. Ecol.* 272: 71-101.

Pueschel, C. M., Judson, B. L. & Wegeberg, S. 2005. Decalcification during epithallial cell turnover in *Jania adhaerens* (Corallinales, Rhodophyta). *Phycologia* 44(2): 156-162.

Ragan, M. 1984. *Fucus* 'lignin': a reassessment. *Phytochemistry* 23(9): 2029-2032.

Raven, P. H. 1993. The evolution of vascular plants in relation to quantitative functioning of dead water-conducting cells and stomata. *Biol. Rev.* 68: 337-363.

Raven, P. H., Evert, R. F. & Eichhorn, S. E. 2003. *Biology of Plants, Sixth Edition*. W. H. Freeman and Company, New York, New York, 944 pp.

Roark, R. J. & Young, W. C. 1975. *Formulas for Stress and Strain, Fifth Edition*. McGraw-Hill Book Company, New York, USA, pp.

Saunders, G. W. & Hommersand, M. H. 2004. Assessing red algal supraordinal diversity and taxonomy in the context of contemporary systematic data. *Am. J. Bot.* 91(10): 1494-1507.

Shaughnessy, F. J., DeWreede, R. E. & Bell, E. C. 1996. Consequences of morphology and tissue strength to blade survivorship of two closely related Rhodophyta species. *Mar. Ecol. Prog. Ser.* 136: 257-266.

South, G. R. & Skelton, P. A. 2003. Catalogue of the marine benthic macroalgae of the Fiji Islands, South Pacific. *Aust. Syst. Bot.* 16: 699-758.

Steneck, R. S. 1983. Escalating herbivory and resulting adaptive trends in calcareous algal crusts. *Paleobiology* 9(1): 44-61.

Steneck, R. S. 1986. The ecology of coralline algal crusts: convergent patterns and adaptive strategies. *Ann. Rev. Ecol. Syst.* 17: 273-303.

Stevens, C., Hurd, C. & Smith, M. 2002. Field measurements of the dynamics of the bull kelp *Durvillaea antarctica* (Chamisso) Heriot. *J. Exp. Mar. Biol. Ecol.* 269: 147-171.

Stevenson, T. T. & Furneaux, R. H. 1991. Chemical methods for the analysis of sulphated galactans from red algae. *Carbohydr. Res.* 210: 277-298.

Stewart, H. L. 2006a. Hydrodynamic consequences of flexural stiffness and buoyancy for seaweeds: a study using physical models. *J. Exp. Biol.* 209: 2170-2181.

Stewart, H. L. 2006b. Ontogenetic changes in buoyancy, breaking strength, extensibility, and reproductive investment in a drifting macroalga *Turbinaria ornata* (Phaeophyta). *J. Phycol.* 42: 43-50.

Stortz, C. A. & Cerezo, A. S. 2000. Novel findings in carrageenans, agaroids and "hybrid" red seaweed galactans. *Curr. Top. in Phytochem.* 4: 121-134.

Tamaoki, D., Karahara, I., Schreiber, L., Wakasugi, T., Yamada, K. & Kamisaka, S. 2006. Effects of hypergravity conditions on elongation growth and lignin formation in the inflorescence stem of *Arabidopsis thaliana*. *J. Plant Res.* 119: 79-84.

Toole, G. A., Gunning, P. A., Parker, M. L., Smith, A. C. & Waldron, K. W. 2001. Fracture mechanics of the cell wall of *Chara corallina*. *Planta* 212: 606-611.

Toole, G. A., Smith, A. C. & Waldron, K. W. 2002. The effect of physical and chemical treatment on the mechanical properties of the cell wall of the alga *Chara corallina*. *Planta* 214: 468-475.

Tsekos, I., Reiss, H. D. & Schnepf, E. 1993. Cell-wall structure and supramolecular organization of the plasma membrane of marine red algae visualized by freeze fracture. *Acta Botanica Neerlandica* 42(2): 119-132.

Turner, S. R. & Somerville, C. R. 1997. Collapsed xylem phenotype of *Arabidopsis* identifies mutants deficient in cellulose deposition in the secondary cell wall. *Plant Cell* 9(5): 689-701.

Underwood, A. J. 1999. *Experiments in Ecology*. Cambridge University Press, Cambridge, UK, 504 pp.

Usov, A. I. 1992. Sulphated polysaccharides of the red seaweeds. *Food Hydrocolloids* 6: 9-23.

Usov, A. I., Bilan, M. I. & Shashkov, A. S. 1997. Structure of a sulfated xylogalactan from the calcareous red alga *Corallina pilulifera* P. *et* R. (Rhodophyta, Corallinaceae). *Carbohydr. Res.* 303: 93-102.

Utter, B. D. & Denny, M. W. 1996. Wave-induced forces on the giant kelp *Macrocystis pyrifera* (Agardh): field test of a computational model. *J. Exp. Biol.* 199: 2645-2654.

Vogel, S. 1994. *Life in Moving Fluids*. Princeton University Press, Princeton, N.J., 467 pp.

Vosburgh, F. 1982. *Acropora reticulata*: structure, mechanics and ecology of a reef coral. *Proc. R. Soc. Lond. B. Biol. Sci.* 214: 481-499.

Waaland, S. D. & Waaland, J. R. 1975. Analysis of cell elongation in red algae by fluorescent labelling. *Planta* 126: 127-138.

Wainwright, S. A., Biggs, W. D., Currey, J. D. & Gosline, J. M. 1982. *Mechanical Design in Organisms*. Princeton University Press, Princeton, NJ, USA, 423 pp.

Woelkerling, W. J. 1988. *The Coralline Red Algae: An Analysis of the Genera and Subfamilies of Nongeniculate Corallinaceae*. Oxford University Press, New York, 268 pp.

Wray, J. L. 1977. *Calcareous Algae*. Elsevier Scientific Publishing Company, New York, 185 pp.

Yendo, K. 1904. A study of the genicula of Corallinae. *J. Coll. Sci. Imp. Univ. Tokyo* 19: 1-45.